INFLUENCE OF PHYSICAL PROPERTIES OF SOILS ON TEMPORAL AND SPATIAL DISTRIBUTION OF POTENTIAL ANOXIC VOLUME AT THE FIELD SCALE

by

HARIOM YADAV

(Under the Direction of NANDITA GAUR)

ABSTRACT

Anoxic soil pores govern carbon retention and the release of potent greenhouse gases like N_2O and CH_4 in agricultural soils. Soil pore-size distribution (PSD) and pore continuity have been known to qualitatively impact oxygen diffusion, a key driver of potential soil anoxia. In this study, this effect was quantified. Soil moisture affected the relationship between PSD and oxygen diffusion and the contribution of pore sizes to potential anoxic volume (POV). Pores ≤ 1 micron contributed significantly to POV in the field, sustaining potentially anoxic conditions for at least 48 hours, while pores > 3 microns had negligible impact. Additionally, the dependence of oxygen diffusivity (OD) on soil structure was quantifiably characterized at different moisture contents. Results showed that van Genuchten's parameters n_1 and n_2, representing soil PSD for a dual porosity system, successfully classified OD for low moisture contents. Results from this research can aid in promoting sustainable agricultural practices.

INDEX WORDS: soil structure; soil hydraulic parameters; oxygen diffusivity; soil moisture; anoxic pore volume; field scale

INFLUENCE OF PHYSICAL PROPERTIES OF SOILS ON TEMPORAL AND SPATIAL DISTRIBUTION OF POTENTIAL SOIL ANOXIC VOLUME AT THE FIELD SCALE

by

HARIOM YADAV

B.S, AGRICULTURE AND FORESTRY UNIVERSITY, NEPAL, 2020

A Thesis Submitted to the Graduate Faculty of The University of Georgia in Partial Fulfillment of the Requirements for the Degree

MASTER OF SCIENCE

ATHENS, GEORGIA

2023

INFLUENCE OF PHYSICAL PROPERTIES OF SOILS ON TEMPORAL AND SPATIAL DISTRIBUTION OF POTENTIAL SOIL ANOXIC VOLUME AT THE FIELD SCALE

by

HARIOM YADAV

Major Professor:	NANDITA GAUR
Committee:	AARON THOMPSON
	CHARLOTTE GARING
	GEORGE VELLIDIS

Electronic Version Approved:

Ron Walcott
Vice Provost for Graduate Education and Dean of the Graduate School
The University of Georgia
August 2023

ACKNOWLEDGEMENTS

I would like to express my heartfelt gratitude to Dr. Nandita Gaur for her invaluable mentorship and the incredible opportunity she provided me to work on this project during my master's program. Her profound knowledge and extensive experience have been instrumental in shaping my ideas and refining my academic research. I am truly grateful for her guidance and unwavering support. Additionally, I would like to extend my thanks to Dr. Aaron Thompson for his valuable suggestions and guidance throughout the project. His insights have been instrumental in enhancing the quality of my work. I would also like to acknowledge and appreciate the assistance of Matthew Thibodeaux, both in the field and in the laboratory. His contributions have been immensely valuable, and I am grateful for his support. Furthermore, I would like to express my sincere appreciation to my committee members for their assistance and input during this entire process. Their expertise and feedback have been crucial in shaping my research. Working with all the individuals associated with this project has been a truly enriching experience, and I have thoroughly enjoyed collaborating with each and every one of them. Lastly, I would like to extend my heartfelt thanks to my family and friends for their unwavering support throughout this journey. Their encouragement and belief in me have been a constant source of motivation, and I am grateful beyond words for their presence in my life.

TABLE OF CONTENTS

Page

LIST OF TABLES

Page

LIST OF FIGURES

Page

CHAPTER 1

INTRODUCTION

Climate-smart agricultural practices are crucial for enhancing the sustainability of agricultural systems. Intensive agricultural practices, such as the use of high-yielding crop varieties, fertilization, irrigation, manuring, and pesticides, have significant local, regional, and global environmental consequences, altering biotic interactions and resource availability in ecosystems (Matson et al., 1997). Long-term studies on organic matter loss have shown a decline in soil organic carbon (SOC) in recently converted agricultural soils (Paul et al., 1996; Wittwer et al., 2021). Fertilized agriculture is a significant source of greenhouse gases, including carbon dioxide (CO_2), nitrous oxide (N_2O), and methane (CH_4), which play a critical role in regulating tropospheric ozone (Agathokleous et al., 2020; Matson et al., 1997). However, these consequences are intricately linked to the interaction between agricultural systems and soil ecological factors (Matson et al., 1997). Therefore, it is essential to understand the impact of intensive agriculture on the soil ecosystem and develop strategies that leverage this interaction to mitigate the adverse effects of management practices and ensure agricultural sustainability.

Soil management practices influence the interactions between the physical, chemical, and biological components of soils. Agricultural practices that involve heavy machinery can impact soil structure by increasing bulk density, causing soil compaction, and reducing aggregate size and stability (Pulido Moncada et al., 2017). Li et al. (2021) demonstrated the long-term effects of cultivation practices on soil physical and hydraulic properties within the 0-100 cm soil profile. Changes in soil structure can affect air-filled porosity, pore architecture, and indices of pore

continuity (such as oxygen diffusivity and tortuosity), which in turn influence soil nutrient dynamics and microbial communities (Ball, 2013; Henault et al., 2012; Sergey & Pete, 2012; Smith, 2017). For instance, water-saturated pores can limit microbial respiration, affecting the exchange of essential plant nutrients between the soil ecosystem and the atmosphere (Keiluweit et al., 2018; Rohe et al., 2021). Conversely, higher pore connectivity and lower pore tortuosity can enhance the oxidation of soil nutrients and microbial activity by improving oxygen transport within soil pores. Understanding this intricate relationship between soil components is crucial for addressing the impacts of intensive agricultural practices.

Soil anoxia is a complex soil condition resulting from the interplay of physical, chemical, and biological phenomena (Haghighi et al., 2010; Selassie et al., 2015; Wei et al., 2006). Anoxic pores are defined as pores devoid of or with limited oxygen concentration, and they form due to high microbial respiration or complete saturation, affecting the redox properties of soil nutrients such as carbon (C), nitrogen (N), iron, and aluminum (Keiluweit et al., 2018; Rohe et al., 2021). Soil organic carbon stocks and applied nitrogenous fertilizers are particularly vulnerable to soil anoxia, as it impacts carbon mineralization and denitrification in the soil (Keiluweit et al., 2017; Ortega-Ramírez et al., 2023). The release of carbon (as CO_2) and nitrogen (as N_2O) significantly affect soil fertility, crop productivity, weather patterns, and the climate. Therefore, understanding the drivers and spatial distribution of anoxic pores is crucial for optimizing fertilizer application and enhancing carbon retention in the soil.

Several factors influence the occurrence and persistence of soil anoxia, including oxygen diffusivity, soil moisture, organic carbon, and microbial hotspots (Lacroix et al., 2021; Schlüter et al., 2019). While the occurrence of anoxia is dependent on microbial respiration or saturation, the maintenance of this condition is attributed to physical properties, particularly soil structure.

Structural characteristics impact the critical drivers of anoxia and determine their overall realization. The architecture, connectivity, and tortuosity of pores affect the transport of molecular oxygen, which is crucial for the microbial degradation of soil organic matter (SOM) (Rohe et al., 2021). When soil moisture exceeds a certain threshold, it can degrade structural attributes, impeding oxygen diffusion in microbial hotspots. Additionally, the soil microbiome is intricately linked to soil structure and can create and sustain anoxic conditions, especially when organic carbon is not limited. Therefore, incorporating soil structural descriptors could provide a better estimation of anoxic soil volume at various scales.

Soil hydraulic properties are influenced by changes in soil physical properties and can serve as descriptors of structural quality (Cook et al., 1992; Horel et al., 2015; Jirků et al., 2013; Kutílek, 2004; Li et al., 2021; Minasny & McBratney, 2007). Hydraulic properties, such as moisture retention and hydraulic conductivity, explain the water-holding and conducting capacity of soils. Kutílek (2004) demonstrated changes in parameters (α and β) of the hydraulic conductivity function due to the destruction of soil structure. Jirků et al. (2013) revealed a positive correlation between the slope of the retention curve at the inflection point and aggregate stability. Many studies have predicted soil water retention properties from the pore-size distribution, which is influenced by soil structure (Beckett & Augarde, 2013; Chang et al., 2019; Minasny & McBratney, 2007). Zeleke and Si (2005) showed spatial dependence between hydraulic properties and soil physical properties. Zhang et al. (2022) used fitted single and dual porosity hydraulic parameters to explain the pore-size distribution and the arrangement of macro- and micropores in soil structures. Therefore, studying the relationship between soil hydraulic parameters and the drivers of soil anoxia could help improve the estimation of anoxic soil volume at different scales.

Multiple models have been used to simulate soil anoxia, each with certain limitations. For instance, the classic 'aggregate model,' which estimates anoxic pore volume based on the balance between oxygen diffusion (supply) into an aggregate and microbial oxygen consumption (demand), has failed to consider the heterogeneity of soil structural units and microbial activity across aggregates (Keiluweit et al., 2018). Furthermore, the prediction of anoxic microsites using this model is limited to mm- or cm-sized aggregates. Keiluweit et al. (2018) quantified the extent of anoxic microsites in soils at the sub-mm scale, even at moderate moisture levels, which accounted for 14-85% of the total pore volume. They used a planar optode imaging system to monitor oxygen dynamics during the incubation of various soils with natural and artificial gradients in texture and organic matter availability. However, this method is not applicable for estimating field-scale soil anoxic volume, which is essential for optimizing fertilizer use and modeling terrestrial soil carbon and nitrogen dynamics.

Most soil carbon models designed to simulate mineralization have failed to consider the potential effect of anoxic volume. Traditional soil carbon models, such as DayCent and RothC, have overlooked the importance of anoxic volume in mineralizing soil residues. In well-aerated soils, mineralization is considered to be an entirely aerobic process (Gottschalk et al., 2012). Mechanistic models developed to precisely predict mineralization rates have incorporated oxygen availability as a factor regulating this process rather than specifically isolating its effect. Some mechanistic models have directly coupled mineralization rates to bulk oxygen concentrations (Davidson et al., 2012). They assumed upland soils to be fully oxygenated, excluding oxygen from their computation, and disregarded the possible effects of anoxic spaces in structurally heterogeneous soils. However, the performance of these carbon models could be enhanced by

incorporating soil physical properties and hydraulic parameters that influence the drivers of soil anoxia or are directly related to it.

This project aims to characterize and quantify the control exerted by the soil's physical structure and wetting dynamics on oxygen diffusivity and estimate the spatio-temporal distribution of potential anoxic volume at the field scale. The second chapter of the thesis discusses fitting retention models to the soil moisture release curve and characterizing the estimates of oxygen diffusivity at different moisture contents based on fitted soil hydraulic parameters. To enhance the transferability of oxygen diffusivity, the lab-estimated oxygen diffusivity at different soil moisture levels was compared with in situ field conditions. An oxygen transport model was also applied to understand the effect of soil structure on oxygen concentration in the soil profile. The third chapter aims to quantify the spatio-temporal distribution of potential anoxic volume at the field scale. A relationship between soil moisture and pore diameter was derived using the soil moisture release curve developed in Chapter 2. The soil pore size thresholds determined by Lacroix et al. (2021) were estimated from the relationship between soil moisture and pore diameter and were used to approximate the field-scale distribution of potential anoxic volume at 24 and 48 hours after rainfall. This work provides valuable information about the effect of soil structure on oxygen diffusivity at different soil moisture levels and allows for the estimation of potential soil anoxia based on soil moisture in distinct pores that are more likely to become anoxic at the field scale. These findings have implications for fertilizer optimization and estimating N_2O emissions from agricultural fields.

REFERENCES

Agathokleous, E., Feng, Z., Oksanen, E., Sicard, P., Wang, Q., Saitanis, C. J., Araminiene, V., Blande, J. D., Hayes, F., Calatayud, V., Domingos, M., Veresoglou, S. D., Peñuelas, J., Wardle, D. A., De Marco, A., Li, Z., Harmens, H., Yuan, X., Vitale, M., & Paoletti, E. (2020). Ozone affects plant, insect, and soil microbial communities: A threat to terrestrial ecosystems and biodiversity. *Science Advances*, *6*(33), eabc1176. https://doi.org/doi:10.1126/sciadv.abc1176

Ball, B. (2013). Soil structure and greenhouse gas emissions: a synthesis of 20 years of experimentation. *European Journal of Soil Science*, *64*(3), 357-373.

Beckett, C. T. S., & Augarde, C. E. (2013). Prediction of soil water retention properties using pore-size distribution and porosity. *Canadian Geotechnical Journal*, *50*(4), 435-450. https://doi.org/10.1139/cgj-2012-0320

Chang, C.-c., Cheng, D.-h., & Qiao, X.-y. (2019). Improving estimation of pore size distribution to predict the soil water retention curve from its particle size distribution. *Geoderma*, *340*, 206-212. https://doi.org/https://doi.org/10.1016/j.geoderma.2019.01.011

Cook, G. D., So, H. B., & Dalal, R. C. (1992). Structural degradation of two Vertisols under continuous cultivation. *Soil and Tillage Research*, *24*(1), 47-64. https://doi.org/https://doi.org/10.1016/0167-1987(92)90071-I

Davidson, E. A., Samanta, S., Caramori, S. S., & Savage, K. (2012). The Dual Arrhenius and Michaelis–Menten kinetics model for decomposition of soil organic matter at hourly to seasonal time scales. *Global change biology*, *18*(1), 371-384.

Gottschalk, P., Smith, J. U., Wattenbach, M., Bellarby, J., Stehfest, E., Arnell, N., Osborn, T., Jones, C., & Smith, P. (2012). How will organic carbon stocks in mineral soils evolve under future climate? Global projections using RothC for a range of climate change scenarios. *Biogeosciences*, *9*(8), 3151-3171.

Haghighi, F., Gorji, M., & Shorafa, M. (2010). A study of the effects of land use changes on soil physical properties and organic matter. *Land Degradation & Development*, *21*(5), 496-502.

HÉNault, C., Grossel, A., Mary, B., Roussel, M., & LÉOnard, J. (2012). Nitrous Oxide Emission by Agricultural Soils: A Review of Spatial and Temporal Variability for Mitigation. *Pedosphere*, *22*(4), 426-433. https://doi.org/https://doi.org/10.1016/S1002-0160(12)60029-0

Horel, Á., Tóth, E., Gelybó, G., Kása, I., Bakacsi, Z., & Farkas, C. (2015). Effects of Land Use and Management on SoilHydraulic Properties. *Open Geosciences*, *7*(1). https://doi.org/doi:10.1515/geo-2015-0053

Jirků, V., Kodešová, R., Nikodem, A., Mühlhanselová, M., & Žigová, A. (2013). Temporal variability of structure and hydraulic properties of topsoil of three soil types. *Geoderma*, *204-205*, 43-58. https://doi.org/https://doi.org/10.1016/j.geoderma.2013.03.024

Keiluweit, M., Gee, K., Denney, A., & Fendorf, S. (2018). Anoxic microsites in upland soils dominantly controlled by clay content. *Soil Biology and Biochemistry*, *118*, 42-50.

Keiluweit, M., Wanzek, T., Kleber, M., Nico, P., & Fendorf, S. (2017). Anaerobic microsites have an unaccounted role in soil carbon stabilization. *Nature Communications*, *8*(1), 1771.

Kutílek, M. (2004). Soil hydraulic properties as related to soil structure. *Soil and Tillage Research*, *79*(2), 175-184. https://doi.org/https://doi.org/10.1016/j.still.2004.07.006

Lacroix, E. M., Rossi, R. J., Bossio, D., & Fendorf, S. (2021). Effects of moisture and physical disturbance on pore-scale oxygen content and anaerobic metabolisms in upland soils. *Science of The Total Environment*, *780*, 146572. https://doi.org/https://doi.org/10.1016/j.scitotenv.2021.146572

Li, H., Yao, Y., Zhang, X., Zhu, H., & Wei, X. (2021). Changes in soil physical and hydraulic properties following the conversion of forest to cropland in the black soil region of Northeast China. *CATENA*, *198*, 104986. https://doi.org/https://doi.org/10.1016/j.catena.2020.104986

Matson, P. A., Parton, W. J., Power, A. G., & Swift, M. J. (1997). Agricultural Intensification and Ecosystem Properties. *Science*, *277*(5325), 504-509. https://doi.org/doi:10.1126/science.277.5325.504

Minasny, B., & McBratney, A. B. (2007). Estimating the Water Retention Shape Parameter from Sand and Clay Content. *Soil Science Society of America Journal*, *71*(4), 1105-1110. https://doi.org/https://doi.org/10.2136/sssaj2006.0298N

Ortega-Ramírez, P., Pot, V., Laville, P., Schlüter, S., Amor-Quiroz, D. A., Hadjar, D., Mazurier, A., Lacoste, M., Caurel, C., Pouteau, V., Chenu, C., Basile-Doelsch, I., Henault, C., & Garnier, P. (2023). Pore distances of particulate organic matter predict N_2O emissions from intact soil at moist conditions. *Geoderma*, *429*, 116224. https://doi.org/https://doi.org/10.1016/j.geoderma.2022.116224

Paul, E. A., Paustian, K. H., Elliott, E., & Cole, C. V. (1996). *Soil Organic Matter in Temperate AgroecosystemsLong Term Experiments in North America*. CRC Press.

Pulido Moncada, M., Helwig Penning, L., Timm, L. C., Gabriels, D., & Cornelis, W. M. (2017). Visual examination of changes in soil structural quality due to land use. *Soil and Tillage Research*, *173*, 83-91. https://doi.org/https://doi.org/10.1016/j.still.2016.08.011

Rohe, L., Apelt, B., Vogel, H.-J., Well, R., Wu, G.-M., & Schlüter, S. (2021). Denitrification in soil as a function of oxygen availability at the microscale. *Biogeosciences*, *18*(3), 1185-1201.

Schlüter, S., Zawallich, J., Vogel, H.-J., & Dörsch, P. (2019). Physical constraints for respiration in microbial hotspots in soil and their importance for denitrification. *Biogeosciences*, *16*(18), 3665-3678.

Selassie, Y. G., Anemut, F., & Addisu, S. (2015). The effects of land use types, management practices and slope classes on selected soil physico-chemical properties in Zikre watershed, North-Western Ethiopia. *Environmental Systems Research*, *4*(1), 1-7.

Sergey, B., & Pete, S. (2012). Soil physics meets soil biology: Towards better mechanistic prediction of greenhouse gas emissions from soil. *Soil Biology & Biochemistry*. https://doi.org/10.1016/J.SOILBIO.2011.12.015

Smith, K. (2017). Changing views of nitrous oxide emissions from agricultural soil: key controlling processes and assessment at different spatial scales. *European Journal of Soil Science*, *68*(2), 137-155.

Wei, C., Gao, M., Shao, J., Xie, D., & Pan, G. (2006). Soil aggregate and its response to land management practices. *China Particuology*, *4*(05), 211-219.

Wittwer, R. A., Bender, S. F., Hartman, K., Hydbom, S., Lima, R. A. A., Loaiza, V., Nemecek, T., Oehl, F., Olsson, P. A., Petchey, O., Prechsl, U. E., Schlaeppi, K., Scholten, T., Seitz, S., Six, J., & van der Heijden, M. G. A. (2021). Organic and conservation agriculture

promote ecosystem multifunctionality. *Science Advances*, *7*(34), eabg6995. https://doi.org/doi:10.1126/sciadv.abg6995

Zeleke, T. B., & Si, B. C. (2005). Scaling relationships between saturated hydraulic conductivity and soil physical properties. *Soil Science Society of America Journal*, *69*(6), 1691-1702.

Zhang, Y., Weihermüller, L., Toth, B., Noman, M., & Vereecken, H. (2022). Analyzing dual porosity in soil hydraulic properties using soil databases for pedotransfer function development. *Vadose Zone Journal*, *21*(5), e20227.

CHAPTER 2

ASSESSING THE IMPACT OF WATER RETENTION PARAMETERS ON OXYGEN DIFFUSIVITY IN AGRICULTURAL SOILS[1]

[1] Yadav, H and Gaur, N. To be Submitted to [Water Resources Research]

ABSTRACT

Soil physical and hydraulic attributes are highly variable in agricultural soils and can significantly influence oxygen diffusion and concentration in soil pores. Although there are models that estimate oxygen diffusion in soils, the effect of soil structure together with resulting moisture dynamics on oxygen diffusion is yet unaccounted. Since oxygen transport is linked to biogeochemical processes, addressing the heterogeneity of soil hydro-physical properties on oxygen diffusion can substantially improve biogeochemical models. In this work, we propose a method to characterize moisture-dependent oxygen diffusivity in structured field soils using soil hydraulic parameters to quantify the impact of soil structure and wetting dynamics on oxygen diffusivity. We estimated soil hydraulic parameters by fitting retention models to soil moisture release curves and linked them with oxygen diffusivity estimates. We used a widely known partitioning algorithm, known as k-medoid, to characterize oxygen diffusivity at different moisture values based on water retention parameters for a near-surface soil. The different moisture contents considered were residual moisture, threshold moisture (≤ 1 micron filled with water), moisture at field capacity, and saturation. Oxygen concentration in the soil profile at 5 cm depth was quantified using a steady-state oxygen transport model. Results showed five statistically significant clusters based on soil hydraulic parameters: n_1 and n_2, which are related to the pore size distribution of soils. The clusters differed for oxygen diffusivity at residual and threshold moisture values. The oxygen concentrations measured in pores at 5 cm depth differed among clusters for residual soil moisture but were similar for diffusivity at threshold moisture. The uncertainties associated with lab-estimated oxygen diffusivity for undisturbed soils were addressed by comparing them with in situ field measurements. The oxygen diffusivity at residual and threshold moisture values were similar, while oxygen diffusivity at field capacity and saturation differed between lab and in situ

field conditions. It is concluded that the influence of soil moisture on oxygen diffusivity is moisture specific, affecting at residual and threshold moisture values, and the diffusivity of oxygen in soils can be compared based on fitted hydraulic parameters: n_1 and n_2. This relationship can be leveraged to develop diffusion models that accurately predict oxygen diffusion in natural soils and improve biogeochemical models.

1 INTRODUCTION

Agricultural practices profoundly influence the diffusion of gases in the soil atmosphere, impacting soil quality, agricultural sustainability, and environmental well-being (Kibret et al., 2023; Lai et al., 1976; Neira et al., 2015; Sergey & Pete, 2012). Increasing agricultural needs drive growers to opt for intensive land use and management practices, such as monoculture, tillage, weed controls, and fertilization, that have detrimental impacts on our ecosystem (Gregory et al., 2002; Noelia & Eguren, 2022; Peng et al., 2022). These practices affect the spatial heterogeneity of soil texture and structure, influencing soil physical and hydrologic attributes such as total porosity, air-filled porosity, water retention, tortuosity, and connectivity of the pore system (Horel et al., 2015; Neira et al., 2015). The modification of these physical properties impacts gaseous diffusion, which, in turn, affects the redox properties of essential nutrients and microbial distribution in the soil (Ball, 2013; Smith, 2017). The cumulative effect of these modifications can change an ecosystem's greenhouse gas (GHG) emission dynamics. Therefore, an in-depth study of the effect of soil's hydro-physical properties on gas diffusion is necessary for the efficient and sustainable use of resources, such as soil and water, and for shaping future decision-making in agricultural and environmental sectors (Horel et al., 2015).

The applied management practices, for instance, tillage, can alter essential soil properties such as structures, pore size distribution, microbial diversity, and their habitats which influences soil hydraulic conductivity K(h), water-conductivity porosity, and shape fitting parameters (α and n) of van Genuchten-Mualem model (Ball, 2013; Horel et al., 2015; Schwen et al., 2011; West et al., 2023). Cook et al. (1992) pointed out that soil tillage can reduce aggregate stability (both dry and wet) by decreasing organic carbon contents and affect water infiltration by sealing aggregate surfaces with clay particles. Additionally, these alterations in soil properties manifest differently

for each suite of management practices, increasing the demand for robust research (Cook et al., 1992; Horel et al., 2015; Jirků et al., 2013; Li et al., 2021; Stolze et al., 2022). However, estimating soil physical and hydraulic parameters can help to address the changes in soil properties due to management practices in diffusion models and improve their prediction.

Soil physical and hydraulic parameters manifest the changes in physico-chemical and biological properties of soil due to management practices (Ball, 2013; Smith, 2017). They are unique to a specific soil structure and texture and could vary based on anthropogenic and climatic factors. The soil structure has substantial control over water retention capacity and pore continuity indices (relative diffusivity, air permeability, and air-filled porosity), influencing soil microbial density and efflux of GHGs (Ball, 2013). Castellano et al. (2010) demonstrated the relevance of air-filled porosity on gaseous efflux by detecting a consistent relationship between N_2O emission and matric potential. Matric potential largely determines unsaturated water flow in a soil system and is attributed to the force of capillary attraction between soil particles and water molecules in soils (Mullins et al., 2000). In addition, the significance of structural attributes such as intra-aggregate pores on the size of anoxic zones and the inter-aggregate macropores on the exchange of O_2 at the boundaries of the aggregates and GHGs with the atmosphere has been mentioned in the synthesis work of Ball (2013). Likewise, soil texture influences the distribution of microbial hotspots inside the soil (Ball, 2013; Schlüter et al., 2019). These microbial habitats are vulnerable to changes in pore spaces due to disturbances and control diffusion of gases in soil aggregates—depending on soil water content and pore continuity. Therefore, the diffusion potential of gases in the soil is related to its structural attributes, which are associated with soil physical and hydraulic parameters.

Knowledge of gaseous diffusion in agricultural soils is essential not only to understand the aeration potential of differently managed soils but also to simulate the soil habitat that could eventually be used for modeling biogeochemical cycles. Gas concentration, mainly oxygen (O_2), is considered vital in the soil as it changes the redox potential of nutrients and microbial activity, which are related to GHG emissions (Turkeltaub et al., 2023). The commonly used parameter for explaining gaseous diffusion, including O_2, in the soil is the gas diffusion coefficient (D_p), which depends upon the texture, structures, pore-size distribution, and architecture of the soil pores (Neira et al., 2015). The gas diffusion coefficient determines the aeration potential of soil and is the ratio of gas flux per unit concentration gradient of gas. It also helps to realize the metabolizing properties of soil microorganisms by emulating soil habitat, which directly impacts soil structures, pore-size distribution, organic carbon decomposition, and the redox potential of nutrients (Neira et al., 2015; Ye et al., 2022). Therefore, the influence of changes in soil physical and hydraulic properties on the gas diffusion coefficient (D_p) is crucial to understand for guiding farmers toward climate-smart farming and predicting the extent of GHG emissions from land management practices.

Several models have been developed to simulate gaseous diffusion, mainly oxygen, for the sustainable management of soils. It is generally challenging to compute oxygen diffusion with data-driven models due to the highly heterogeneous nature of the soil system in terms of physico-chemical and biological properties. These models often fail to consider essential soil attributes, like aggregation and structures and the fraction of macropores, that restrict their coupling with biogeochemical models (Sergey & Pete, 2012). However, since the majority of oxygen transport occurs through diffusion, a simple Fick's first law is generally used to explain the movement of O_2

molecules under steady-state conditions, which is stated as (Neira et al., 2015; Sergey & Pete, 2012):

$$q_x = -D_p \left(\frac{\delta C}{\delta x}\right)$$

Where q_x is the diffusive flux of O_2 (mass per unit area per unit time) in x directions in soil (g m^{-2} s^{-1}), D_p is the effective diffusion coefficient (m^2 s^{-1}), C is the O_2 concentration (g m^{-3}), and x is the distance along the line of the flow (m). The effective diffusion coefficient (D_p) is an essential parameter for estimating oxygen diffusion, which is generally measured as relative diffusivity (D_p/D_o), where D_o refers to diffusion in a gaseous medium.

Numerous models have been developed to predict *Dp* with certain limitations. For instance, Sergey and Pete (2012) have categorized these D_p models into mainly three categories based on the level of complexity. The first group of models (Campbell, 1985; Millington, 1959; Moldrup et al., 2004; Troeh et al., 1982) link D_p with air-filled porosity, while the second group of D_p models (Millington & Quirk, 1960; Millington & Quirk, 1961) depends on air-filled porosity and total soil porosity. The usability of these models is limited because they need parameterization for a particular soil texture type. Also, the linkage between parameters used in the model is still to be validated for various soils. The third group of models incorporates Campbell water retention parameter *b* (Campbell, 1974) and air-filled porosity at a fixed value of soil water potential in addition to air-filled porosity and the total porosity (Moldrup et al., 1996; Moldrup et al., 2000). The model proposed by Moldrup et al. (1996) is vital for estimating the D_p of undisturbed soil cores and modeling GHG emissions from soils. Although this model has tried to address soil heterogeneity by incorporating the water retention parameter *b*, an in-depth investigation of the effects of these parameters on oxygen diffusivity is missing in the literature.

The objective of this research is to characterize and quantify the control exerted by the soil's physical structure and wetting dynamics on oxygen diffusivity. The approach consisted examining the relationship between soil hydraulic parameters—linked to soil moisture release curve—and oxygen diffusivity at different moisture conditions for soils with variable soil physical properties. The moisture states considered were residual, threshold, field capacity, and saturation. While residual moisture is mostly a fitting parameter in the water retention curve, it can signify the absence of capillary water in a soil system, while threshold moisture represents water content needed to saturate pores equal to or less than 1 micron. Threshold moisture has significance in determining soil anoxia as shown by Lacroix et al. (2021). Field capacity refers to the optimal water content at -0.1 bar, and saturation describes the complete filling of capillary pores with water. To achieve our objective, we developed high-resolution, complete soil moisture release curves using undisturbed soil cores and tested the fit of two retention models: van Genuchten and Dual porosity models, to describe the release curves and estimate water retention parameters. These models have been widely applied to simulate the relationship between soil moisture and matric potential (Li et al., 2021; Schwen et al., 2011; Zhang et al., 2022). Based on the water retention parameters, soil cores were clustered, and O_2 diffusivity at residual, threshold, field capacity, and saturation were compared between clusters to study the effect of hydro-physical attributes of soils on oxygen diffusivity. Using field-based water retention parameters, the oxygen diffusivity estimates at different moisture values were quantified for the field and compared with lab-based O_2 diffusivity estimates to enhance the applicability of this work. Furthermore, the oxygen concentration approximated using a steady-state oxygen transport model was compared between the lab and the field conditions.

2 MATERIALS AND METHODS

2.1 SITE DESCRIPTION

The study was conducted at the University of Georgia's Iron Horse Farm (IHF), which lies in the Blue Ridge and Piedmont region in Oconee County, Georgia (GA), USA. Soils in this region are very deep, well-drained, moderately permeable, and eroded, formed on the ridges and the sides of the Piedmont uplands (California Soil Resource Lab and USDA Natural Resources Conservation Service). They are classified within USDA taxonomy as Cecil (Fine, Kaolinitic, thermic Typic Kanhapludults) with sandy loam texture (Soil Survey Staff Natural Resources Conservation Service United States Department of Agriculture, 2017) and have 2 to 10 percent slopes. The average annual temperature in this region is 19.6 ^{o}C, and annual precipitation is 1354.1 mm yr^{-1} (University of GA Environmental Monitoring Network, 1957–2016).

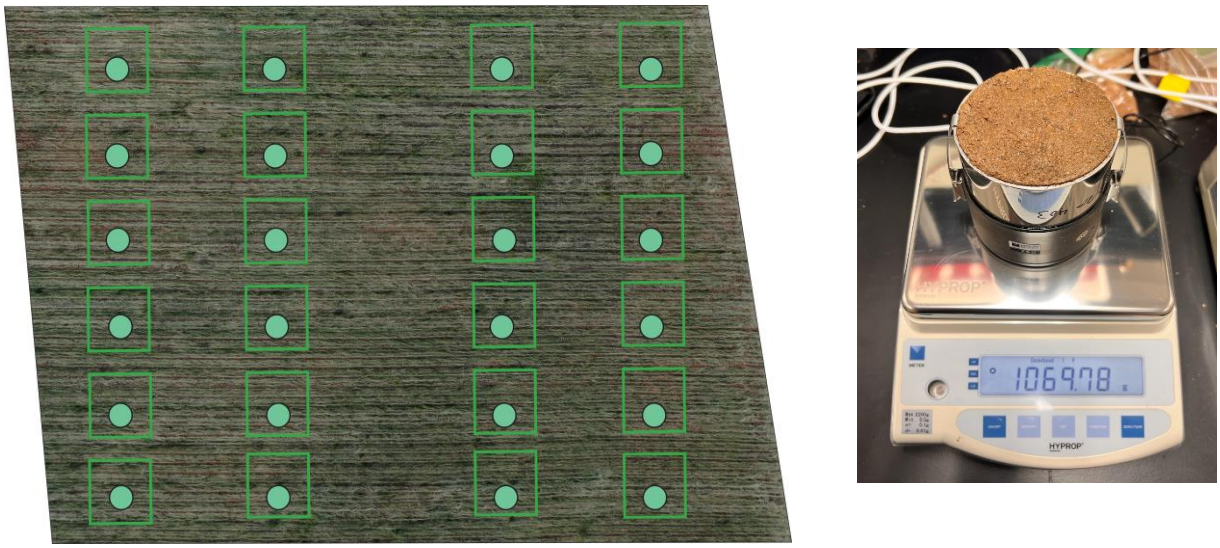

Figure 2.1. Schematic representation of the study area. The rectangular boxes indicate plots, and the green circles represent points from where soil cores were collected —not drawn to scale. The picture on the right shows a soil core mounted on a HYPROP instrument in the lab.

The plantation of crops at IHF began in 2018— which was initially covered with forests. Studies were conducted afterward to seek the best possible combination of herbicides and cover

crops for corn production. In 2022, the field site (0.06 ha) was divided into four blocks, each with 6 experimental plots (0.0021 ha) as displayed in Figure 2.1 (left), and was planted with corn. The treatment combinations include a rye cover crop or no cover crop (both no-till) and a range of herbicide application rates (High, Low, No). These treatment combinations were randomly distributed in experimental plots, with all six combinations in each block. There were 24 experimental plots in total, and fertilizers (NPK) and irrigation amounts were applied in equal amounts in these plots during maize growth.

2.2 SOIL CORE COLLECTION

A total of 24 undisturbed soil cores of 0.08 m diameter and 0.063 m length were collected from the field, one from each experimental plot in August 2022. Stainless steel cores were pushed horizontally into the Ap horizon using a rubber mallet to collect cores from the top horizon of the soil. Soil cores were capped with plastic caps and brought to Environmental Soil Physics lab at University of Georgia. In the lab, soil cores were kept in a refrigerator to avoid moisture loss.

2.3. LAB MEASUREMENTS

2.3.1 THE HYPROP MEASUREMENT

We developed a complete soil moisture release curve to evaluate the relationship between volumetric water content (VWC) and the matric potential (h) for each soil core. The HYPROP evaporation method was used for the wet range (0 to -0.1 MPa) and the WP4C psychrometer method for the dry range (-0.1 to -300 MPa) of a soil moisture release curve (Meter Group, Inc., Pullman, WA, USA).

The HYPROP setup includes matric potential measurements at two depths within a 6.3 cm long saturated soil core using tensiometer shafts (2.5 cm and 5 cm long). Soil cores were prepared by saturating them in a plastic trough from the bottom for 24 hours. After saturation, a small rotary

auger was used to drill circular holes vertically through the core to insert tensiometers. The tensiometers were aligned in the holes such that the middle of the tensiometers cups was located at 1.25 cm and 3.75 cm for the bottom of the core. The upper side of the core was opened to the atmosphere so that soil moisture could evaporate. The difference in the soil mass over time was measured by automated weighing of the core and was used to calculate VWC. The medial matric potential was calculated based on the average value of the two tensions. More information about the standard HYPROP system and the evaporation methodology is provided by Pertassek et al. (2015) and METER (2015). Our experimental protocol limited hydraulic measurements using the HYPROP setup down to a pressure head of about – 100 kPa as the tensiometers experience bubble formation and subsequent expansion beyond this point (Lipovetsky et al., 2020). We used a WP4C dewpoint potentiometer to measure matric potential in the dry range.

2.3.2 WP4C MEASUREMENT

The WP4C psychrometer measurements were conducted for three subsamples prepared from each soil core. Once the soil cores were done with HYPROP measurements, the soil was transferred to Ziploc bags, which were crushed to disintegrate larger soil aggregates. We took three subsamples: one without moisture manipulation and two after moisture manipulation with a dripper to a water content slightly above the initial condition. Meanwhile, the remaining samples were kept aside for estimating particle size and organic carbon. The subsamples were placed in stainless steel cups such that the soil completely covered the bottom of the cup. Each WP4C measurement was preceded by equilibrating the cup and the sample temperature on a cold surface as recommended by METER (Meter Group, Inc., Pullman, WA, USA). Following WP4C measurements, the samples were dried in an oven at 105 ^{o}C to estimate the samples' dry weight as the change in dry weight of soil is minimum beyond this temperature (Gardner, 1965).

2.3.3 PARTICLE SIZE DISTRIBUTION

An LS13 320 Laser diffraction particle size analyzer (LPSA) (Beckman Coulter Inc., Miami, FL) was used to estimate the sand, silt, and clay percentage in each soil core. This instrument measures the diameter of particles between 2000 to 0.04 μm by implementing a polarization intensity differential scattering (PIDS) technique, which improves the measurements in the clay-sized region (Arriaga et al., 2006; Stevenson et al., 2023). For measurement, air-dried soil samples were ground with a wooden rolling pin and sieved through a 2 mm sieve. Before the texture estimation, samples were pretreated with 30% H_2O_2 to remove organic matter. Two subsamples were prepared for each sample in 15 ml centrifuge tubes for the pretreatment. Once the pretreatments were completed, the tubes were centrifuged for 10 min at 4000 rpm in Tachometer. After centrifugation, about 5 ml of $(NaPO_3)_6$ was added to tubes to facilitate dispersion, and the tubes were shaken overnight at 120 oscillations per minute. The prepared samples were transferred to 13 ml test tubes for LPSA operations. Finally, we calculated the % sand, silt, and clay according to the United States Department of Agriculture (USDA) soil texture classification standard.

2.3.4 ORGANIC CARBON ESTIMATION

The loss-on-ignition (LOI) method was used to estimate the LOI carbon percentage in each soil core. The samples were ground with a wooden rolling pin and sieved through a 2 mm sieve. About 1 gm of the sample was then placed in a completely dry crucible and dried in an oven for 24 hours for moisture correction. The treated samples were weighed in a weighing balance for pre-ignition weight and, finally, heated at 550 ^{o}C for 8 hours in a Thermolyne muffle furnace (model F6010, Thermo Fisher Scientific Inc., Asheville, NC, USA). Upon completion, the crucibles were transferred to a desiccator to restrict moisture absorption. After 30 min, the post-ignition weights

were recorded, and the LOI carbon (%) was estimated by taking the difference between pre-and post-ignition weights and dividing the result by the pre-ignition weight. Hendricks et al. (2019) revealed a strong linear relationship (R^2 = 0.90) between SOC concentration and LOI carbon in southern piedmont pastures where SOC was 0.47 times LOI; however, this conversion factor could differ based on crop type and biomass coverage, topography, weather patterns, and management practices (Subedi et al., 2022).

2.4 IN SITU FIELD MEASUREMENTS

Soil moisture (ECH20 10 HS and 5 TE, Decagon Devices, Inc., Pullman, WA, USA) and water potential (TEROS 21, Meter Group, Inc., Pullman, WA, USA) sensors were installed at 10 cm depth in ten plots to measure in situ variation in VWC at different matric potential. Soil moisture sensors measured VWC (factory calibrated accuracy: ± 2% VWC) every minute during the span of maize growth (April to September) while matric potential data (ψ) were recorded [factory calibrated accuracy: ± (10% of reading + 2 kPa)] every 60 min from mid-August to mid-September. The moisture sensors were connected to two different data loggers that were ZL6 (Meter Group, Inc., Pullman, WA, USA) and Em50 data logger (Decagon Devices, Inc., Pullman, WA, USA), based on availability. In situ soil moisture release curves were developed using measured moisture and matric potential data. Retention models were fitted to compute and compare hydraulic parameters of the lab and in situ hydraulic parameters, as described in the following sub-sections.

2.5 ANALYTICAL MODELS

2.5.1 HYDRAULIC RETENTION MODELS

Two retention models, van Genuchten (Van Genuchten, 1980) and Dual porosity (Durner, 1994), were fitted to the data pairs of VWC (θ) versus matric potential (h) to predict the complete

soil moisture release curve, $\theta(h)$ in MATLAB (R2022a, The MathWorks, Inc.). The van Genuchten model (Van Genuchten, 1980) is the most popular model commonly used to explain the single-porosity system, which estimates $\theta(h)$ based on the following general equation,

$$\frac{\theta(h) - \theta_r}{\theta_s - \theta_r} = \frac{1}{[1 + |\alpha h|^n]^m}$$

where $\theta(h)$ is the volumetric water content ($m^3\ m^{-3}$), θ_s and θ_r are the saturated and residual values of the soil water content, α and n are dimensionless curve shape parameters, and m = 1-1/n. However, its applicability is limited to homogeneous soils with unimodal pore-size distribution (Durner, 1994; Fatichi et al., 2020). We fitted the Dual porosity model (Durner, 1992, 1994), constructed by a linear supposition of two van Genuchten models, to account for distinct but interacting structural (inter-aggregate) and micro (intra-aggregate) pores. This model describes the role of soil structure in the hydraulic properties and is generally expressed as follows:

$$\frac{\theta(h) - \theta_r}{\theta_s - \theta_r} = \frac{w_1}{[1 + |\alpha_1 h|^{n_1}]^{m_1}} + \frac{1 - w_1}{[1 + |\alpha_2 h|^{n_2}]^{m_2}}$$

where α_i and n_i (i = 1, 2) are the same as in the van Genuchten model for the structural and micro pore regions, respectively, while w_i (i = 1, 2) are weighing factors for these distinct pore regions.

2.5.2 GAS DIFFUSIVITY MODEL

The relative oxygen diffusion coefficients (D_p/D_o) at different air-filled porosity were estimated using a soil-type dependent model suggested by Moldrup et al. (1996). This model calculates D_p/D_o for undisturbed soils based on the soil moisture release curve with higher accuracy (Sergey & Pete, 2012). The release-curve-dependent gas diffusivity model is stated as follows:

$$\frac{D_P}{D_O} = (2\varepsilon^3{}_{100} + 0.04\varepsilon_{100})(\frac{\varepsilon}{\varepsilon_{100}})^{2+3/b}$$

where *b* is the Campbell (1974) soil water retention parameter (equal to the slope of the SMRC curve in a log-log coordinate system), D_P is the gas diffusivity coefficient in soil (cm^3 soil air cm^{-1} soil h^{-1}), D_O is the gas diffusivity coefficient in the air (cm^2 h^{-1}), ε_{100} is the air-filled porosity at ψ = -100 cm (estimated from SMRC), and ε is the air-filled porosity. The air-filled porosity was plotted against their relative oxygen diffusion coefficient for studying oxygen transport in soil pores at different soil moisture contents. This relationship was used to estimate the relative oxygen diffusion coefficients at residual moisture, threshold moisture, field capacity, and saturation. The O_2 diffusivity at threshold moisture reflects the diffusivity coefficient when pores less than or equal to 1 μm are saturated with water (Lacroix et al., 2021).

2.4.3 OXYGEN TRANSPORT MODEL

The modified steady-state transport model proposed by Kanwar (1986) was used to analyze the movement of oxygen in undisturbed soil cores at different depths, which is expressed as:

$$c(x,t) = c_o - \alpha t + \alpha[\left(t + \frac{x^2}{2D}\right) erfc\left(\frac{x}{2\sqrt{Dt}}\right) - x\left(\frac{t}{\pi D}\right)^2 exp\left(-\frac{x^2}{4Dt}\right)]$$

where *c* is the oxygen concentration in the soil air (cm^3 cm^{-3}) at depth *x* in cm and time *t* in hr, c_o is the oxygen concentration in the atmosphere (cm^3 cm^{-3}), α is the rate of oxygen consumption by biological and chemical processes within the soil mass (cm^3 cm^{-3} hr^{-1}), *D* is the oxygen diffusion coefficient in the soil (cm^2 hr^{-1}), and *erfc* is the complementary error function. This model assumes

that the oxygen concentration remains constant throughout the soil core at the beginning of the measurement and is equal to the atmospheric oxygen concentration [$c\ (x,\ t) = c_o$]. Further, the model assumes that the change in oxygen concentration with depth remains constant and is equal to zero ($\delta c/\ \delta x = 0$ as $x \rightarrow \infty$, $t > 0$). For simplicity, we assumed α to be constant and equal to 0.002125 $cm^3\ cm^{-3}\ hr^{-1}$ for all the simulations because the overall effect of change in α on oxygen transport is almost insignificant for a short period of 24 to 48 hours (Kanwar et al., 1989). The relationship between relative oxygen concentration (c/c_o) and soil depth (x) was plotted for different oxygen diffusion coefficients (estimated using the above-stated diffusivity model) to describe the effects of diffusion coefficients, altered due to management practices, on oxygen concentration in the soil. This relationship was leveraged to estimate relative oxygen concentrations at 5 cm soil depth at 12, 24, 36, and 48 hours after the initial equilibrium condition.

2.6 STATISTICAL ANALYSIS

The hydraulic parameters from the release curves were estimated by fitting retention models using a global optimization algorithm developed in MATLAB (R2022a, The MathWorks, Inc.) We did 2000 iterations per model per sample by fixing the lower and upper bound of the parameters. The lower bounds for the shape parameters (α, n, and m) were set as suggested by van Genuchten (1980) and Durner (1994), while the upper bounds were determined based on literature review and initial model fitting. The hydraulic parameters estimated by van Genuchten for clay loam were used as the initial value of the parameters because most of the samples had clay loam texture. The performance of the retention models was evaluated based on root mean square error (RMSE) and akaike information criterion (AIC). The smaller the values of these parameters, the better the model. The codes for fitting oxygen diffusivity and transport models were also generated in MATLAB.

In order to classify oxygen diffusivity behavior as controlled by soil structural parameters, we did k-medoid clustering for partitioning hydraulic parameters into the possible number of clusters and assessed differences in oxygen diffusivity between clusters. This method minimizes the sum of pairwise dissimilarities between points such that the points in a cluster are highly similar to those in another cluster. To find the optimum number of clusters for the data, we applied the medoid silhouette method, which computes the average silhouette width for the selected number of clusters. Higher silhouette width indicates that the points are well-matched to their cluster and poorly matched to others. In order to check the collinearity between variables, the variance inflation factor (VIF) was estimated, and the threshold value equal to 10 was used for the determination—higher values indicate collinearity. Before comparing the clusters, the distribution of the variables was analyzed, and the non-normally distributed variables were transformed using the box-cox transformation method. Analysis of variance (ANOVA) test was performed to compare clusters for the normally distributed variables, while the Kruskal-Wallis rank sum test was used for non-normally distributed variables. The post hoc tests, such as Tukey's test (for normal data) and Dunn's test (for non-normal data), were applied to find the clusters that differ. The *p* values were corrected for multiple comparisons, and the adjusted p values ≤ 0.05 were considered significant. The figures and graphs for explanations and comparisons were developed in MATLAB and R (R core Team, Version 2023.03.0).

3 RESULTS

3.1 FITTED HYDRAULIC PARAMETERS

The retention models, namely van Genuchten and Dual porosity, were fitted to the soil moisture release curves developed for the 24 soil cores (Appendix A1). An example of a soil moisture release curve is displayed in Figure 2.2 (for sample 5), and fitted values are listed for all samples in Table 2.1. The dual porosity model performed relatively well compared to van Genuchten's model for all the cores, which were compared based on RMSE and AIC values.

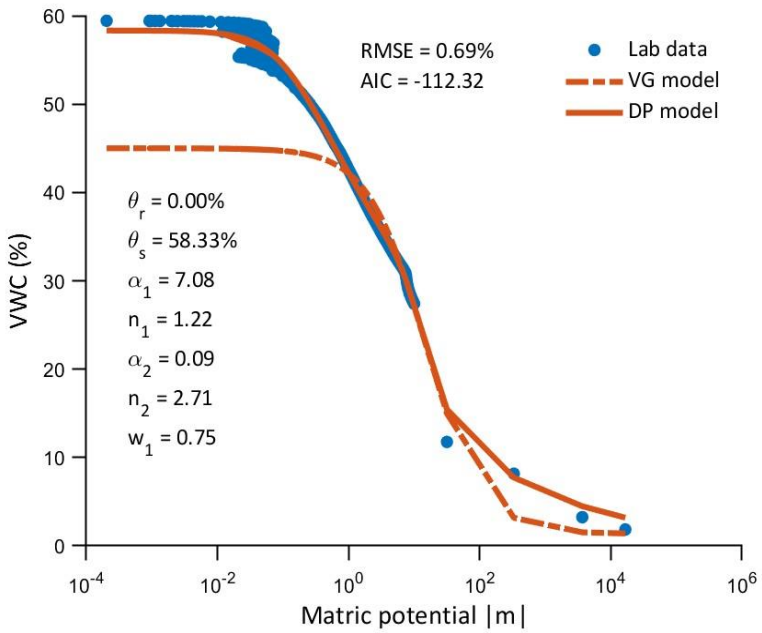

Figure 2.2. Soil moisture release curve developed in the lab for a soil core (Sample 5). The blue dots represent volumetric water content (%) at different matric potentials (m). The solid red line reflects the fitted dual porosity model (Durner, 1994), while the dotted red line is the fitted single porosity model (van Genuchten, 1980). The remaining SMCC curves (N = 23) are shown in Appendix A1.

The van Genuchten model could not simulate soil moisture near saturation (as depicted in Figure 2.2). This indicates that the soil cores had bimodal pore-size distribution consisting of

micropores and macropores enmeshed to form a heterogeneous matrix. Table 2.1 shows the fitted hydraulic parameters to moisture release curves using the dual porosity model.

Table 2.1. Fitted hydraulic parameter values of Dual porosity model for all soil samples (N = 24)

Sample	θ_r (%)	θ_s (%)	α_1 (m^{-1})	n_1	α_2 (m^{-1})	n_2	w_1	RMSE (%)
1	10.00	54.00	2.91	1.29	0.03	5.00	0.85	0.46
2	0.56	59.32	0.31	1.63	10.00	1.12	0.14	0.29
3	0.00	49.85	2.48	1.23	0.05	1.50	0.76	0.42
4	2.92	52.86	0.09	5.00	3.59	1.31	0.31	0.35
5	0.00	58.33	7.08	1.22	0.09	2.71	0.75	0.69
6	3.91	59.31	0.10	5.00	7.26	1.30	0.24	0.25
7	8.22	54.92	8.52	1.83	0.60	1.38	0.45	0.53
8	0.00	53.38	7.24	1.87	0.41	1.35	0.34	0.28
9	7.01	54.28	5.85	1.43	0.12	5.00	0.68	0.62
10	0.00	43.91	0.11	4.58	5.11	1.15	0.29	0.37
11	9.91	50.30	10.00	1.41	0.11	2.97	0.62	0.27
12	10.00	43.98	5.69	1.32	0.12	5.00	0.77	0.22
13	0.00	44.63	2.87	1.21	3.67	5.00	0.81	0.78
14	10.00	45.86	0.14	5.00	7.79	1.46	0.15	0.39
15	0.00	52.36	0.03	5.00	10.00	1.23	0.20	0.29
16	2.85	58.79	0.08	5.00	10.00	1.19	0.35	0.30
17	8.35	45.86	9.97	1.47	0.09	3.03	0.70	0.38
18	10.00	47.21	10.00	1.28	0.13	5.00	0.84	0.42
19	4.88	45.06	1.99	3.62	6.75	1.37	0.13	0.50
20	0.00	44.67	5.33	1.83	0.08	1.62	0.49	0.51
21	0.08	35.80	5.31	1.66	0.23	1.28	0.48	0.46
22	0.00	36.57	3.34	1.24	0.01	4.59	0.75	0.66
23	9.67	43.97	7.42	1.29	0.13	5.00	0.89	0.39
24	2.42	28.15	0.20	2.90	6.23	1.39	0.34	0.31

3.2 CLUSTERING APPROACH

We did k-medoid clustering to characterize soil samples with similar soil structures and identify specific soil hydraulic parameters as represented by their water retention curves that classify the variation in O_2 diffusivity in soils. Clustering was done with the possible combinations of hydraulic parameters, and the estimates of oxygen diffusion coefficient at different moisture contents, such as residual moisture (maximum diffusivity), threshold moisture, field capacity, and saturation (minimum diffusivity), were evaluated among the clusters. The oxygen diffusivities at different soil moisture were computed from a curve demonstrating the variation in relative diffusion coefficient as a function of air-filled porosity developed using a gas diffusivity model formulated by Moldrup et al. (1996) (Figure 2.3). These diffusivity estimates were computed for each soil core to examine their relationship with soil hydraulic parameters.

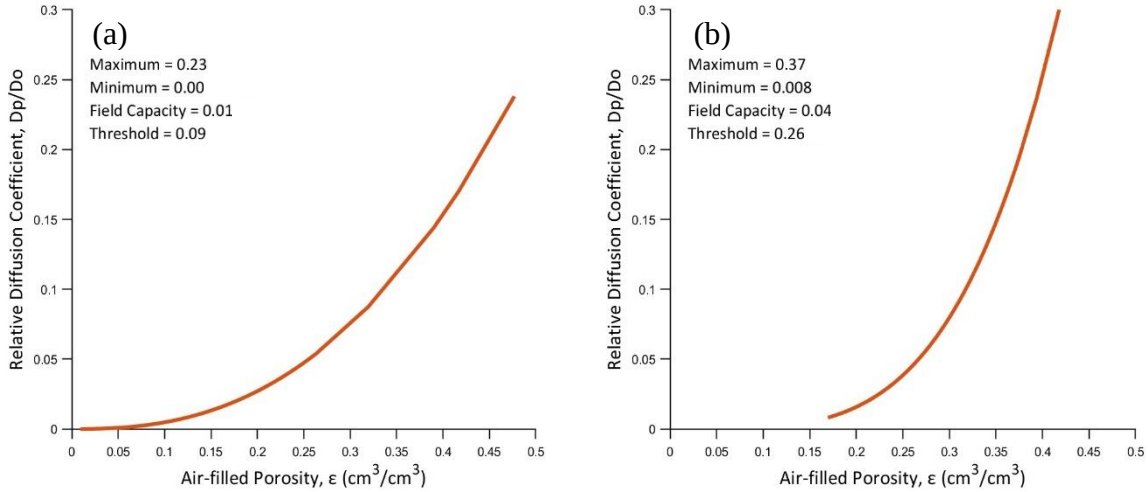

Figure 2.3. Relative oxygen diffusivity as a function of air-filled porosity. Figures (a) and (b) represent the variation in oxygen diffusivity for two different soil cores. The oxygen diffusivities at different soil moistures for a soil core were estimated from the curve, and estimates of 24 soil cores were compiled and presented in the form of box plots.

For most of the combinations, the mean values of oxygen diffusivity at residual moisture, threshold moisture, field capacity, and saturation were similar among clusters ($p > 0.05$). However,

the mean values of O_2 diffusivity at residual and threshold moisture were significantly different ($p < 0.05$) among clusters when partitioned using hydraulic parameters: n_1 and n_2. These hydraulic parameters are related to the slope of the moisture release curves and influence the width of the pore size distribution. Five clusters were formed with different sample sizes (Figure 2.4); cluster 1 had 7 samples, while clusters 2 and 3 had 6 samples each. Also, clusters 4 and 5 had 3 and 2 samples, respectively. The number of clusters was determined based on the average silhouette value, which was higher (0.42) for five clusters. We used clusters formed based on n_1 and n_2 parameters for further analysis to utilize the most parsimonious model.

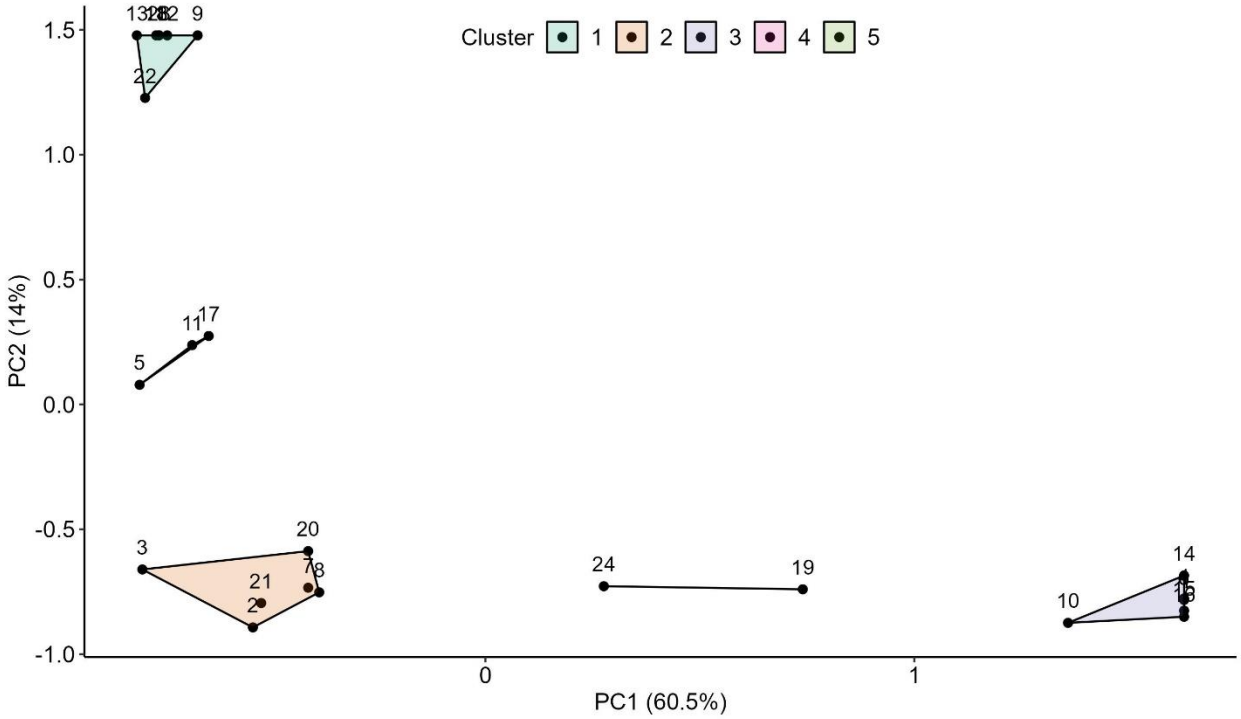

Figure 2.4. K-medoid clustering approach using n_1 and n_2 hydraulic parameters. Different shapes indicate clusters formed by minimizing a sum of pairwise dissimilarities between samples for n_1 and n_2 parameters.

Figure 2.5 shows the distribution of the O_2 diffusivity at residual moisture, threshold moisture, field capacity, and saturation in five clusters. Statistical results showed a significant

difference ($p < 0.05$) in the mean values of O_2 diffusivity at residual and threshold moisture among clusters (Figures 2.5a, 2.5b). We found that cluster 5 had higher mean values of O_2 diffusivity at residual (confidence interval (CI): 0.012 to 0.332) and threshold (CI: 0.011 to 0.232) moisture than cluster 1. In contrast, the mean values of clusters were similar ($p > 0.05$) between cluster pairs for O_2 diffusivity at field capacity and saturation (Figures 2.5c, 2.5d).

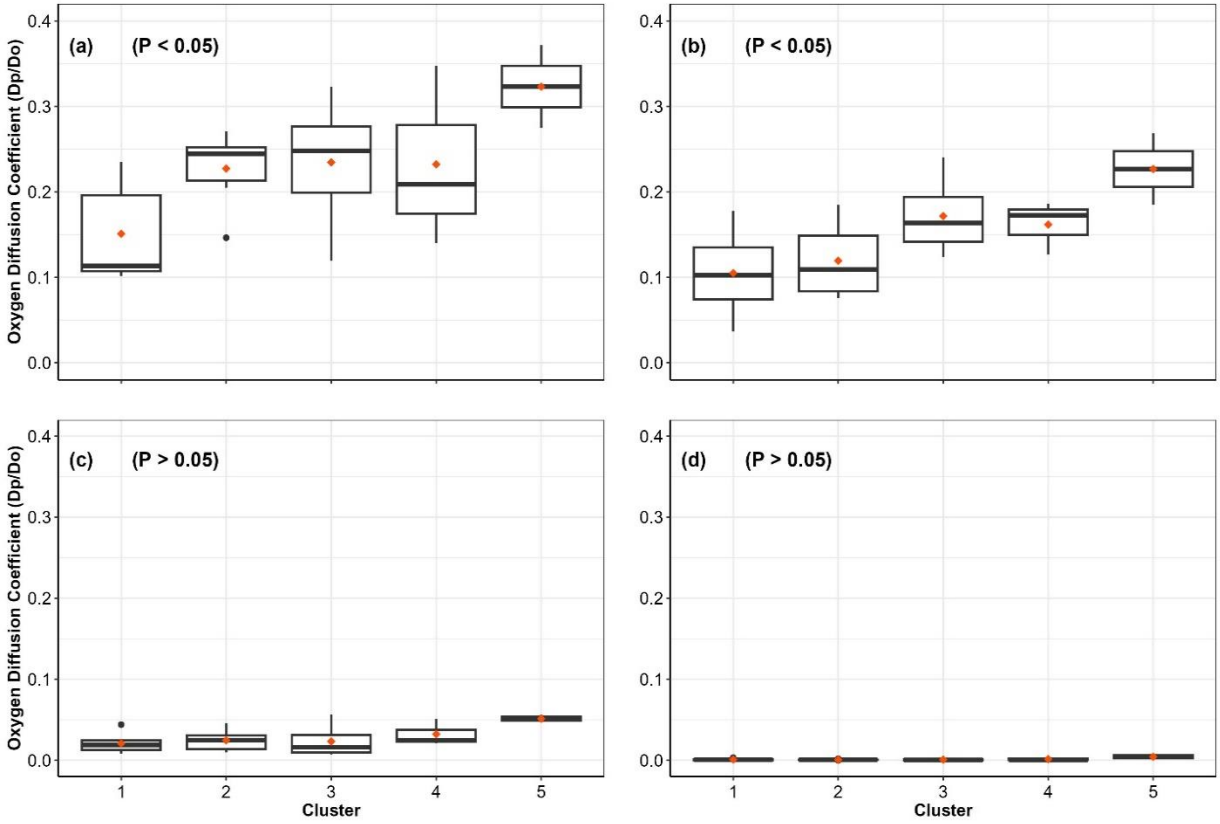

Figure 2.5. Distribution of O_2 diffusivity at (a) residual moisture, (b) threshold moisture, (c) field capacity (FC), and (d) saturation in five clusters. The centerline of the box plots indicates the median, the upper and lower represent the 25th and 75th quantiles, and the red dot reflects a cluster's arithmetic mean O_2 diffusivity/diffusion coefficient. The p value ($p < 0.05$) represents a significant cluster difference. For multiple comparisons, we used adjusted p values.

3.2.1 COMPARISON OF SOIL HYDRAULIC PARAMETERS

The soil hydraulic parameters represent important physical and hydraulic attributes such as pore-size distribution, soil structure, and water retention capacity that regulate the diffusion and transport of oxygen in soils. The differences in hydraulic parameters among clusters can provide substantial information about the soil's hydro-physical properties and the magnitude of O_2 diffusivity and O_2 concentration in soil layers. We evaluated the distribution of hydraulic parameters of clusters and found significant differences ($p < 0.05$) in mean values of shape fitting parameters: n_1, n_2 α_1, α_2, w_1, and w_2 among clusters (Figure 2.6a, 2.6b, and Figure 2.7c-f). However, the mean values of residual water content (θ_r) and saturated water content (θ_s) were similar among clusters (Figure 2.7a, 2.7b).

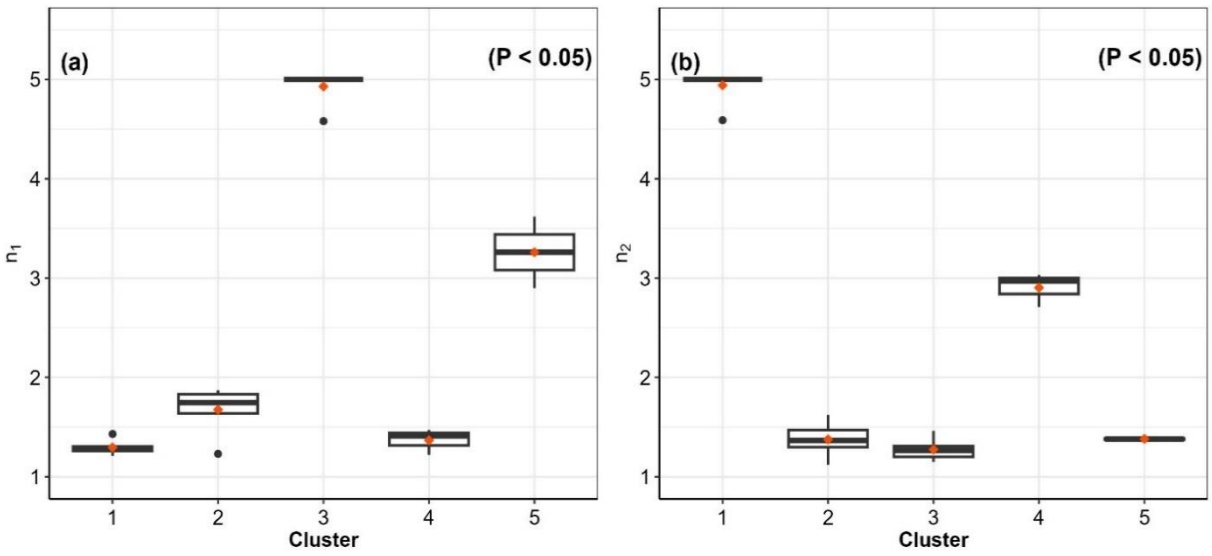

Figure 2.6. Distribution of soil hydraulic parameters n_1 and n_2 in five clusters. The p value < 0.05 indicates a significant difference among clusters. The centerline of the box plots indicates the median, the upper and lower represent the 25^{th} and 75^{th} quantiles, and the red dot reflects the arithmetic mean n_1 and n_2 parameters of a cluster. The related p values were corrected for multiple comparisons according to Benjamini and Hochberg (1995).

The results showed that cluster 1 had lower n_1, α_2, and w_2 mean values and higher n_2, α_1, and w_1 mean values than cluster 3 (Figures 2.6a, 2.6b, and 2.7c-f). Also, cluster 1 had higher mean values of n_2 and w_1 and lower mean w_2 than cluster 2. In addition, the mean of w_1 was higher, but the mean of w_2 was lower in cluster 1 compared to cluster 5 (Figure 2.7e, 2.7f). Moreover, clusters 2 and 4 had a significantly higher mean value of α_1 than cluster 3 (Figure 2.7c). The mean values of n_1 and α_2 were significantly lower in cluster 4 compared to cluster 3 (Figures 2.6a, 2.7d).

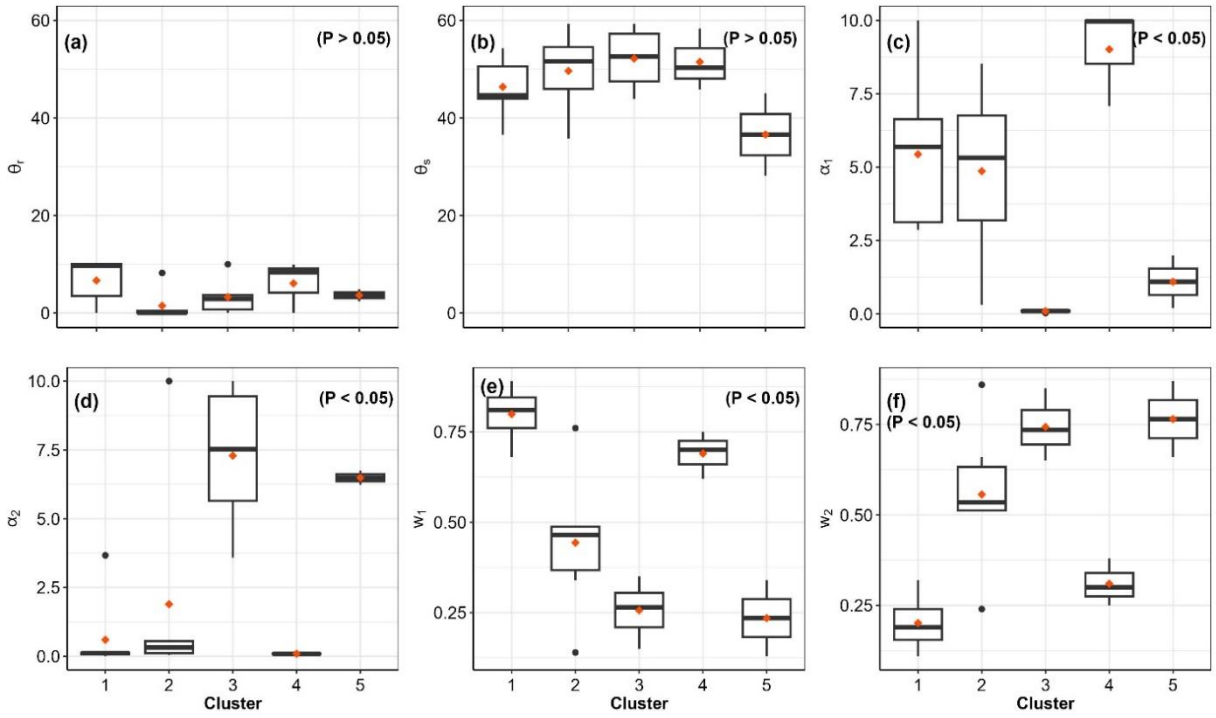

Figure 2.7. Distribution of soil hydraulic parameters such as (a) residual water content θ_r, (b) saturated water content θ_s, and shape fitting parameters [(c) α_1, (d) α_2, (e) w_1, and (f) w_2] in five clusters. The centerline of the box plots indicates the median, the upper and lower represent the 25^{th} and 75^{th} quantiles, and the red dot reflects the arithmetic mean of a parameter for a cluster. The p value ($p < 0.05$) indicates a significant cluster difference. The related p values were corrected for multiple comparisons according to Benjamini and Hochberg (1995).

3.2.2 COMPARISON OF SOIL PHYSICAL ATTRIBUTES

The clusters were evaluated for the differences in porosity, clay, sand, bulk density, and loss-on-ignition (LOI) carbon using the analysis of variance (ANOVA) method. The comparison

revealed no statistically significant differences ($p > 0.05$) among clusters for these soil physical attributes (Figure 2.8). However, the mean values of these attributes were slightly different between clusters despite the statistical similarity. Meanwhile, LOI carbon was positively correlated with sand (0.62) and porosity (0.78) and negatively correlated with bulk density (0.78). We also observed a negative correlation (1.0) between bulk density and porosity. Lastly, we observed a negative correlation between sand and bulk density (0.47) and a positive correlation between sand and porosity (0.47).

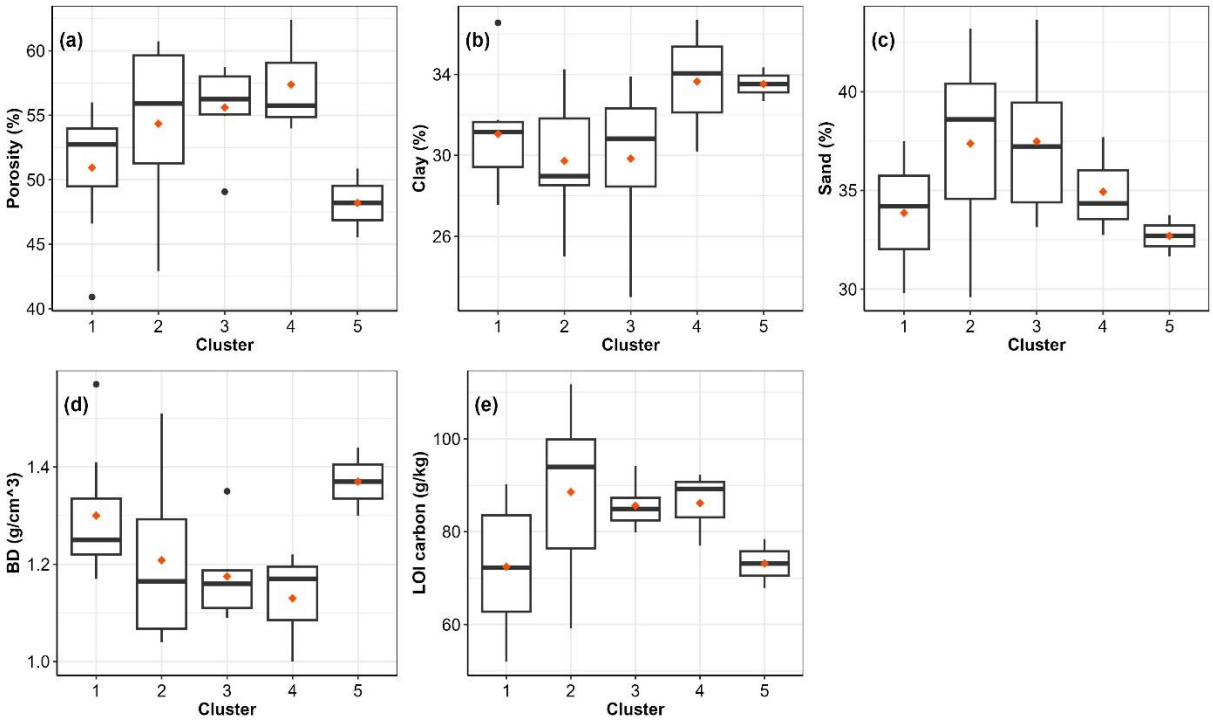

Figure 2.8. Distribution of soil physical features: (a) porosity (%), (b) clay (%), (c) sand (%), (d) bulk density (g/cm^3), and (e) loss-on-ignition (LOI) carbon in five clusters. The centerline of the box plots indicates the median, the upper and lower represent the 25th and 75th quantiles, and the red dot reflects the arithmetic mean of physical features for a cluster. The mean comparison using ANOVA resulted in insignificant differences ($P > 0.05$) among clusters for all these attributes.

3.2.3 COMPARISON OF RELATIVE OXYGEN CONCENTRATION BETWEEN CLUSTERS

We estimated oxygen concentration relative to atmospheric O_2 concentration at 5 cm soil depth for oxygen diffusivity at residual and threshold moisture using the O_2 transport model proposed by Kanwar (1986). The initial concentration of O_2 was assumed to be equal to the atmospheric concentration, and the change in O_2 concentration with depth was assumed to be constant and equal to zero. The O_2 concentrations were computed at 12, 24, 36, and 48 hours after the initial concentration equal to atmospheric (Figure 2.9). The estimated relative oxygen concentrations of 24 soil cores were compiled based on clusters for O_2 diffusivity at residual and threshold moisture and depicted in boxplots (Figure 2.10).

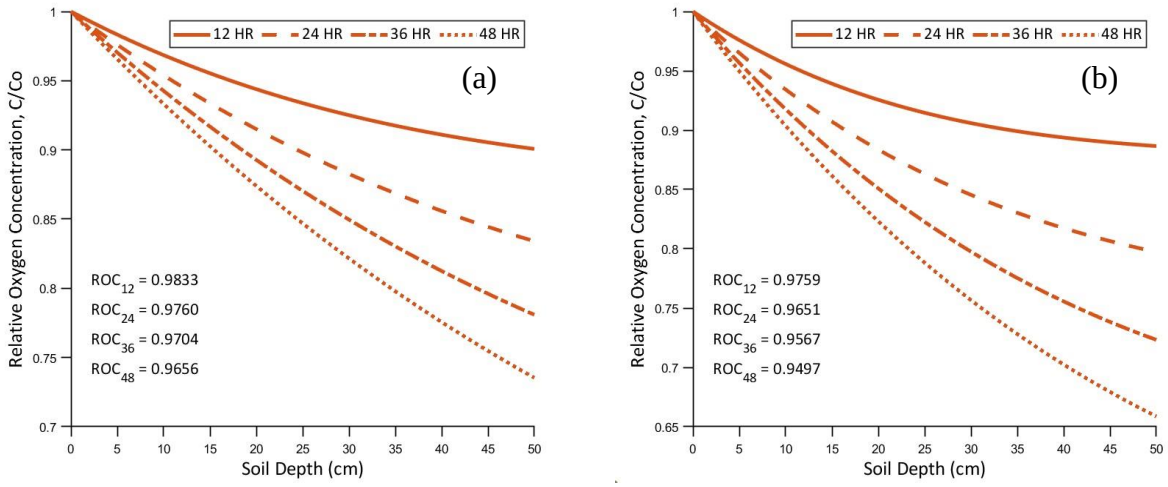

Figure 2.9. Modeled variation in soil oxygen concentration relative to atmospheric with soil depth for oxygen diffusivity at (a) residual moisture and (b) threshold moisture. The line gradient represents the change in oxygen concentrations for a particular time after equilibrium (equal to atmospheric concentration) at different depths. The relative oxygen concentration in the soil profile at 5 cm depth was computed from these curves and used for comparison between clusters.

The results showed significant differences ($P < 0.05$) in the mean values of O_2 concentrations for O_2 diffusivity at residual moisture among clusters for all time points (Figure 2.10a-d). Nonetheless, the mean values of O_2 concentrations for diffusivity at threshold moisture

were similar among clusters ($P > 0.05$) (Appendix A2a-d). Additionally, a post hoc test revealed a higher mean value of relative O_2 concentration estimated for diffusivity at residual moisture in cluster 5 than in cluster 1 at 12 hours after equilibrium (Figure 2.10a). Although the statistical test did not find the differences in O_2 concentration between clusters 1 and 5 at 24, 36, and 48 hours, both clusters followed the same pattern as 12 hours at these time points.

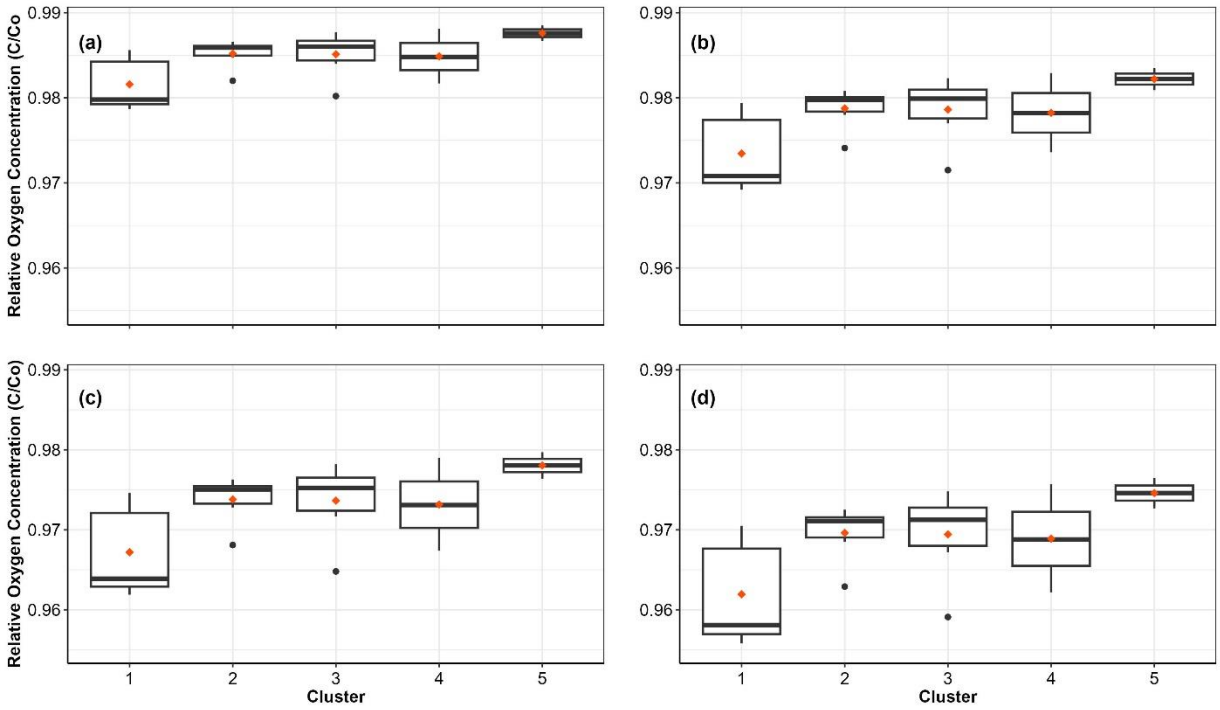

Figure 2.10. Distribution of relative O_2 concentration in clusters estimated for O_2 diffusivity at residual moisture at (a) 12 hours, (b) 24 hours, (c) 36 hours, and (d) 48 hours after equilibrium concentration with atmosphere. The centerline of the box plots indicates the median, the upper and lower represent the 25^{th} and 75^{th} quantiles, and the red dot reflects the arithmetic mean of relative O_2 concentration for clusters. The relative oxygen concentrations differed significantly ($p < 0.05$) among clusters at all time points. Dunn test was performed for multiple comparisons by correcting the *p* value using Benjamini and Hochberg (1995).

3.3 UNCERTAINTIES ASSOCIATED WITH THE LAB-MEASURED SOIL HYDRAULIC PARAMETERS FOR OXYGEN DIFFUSION

The in situ field soil moisture release curves were developed and fitted to retention models. We observed better performance of the dual porosity model for all the release curves (Figure

2.11b). The fitted hydraulic parameters of release curves were recorded and compared with lab-fitted hydraulic parameters.

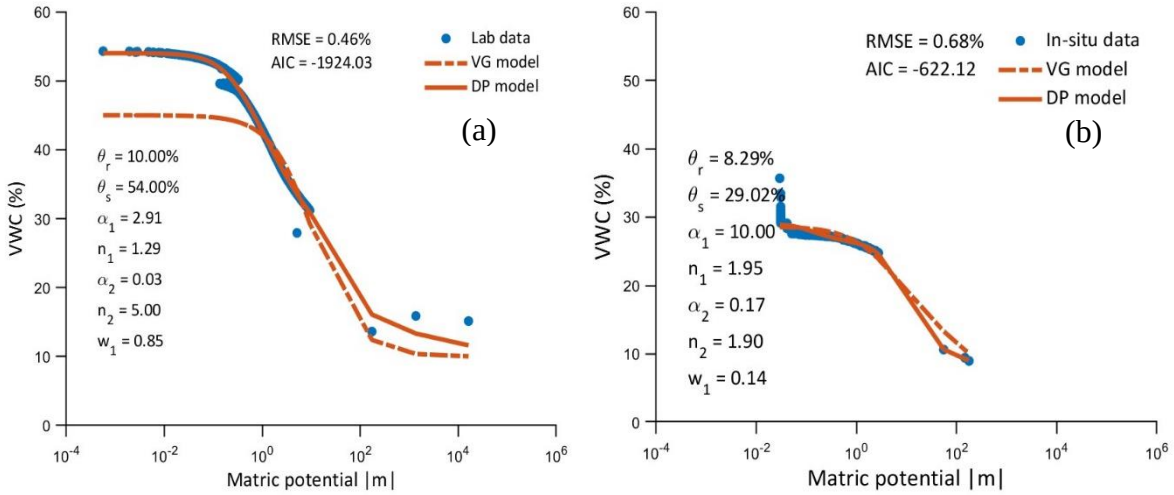

Figure 2.11. Soil moisture release curves developed using (a) a soil core in the lab and (b) in situ field-based measurements. The solid light red line reflects the fitted dual porosity model (Durner, 1994), while the dotted light red line is the fitted single porosity model (van Genuchten, 1980). For ten sites, the field-based moisture release curves were developed, which are shown in Appendix A3.

The results showed a significant difference ($p < 0.05$) in the mean value of saturated water content between lab (45.36%) and in situ field (21.58%) conditions (Figure 2.12b). However, all other hydraulic parameters were statistically similar between lab and in situ field conditions (Figure 2.12a, 2.12c, and 2.12d and Appendix A4).

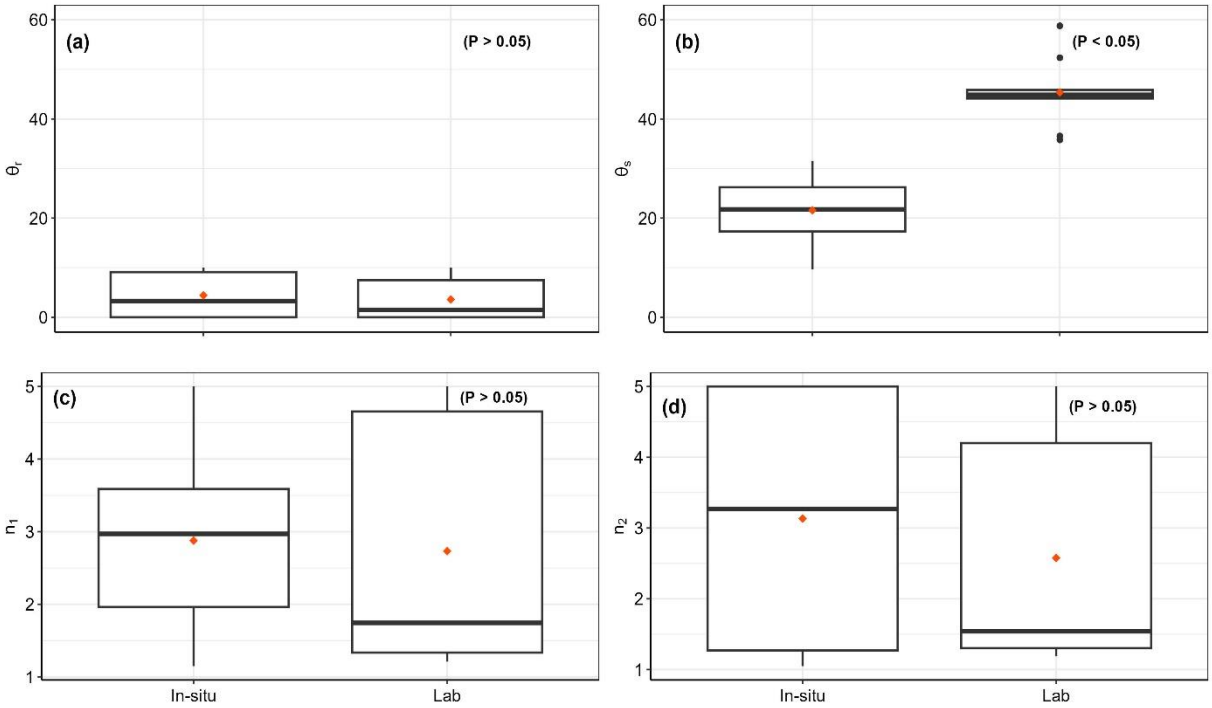

Figure 2.12. Distribution of soil hydraulic parameters such as (a) residual water content θ_r, (b) saturated water content θ_s, (c) n_1, and (d) n_2 between lab and in situ field conditions. The normally distributed data were compared using Student's t-test, while non-normal data were compared using the Mann-Whitley-Wilcoxon test. The centerline of the box plots indicates the median, the upper and lower represent the 25^{th} and 75^{th} quantiles, and the red dot reflects the arithmetic mean of hydraulic parameters for clusters. The p value ($p < 0.05$) indicates a significant difference in the mean estimates between the lab and the field.

Figure 2.13 shows the variation in oxygen diffusivity at different air-filled porosity and the change in oxygen concentration with soil depth for a soil core and in situ field condition. The estimates of oxygen diffusivity at residual moisture, threshold moisture, field capacity, and saturation were compared between the lab and the field. The mean values of O_2 diffusivity at residual and threshold moisture were similar between lab and field conditions, indicating that lab-based measurements may suffice for determining oxygen transport in the field under these conditions. In contrast, the O_2 diffusivity at field capacity and saturation differed between lab and in situ field conditions (Appendix A5 a-d). Moreover, the mean computed O_2 concentrations at 5

cm soil depth, at 12, 24, 36, and 48 hours after uniform O_2 distribution (equal to atmospheric concentration), were similar between lab and in situ field conditions (Appendix A6 a-g) for diffusivity at residual and threshold moisture.

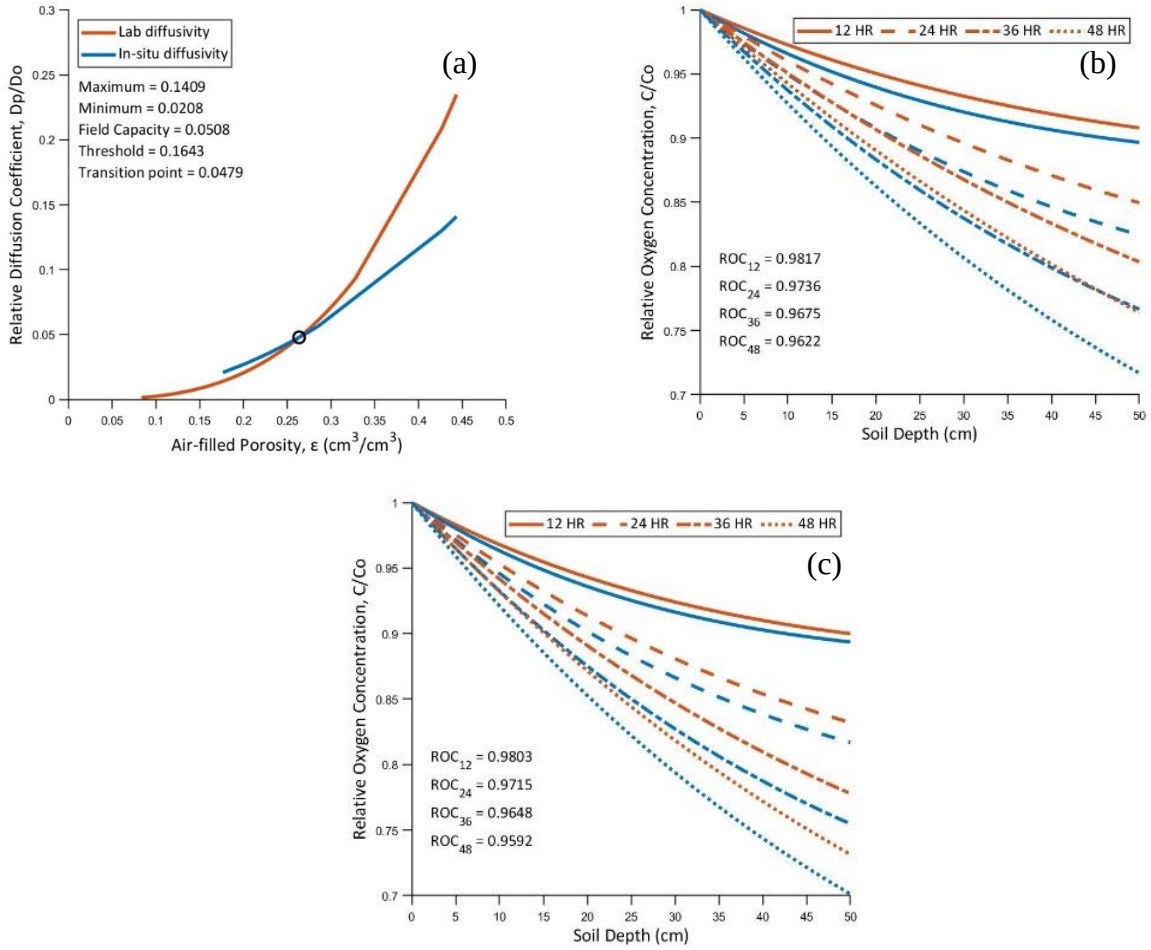

Figure 2.13. (a) Variation in relative oxygen diffusivity as a function of air-filled porosity in the lab soil core (light red) and the field (blue); changes in relative O_2 concentrations with soil depths in the lab and the field computed for O_2 diffusivity at (b) residual moisture (c) threshold moisture. The changes in oxygen concentrations were estimated at 12, 24, 36, and 48 hours after equilibrium, represented by different line gradients. ROC stands for relative oxygen concentration. All these estimates were compiled for the lab and the field and presented in the form of boxplots.

4 DISCUSSION

The interaction between soil attributes, namely physical, chemical, and biological, influence the uptake and transport of gases within soil pores that impact pore-scale biogeochemical processes (Brussaard et al., 1997; Hayes, 2017; Horel et al., 2015; Jones & Bradford, 2001; Schwen et al., 2011). As agricultural management practices affect the interaction between soil attributes, parameters that manifest the effect of management practices in soils are essential for developing a conceptual framework related to the dynamics of gases in soils and differentiating soils based on their potential to become oxygenated. This study is focused on applying diffusivity (Moldrup et al., 1996) and retention models (Durner, 1994; Van Genuchten, 1980) for characterizing oxygen diffusion coefficients of soils based on hydraulic parameters and study the effect of soil structure on oxygen diffusivity at key moisture states. The moisture values considered were residual, threshold, field capacity, and saturation. Understanding the oxygen diffusivity of soils with changes in soil structure and moisture has implications for modeling greenhouse gas emissions and improving soil management practices.

Variation in pore architecture

By fitting retention models, we found that the bi-modal pore size distribution was a better representation of all our undisturbed soil cores (Appendix A1). The bi-model pore size might be due to the presence of above-ground biomass, which influences the formation of biopores (Bodner et al., 2014; Wendel et al., 2022). These biopores are formed due to the penetration of plant roots, soil faunal activity, and physical disturbance and have pore sizes usually different from the normal pores (Wendel et al., 2022). Moreover, the bi-modal pore size distribution could have been due to unusually wide macropores formed due to the cracking of aggregates (Ball, 2013). These bigger pores can hold a comparatively high amount of water at less negative matric potential, resulting in

poor performance of the single porosity (van Genuchten) model as they cannot simulate water content in large pores. Using X-ray microtomography, the presence of bi-modal pore-size distribution can be verified (Pires et al., 2020). This result is in accordance with Haws et al. findings, where they documented better performance of the dual porosity model while simulating solute flows from the subsurface of agricultural soils using retention models (2005). The dual-domain model better predicted solute flow at less negative matric potential.

Variation in oxygen diffusivity with soil moisture

Soil moisture plays a pivotal role in influencing oxygen diffusion in soil pores, primarily by decreasing air-phase pore connectivity and increasing the path length traveled by O_2 molecules (pore tortuosity) (CURRIE, 1984; Neira et al., 2015; Sergey & Pete, 2012). Given the inherent spatial and temporal variability of soil moisture in the field, understanding the dynamics of oxygen necessitates consideration of key moisture states: residual moisture, threshold moisture, field capacity, and saturation. By examining these dominant moisture states, we can gain valuable insights into the intricate behavior of oxygen in the field. Soil hydraulic parameters describing pore-size distribution (n_1 and n_2) clustered oxygen diffusivity at residual and threshold moisture, whereas these parameters did not influence oxygen diffusivity at field capacity and saturation. This result revealed that oxygen diffusivity at residual and threshold moisture are affected by soil structural features, while oxygen diffusivity at field capacity and saturation are not influenced. This discrepancy may be due to the higher connectivity of the water phase at field capacity and saturation, reducing air-filled porosity and the impact of pore-size distribution—which are influenced by soil structure (Bakhshian et al., 2021; Berg et al., 2013).

The within-cluster differences for O_2 diffusivity at residual and threshold moisture were found between clusters 1 and 5; cluster 5 had higher diffusivities when the soil was completely dry

and soil pores less than or equal to 1 micron were filled with water. The relatively higher mean value of O_2 diffusivity at residual and threshold moisture in the soil that falls in cluster 5 might be due to uniform pore-size distribution (PSD) and greater pore continuity as indicated by the presence of higher mean value of clay and lower value of weighting parameter w_1 (Jiao et al., 2021; Zhang et al., 2022). Higher clay content favors soil aggregation and the formation of uniform inter- and intra-aggregate pores, which are highly connected (Nimmo, 2004). On the other hand, a lower value of w_1 indicates the dominance of the micro-and mesopores domain, resulting in uniform pore-size distribution (Zhang et al., 2022). The abundance of uniform pores and high pore connectivity can also be explained by the ratio of α parameters (α_1/α_2). A higher ratio of α_1/α_2 indicates a soil matrix with a large number of macropores embedded in micro-and mesopores, as was observed for cluster 1 (Fatichi et al., 2020; Zhang et al., 2022). Cluster 5 had a lower α_1/α_2 ratio, reflecting the minimum influence of macropores on pore-size distribution and supporting the presence of uniform soil pores. Homogeneous and well-connected soil pores drain simultaneously, leading to greater air-filled porosity and higher O_2 diffusivities at residual and threshold moisture. On the contrary, water can remain in smaller pores in a heterogenous PSD—having a huge difference in micropores and macropores, due to strong tension and hysteretic effect, during a drying cycle, thereby decreasing air-filled porosity and O_2 diffusivity.

Variation in n parameters within clusters

The n parameter of the retention models represents the range of pore-size distribution of soils; a higher n value generally indicates sandy soils with narrow pore-size distribution, while a lower value denotes a wide range of pore-size distribution (Zhang et al., 2022). The results showed significant differences among clusters for both n_1 and n_2 parameters. This finding implies that there are significant structural differences among clusters. A post hoc analysis revealed statistically

insignificant differences between clusters 1 and 5 for n parameters; however, the mean value of n_1 was relatively higher in cluster 5 than in cluster 1, while n_2 varied exactly the opposite. This anomaly in the post hoc statistical test might have resulted due to too many ties in the ranks, which renders non-parametric tests inappropriate to encounter the difference. The higher n_1 parameter of cluster 5 typically signifies a narrow pore-size distribution with greater sand percentage, as n_1 represents structural macropores. But we observed a comparatively greater percentage of clay in cluster 5 with a wide range of pore size distribution. Our observation was supported by the lower estimate of w and the ratio of α parameters (α_1/α_2), which signify broad pore-size distribution. The discrepancy in the observation and the notion related to n_1 might have been due to two reasons. One is the higher uncertainty in the estimation of n_1 which was also noted by Zhang et al. (2022), where they found unclear correlations between the ratio of n parameters (n_1/ n_2) and weighting parameter w. Another reason relates to macropores inside soil aggregates formed by clay particles (Nimmo, 2004). However, the average estimate of n_1 and n_2 aligned with the notion related to the n parameter, which was higher in cluster 1 compared to cluster 5, with a greater sand percentage.

Variation in oxygen concentration

The O_2 transport in soil pores depends on the oxygen diffusion coefficient (Kanwar, 1986; Kanwar et al., 1989; Moldrup et al., 2000; Sergey & Pete, 2012). Variations in pore geometry and connectivity influence oxygen uptake by altering oxygen diffusivity. Well-connected pores lead to higher diffusivity, replenishing the consumed oxygen by microbes and maintaining optimum O_2 concentration in soil pores. The applied oxygen transport model in this study revealed that there are likely differences in oxygen concentration at 5 cm soil depth among clusters for maximum diffusivity. The results indicate higher oxygen concentration in cluster 5 soils than in cluster 1 soils after 12 hours of equilibrium concentration. We did not find significant differences at 24, 36, and

48 hours after equilibrium, but the mean values were comparatively higher in cluster 5 than in cluster 1. One of the plausible explanations of the observed results is the presence of uniform pore geometry, indicated by higher clay content and a lower ratio of α_1 and α_2 parameters. However, the mean oxygen concentrations were similar among clusters for diffusivity at threshold moisture. This may have resulted due to the significant contribution of smaller pores (< 1 μm) to the total pore volume of soils in clusters 1 and 5. When these smaller pores became saturated, the highly disconnected bigger pores (> 1 μm) could not contribute substantially to the soil's oxygen concentration. Wendel et al. (2022) have also noted the significant effect of smaller pores on the oxygen concentration in soil. We would also like to note that these inferences are based on a model under one set of boundary conditions, and results may not be transferred to other conditions without adequate validation.

Variation between lab and in situ field-based estimations

The uncertainty associated with estimated hydraulic parameters needs to be examined by comparing them with field-based hydraulic parameters to ensure accuracy and enhance the applicability of our work. The comparison of the lab and in situ hydraulic parameters indicated statistically insignificant differences in the mean values of n_1 and n_2 parameters. This result provides insights into the simulation of undisturbed soil cores that can represent field heterogeneity. Similarly, other hydraulic parameters except saturated water content (θ_s) were statistically similar between lab and in situ conditions. The fitted saturated water content (θ_s) was lower in the field than in the lab. This may have resulted due to differences in the wetting process of soils in the lab and field conditions. Since water moves from the surface into soil pores in the field, air initially present in pores gets compressed and precludes soil pores from complete saturation (Nimmo & Likens, 2009; van Dam et al., 1996). In addition, the saturation of field soils

depends on the intensity of rainfall and topography (Wang et al., 2022; Xue & Gavin, 2008). However, the air inside soil pores gets released during saturation under controlled conditions in the lab as a result of capillarity, resulting in higher water content.

The statistical similarity between the lab and the field for O_2 diffusivity at residual and threshold moisture may have resulted from an accurate prediction of air-conducting pores during complete dry conditions and when smaller pores (≤ 1 μm) were filled with water. However, we observed higher O_2 diffusivity at field capacity and saturation in the field than in the lab. This discrepancy could be due to the differences in water content at saturation and the fraction of structural pores between in situ and lab conditions. Field soils had lower fitted saturated water content (θ_s) than the lab soils, indicating the presence of air-filled pores at saturation. Lower saturation could be due to the presence of non-capillary or macropores that drain quickly—removing water through downward or lateral flow—and can substantially increase oxygen diffusivity at field capacity and saturation. The lower oxygen diffusivity in the lab may have resulted from destroying air-conducting macropores during sampling using a soil core (Suzanne et al., 2008). Consequently, the result suggests that estimating oxygen diffusivity at saturation and field capacity based on lab-computed parameters should be guided with proper considerations.

Limitations

Some limitations need to be considered when utilizing the interpretation outlined in this study. While both diffusion and convection influence the movement of oxygen in soil pores, this research primarily focused on diffusion due to its predominant contribution to oxygen dynamics (Frederick et al., 1982; Neira et al., 2015; Sergey & Pete, 2012; Suzanne et al., 2008). It is essential to recognize that soils exhibit significant diversity in terms of microbial species and populations, which impact the demand and supply of oxygen into soil pores in a multifaceted manner.

Consequently, the variations in oxygen diffusivity resulting from structural differences and soil moisture levels do not encompass the entirety of the situation. Additionally, it should be noted that some of the fitted hydraulic parameters approached the upper limits of the dual porosity model's range, but this only represents a small fraction of the total fitted values. Therefore, care should be taken when interpreting the fitted hydraulic parameters and oxygen diffusivity.

5 CONCLUSIONS

This study investigated the potential of classifying oxygen diffusivity in agricultural soils at different moisture contents based on soil structure as studied using soil hydraulic parameters from the water retention curve. We found that soils clustered into similar soil structure groups using hydraulic parameters n_1 and n_2 categorized oxygen diffusivity for low moisture contents, specifically, moisture required to saturate soil pores < 1 micron and residual saturation. The effect of structural differences on oxygen diffusivity was moisture specific, and no impacts were observed for higher moisture contents. Soils with uniform pore-size distribution, depicted by a greater percentage of clay and a lower proportion of structural pores, had higher oxygen diffusivity at residual and threshold moisture. Comparison between lab- and field-based estimations revealed that the oxygen diffusivity quantified at residual and threshold moisture in the lab can simulate the field condition. These findings have implications for modeling oxygen diffusivity of undisturbed soils and improving biogeochemical models. Accurate estimation and interpretation of biogeochemical cycles of croplands will aid in sustainable soil management practices while enhancing crop productivity.

REFERENCES

Arriaga, F. J., Lowery, B., & Mays, M. D. (2006). A fast method for determining soil particle size distribution using a laser instrument. *Soil Science*, *171*(9), 663-674.

Bakhshian, S., Rabbani, H. S., & Shokri, N. (2021). Physics-driven investigation of wettability effects on two-phase flow in natural porous media: Recent advances, new insights, and future perspectives. *Transport in Porous Media*, *140*, 85-106.

Ball, B. (2013). Soil structure and greenhouse gas emissions: a synthesis of 20 years of experimentation. *European Journal of Soil Science, 64*(3), 357-373.

Berg, S., Ott, H., Klapp, S. A., Schwing, A., Neiteler, R., Brussee, N., Makurat, A., Leu, L., Enzmann, F., Schwarz, J.-O., Kersten, M., Irvine, S., & Stampanoni, M. (2013). Real-time 3D imaging of Haines jumps in porous media flow. *Proceedings of the National Academy of Sciences*, *110*(10), 3755-3759. https://doi.org/doi:10.1073/pnas.1221373110

Bodner, G., Leitner, D., & Kaul, H.-P. (2014). Coarse and fine root plants affect pore size distributions differently. *Plant and Soil*, *380*, 133 - 151.

Brussaard, L., Behan-Pelletier, V. M., Bignell, D. E., Brown, V. K., Didden, W. A. M., Folgarait, P. J., Fragoso, C. E., Freckman, D. W., Gupta, V. V. S. R., & Hattori, T. (1997). Biodiversity and ecosystem functioning in soil. *AMBIO: A Journal of the Human Environment*, *26*, 563-570.

Campbell, G. S. (1974). A simple method for determining unsaturated conductivity from moisture retention data. *Soil Science*, *117*(6), 311-314.

Campbell, G. S. (1985). *Soil physics with BASIC: transport models for soil-plant systems*. Elsevier.

Castellano, M. J., Schmidt, J. P., Kaye, J. P., Walker, C., Graham, C. B., Lin, H., & Dell, C. J. (2010). Hydrological and biogeochemical controls on the timing and magnitude of nitrous oxide flux across an agricultural landscape. *Global change biology*, *16*(10), 2711-2720.

Cook, G. D., So, H. B., & Dalal, R. C. (1992). Structural degradation of two Vertisols under continuous cultivation. *Soil and Tillage Research*, *24*(1), 47-64. https://doi.org/https://doi.org/10.1016/0167-1987(92)90071-I

CURRIE, J. A. (1984). Gas diffusion through soil crumbs: the effects of compaction and wetting. *Journal of Soil Science*, *35*(1), 1-10. https://doi.org/https://doi.org/10.1111/j.1365-2389.1984.tb00253.x

Durner, W. (1994). Hydraulic conductivity estimation for soils with heterogeneous pore structure. *Water Resources Research*, *30*(2), 211-223.

Fatichi, S., Or, D., Walko, R., Vereecken, H., Young, M. H., Ghezzehei, T. A., Hengl, T., Kollet, S., Agam, N., & Avissar, R. (2020). Soil structure is an important omission in Earth System Models. *Nature Communications*, *11*(1), 522. https://doi.org/10.1038/s41467-020-14411-z

Frederick, R. T., Jalal, D. J., & Don, K. (1982). Gaseous diffusion equations for porous materials. *Geoderma*. https://doi.org/10.1016/0016-7061(82)90033-7

Gregory, P. J., Ingram, J. S. I., Andersson, R., Betts, R. A., Brovkin, V., Chase, T. N., Grace, P. R., Gray, A. J., Hamilton, N., Hardy, T. B., Howden, S. M., Jenkins, A., Meybeck, M., Olsson, M., Ortiz-Monasterio, I., Palm, C. A., Payn, T. W., Rummukainen, M., Schulze, R. E., . . . Wilkinson, M. J. (2002). Environmental consequences of alternative practices for intensifying crop production. *Agriculture, Ecosystems & Environment*, *88*(3), 279-290. https://doi.org/https://doi.org/10.1016/S0167-8809(01)00263-8

Haws, N. W., Rao, P. S. C., Simunek, J., & Poyer, I. C. (2005). Single-porosity and dual-porosity modeling of water flow and solute transport in subsurface-drained fields using effective field-scale parameters. *Journal of Hydrology*, *313*(3-4), 257-273.

Hayes, A. (2017). Soil Physical Properties. *Properties and Management of Soils in the Tropics*.

Hendricks, T., Franklin, D., Dahal, S., Hancock, D., Stewart, L., Cabrera, M., & Hawkins, G. (2019). Soil carbon and bulk density distribution within 10 Southern Piedmont grazing systems. *Journal of Soil and Water Conservation*, *74*(4), 323-333.

Horel, Á., Tóth, E., Gelybó, G., Kása, I., Bakacsi, Z., & Farkas, C. (2015). Effects of Land Use and Management on SoilHydraulic Properties. *Open Geosciences*, *7*(1). https://doi.org/doi:10.1515/geo-2015-0053

Jiao, W., Zhou, D., & Wang, Y. (2021). Effects of Clay Content on Pore Structure Characteristics of Marine Soft Soil. *Water*, *13*(9), 1160. https://www.mdpi.com/2073-4441/13/9/1160

Jirků, V., Kodešová, R., Nikodem, A., Mühlhanselová, M., & Žigová, A. (2013). Temporal variability of structure and hydraulic properties of topsoil of three soil types. *Geoderma, 204-205*, 43-58. https://doi.org/https://doi.org/10.1016/j.geoderma.2013.03.024

Jones, T. H., & Bradford, M. A. (2001). Assessing the functional implications of soil biodiversity in ecosystems. *Ecological Research, 16*, 845-858.

Kanwar, R. (1986). Analytical solutions of the transient state oxygen diffusion equation in soils with a production term. *Journal of Agronomy and Crop Science, 156*(2), 101-109.

Kanwar, R. S., Mukhtar, S., & Singh, P. K. (1989). Transient-State Oxygen Diffusion Through Undisturbed Soil Columns. *Transactions of the ASABE, 32*, 1645-1650.

Kibret, K., Beyene, S., & Erkossa, T. (2023). Soil Fertility and Soil Health. In S. Beyene, A. Regassa, B. B. Mishra, & M. Haile (Eds.), *The Soils of Ethiopia* (pp. 157-192). Springer International Publishing. https://doi.org/10.1007/978-3-031-17012-6_8

Lacroix, E. M., Rossi, R. J., Bossio, D., & Fendorf, S. (2021). Effects of moisture and physical disturbance on pore-scale oxygen content and anaerobic metabolisms in upland soils. *Science of The Total Environment, 780*, 146572. https://doi.org/https://doi.org/10.1016/j.scitotenv.2021.146572

Lai, S.-H., Tiedje, J. M., & Erickson, A. E. (1976). In situ Measurement of Gas Diffusion Coefficient in Soils. *Soil Science Society of America Journal, 40*(1), 3-6. https://doi.org/https://doi.org/10.2136/sssaj1976.03615995004000010006x

Li, H., Yao, Y., Zhang, X., Zhu, H., & Wei, X. (2021). Changes in soil physical and hydraulic properties following the conversion of forest to cropland in the black soil region of

Northeast China. *CATENA, 198*, 104986. https://doi.org/https://doi.org/10.1016/j.catena.2020.104986

Lipovetsky, T., Zhuang, L., Teixeira, W. G., Boyd, A., Pontedeiro, E. M., Moriconi, L., Alves, J. L., Couto, P., & van Genuchten, M. T. (2020). HYPROP measurements of the unsaturated hydraulic properties of a carbonate rock sample. *Journal of Hydrology, 591*, 125706.

Millington, R. (1959). Gas diffusion in porous media. *Science, 130*(3367), 100-102.

Millington, R., & Quirk, J. (1960). Transport in porous media. p. 97–106. FA Van Beren et al.(ed.) Trans. Int. Congr. of Soil Sci., 7th, Madison, WI. 14–24 Aug. 1960. Vol. 1. Elsevier, Amsterdam. *Transport in porous media. p. 97–106. In FA Van Beren et al.(ed.) Trans. Int. Congr. of Soil Sci., 7th, Madison, WI. 14–24 Aug. 1960. Vol. 1. Elsevier, Amsterdam.*, -.

Millington, R., & Quirk, J. (1961). Permeability of porous solids. *Transactions of the Faraday Society, 57*, 1200-1207.

Moldrup, P., Kruse, C., Rolston, D., & Yamaguchi, T. (1996). Modeling diffusion and reaction in soils: III. Predicting gas diffusivity from the Campbell soil-water retention model. *Soil Science, 161*(6), 366-375.

Moldrup, P., Olesen, T., Schjonning, P., Yamaguchi, T., & Rolston, D. E. (2000). Predicting the gas diffusion coefficient in undisturbed soil from soil water characteristics. *Soil Science Society of America Journal, 64*(1), 94-100. https://doi.org/DOI10.2136/sssaj2000.64194x

Moldrup, P., Olesen, T., Yamaguchi, T., Schjonning, P., & Rolston, D. E. (1999). Modeling diffusion and reaction in soils: IX. The Buckingham-Burdine-Campbell equation for gas diffusivity in undisturbed soil. *Soil Science*, *164*(8), 542-551. https://doi.org/Doi10.1097/00010694-199908000-00002

Moldrup, P., Olesen, T., Yoshikawa, S., Komatsu, T., & Rolston, D. E. (2004). Three-porosity model for predicting the gas diffusion coefficient in undisturbed soil. *Soil Science Society of America Journal*, *68*(3), 750-759.

Neira, J., Ortiz, M., Morales, L., & Acevedo, E. (2015). Oxygen diffusion in soils: Understanding the factors and processes needed for modeling. *Chilean journal of agricultural research*, *75*, 35-44. http://www.scielo.cl/scielo.php?script=sci_arttext&pid=S071858392015000300005&nrm=iso

Nimmo, J. R. (2004). Porosity and pore size distribution. *Encyclopedia of Soils in the Environment*, *3*(1), 295-303.

Noelia, R.-R., & Eguren, G. (2022). Evaluation of Sustainability of Cropping Sequences on Production Systems: Agricultural Intensification Indices.

Peng, H., Dan, L., Hua, X., Chaoli, L., Hayat, U., Yang, X., Changhong, S., Chunsheng, D., Yuanlai, C., & Yufeng, L. (2022). Assessment of paddy expansion impact on regional climate using WRF model: a case study in Sanjiang Plain, Northeast China. https://doi.org/10.1007/S00704-022-04145-X

Schlüter, S., Zawallich, J., Vogel, H.-J., & Dörsch, P. (2019). Physical constraints for respiration in microbial hotspots in soil and their importance for denitrification. *Biogeosciences*, *16*(18), 3665-3678.

Schwen, A., Bodner, G., Scholl, P., Buchan, G. D., & Loiskandl, W. (2011). Temporal dynamics of soil hydraulic properties and the water-conducting porosity under different tillage. *Soil and Tillage Research*, *113*(2), 89-98. https://doi.org/https://doi.org/10.1016/j.still.2011.02.005

Sergey, B., & Pete, S. (2012). Soil physics meets soil biology: Towards better mechanistic prediction of greenhouse gas emissions from soil. *Soil Biology & Biochemistry*. https://doi.org/10.1016/J.SOILBIO.2011.12.015

Smith, K. (2017). Changing views of nitrous oxide emissions from agricultural soil: key controlling processes and assessment at different spatial scales. *European Journal of Soil Science*, *68*(2), 137-155.

Stevenson, A., Hartemink, A. E., & Zhang, Y. (2023). Measuring sand content using sedimentation, spectroscopy, and laser diffraction. *Geoderma*, *429*, 116268. https://doi.org/https://doi.org/10.1016/j.geoderma.2022.116268

Stolze, K., Barnes, A. D., Eisenhauer, N., & Totsche, K. U. (2022). Depth-differentiated, multivariate control of biopore number under different land-use practices. *Geoderma*, *418*, 115852. https://doi.org/https://doi.org/10.1016/j.geoderma.2022.115852

Subedi, A., Franklin, D., Cabrera, M., Dahal, S., Hancock, D., McPherson, A., & Stewart, L. (2022). Extreme Weather and Grazing Management Influence Soil Carbon and Compaction. *Agronomy*, *12*(9), 2073.

Suzanne, E. A., Jonathan, A. L., Alexandre, R. C., & Sébastien, F. L. (2008). Measurement of gas diffusion through soils: comparison of laboratory methods. *Journal of Environmental Monitoring*. https://doi.org/10.1039/B809461F

Troeh, F. R., Jabro, J. D., & Kirkham, D. (1982). Gaseous diffusion equations for porous materials. *Geoderma*, *27*(3), 239-253.

Turkeltaub, T., Mannheim, R., Furman, A., & Weisbrod, N. (2023). Elucidating the relationship between gaseous O2 and redox potential in a soil aquifer treatment system using data driven approaches and an oxygen diffusion model. *Journal of Hydrology*, *618*, 129168. https://doi.org/https://doi.org/10.1016/j.jhydrol.2023.129168

Van Genuchten, M. T. (1980). A closed-form equation for predicting the hydraulic conductivity of unsaturated soils. *Soil Science Society of America Journal*, *44*(5), 892-898.

Wang, R., Wen, S., & Sun, Z. (2022). Analytical Solution of Rainfall Infiltration in Unsaturated Soil Slopes Considering Initial Water Content Distribution. *KSCE Journal of Civil Engineering*, *26*(11), 4419-4431. https://doi.org/10.1007/s12205-022-1750-5

Wendel, A. S., Bauke, S. L., Amelung, W., & Knief, C. (2022). Root-rhizosphere-soil interactions in biopores. *Plant and Soil*, *475*(1-2), 253-277.

West, J. R., Lauer, J. G., & Whitman, T. (2023). Tillage homogenizes soil bacterial communities in microaggregate fractions by facilitating dispersal. *bioRxiv*, 2023.2003. 2008.531801.

Xue, J., & Gavin, K. (2008). Effect of Rainfall Intensity on Infiltration into Partly Saturated Slopes. *Geotechnical and Geological Engineering*, *26*(2), 199-209. https://doi.org/10.1007/s10706-007-9157-0

Ye, L., Zengming, C., Ji, C., Michael, J. C., Chenglong, Y., Nan, Z., Yuncai, M., Huijie, Z., Junjie, L., Weixin, D., Ye, L., Zengming, C., Ji, C., Michael, J. C., Chenglong, Y., Nan, Z., Yuncai, M., Huijie, Z., Junjie, L., & Weixin, D. (2022). Oxygen availability regulates the quality of soil dissolved organic matter by mediating microbial metabolism and iron oxidation. https://doi.org/10.1111/GCB.16445

Zhang, Y., Weihermüller, L., Toth, B., Noman, M., & Vereecken, H. (2022). Analyzing dual porosity in soil hydraulic properties using soil databases for pedotransfer function development. *Vadose Zone Journal*, *21*(5), e20227.

APPENDIX 2.1

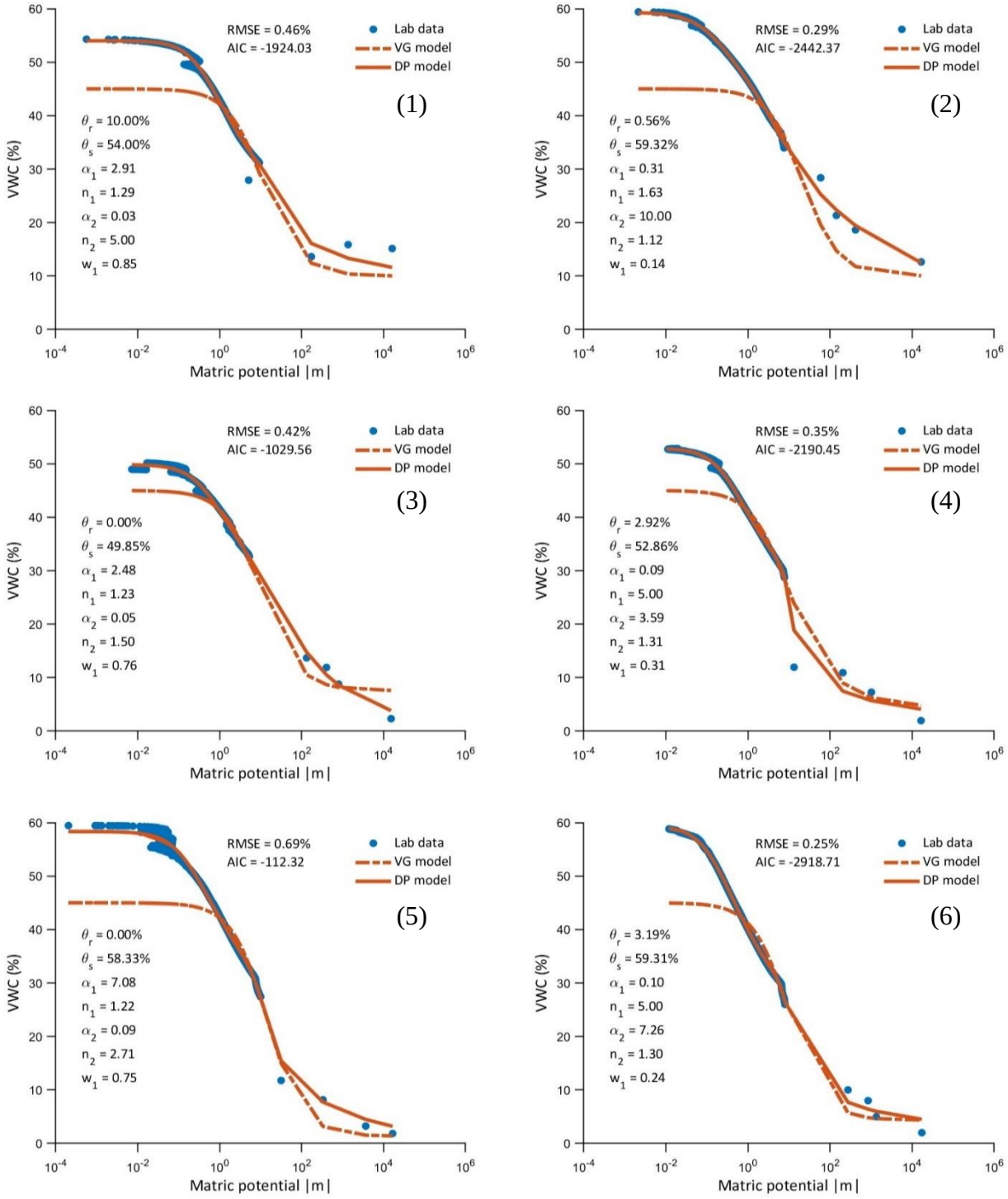
RMSE = 0.46%
AIC = -1924.03
Lab data
VG model
DP model
(1)
θ_r = 10.00%
θ_s = 54.00%
α_1 = 2.91
n_1 = 1.29
α_2 = 0.03
n_2 = 5.00
w_1 = 0.85
VWC (%)
Matric potential |m|
RMSE = 0.29%
AIC = -2442.37
(2)
θ_r = 0.56%
θ_s = 59.32%
α_1 = 0.31
n_1 = 1.63
α_2 = 10.00
n_2 = 1.12
w_1 = 0.14
RMSE = 0.42%
AIC = -1029.56
(3)
θ_r = 0.00%
θ_s = 49.85%
α_1 = 2.48
n_1 = 1.23
α_2 = 0.05
n_2 = 1.50
w_1 = 0.76
RMSE = 0.35%
AIC = -2190.45
(4)
θ_r = 2.92%
θ_s = 52.86%
α_1 = 0.09
n_1 = 5.00
α_2 = 3.59
n_2 = 1.31
w_1 = 0.31
RMSE = 0.69%
AIC = -112.32
(5)
θ_r = 0.00%
θ_s = 58.33%
α_1 = 7.08
n_1 = 1.22
α_2 = 0.09
n_2 = 2.71
w_1 = 0.75
RMSE = 0.25%
AIC = -2918.71
(6)
θ_r = 3.19%
θ_s = 59.31%
α_1 = 0.10
n_1 = 5.00
α_2 = 7.26
n_2 = 1.30
w_1 = 0.24

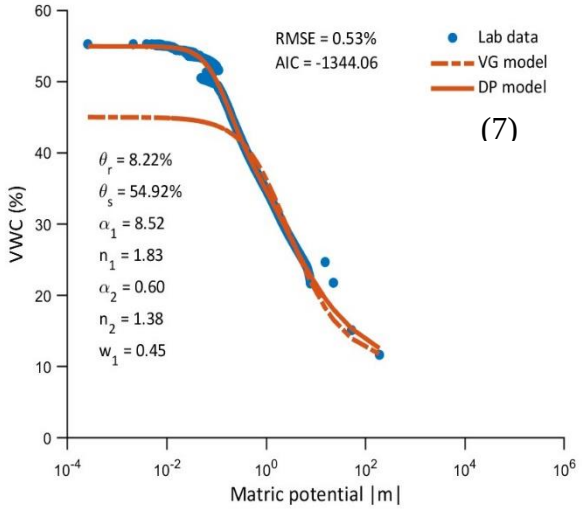
RMSE = 0.53%
AIC = -1344.06
Lab data
VG model
DP model
θ_r = 8.22%
θ_s = 54.92%
α_1 = 8.52
n_1 = 1.83
α_2 = 0.60
n_2 = 1.38
w_1 = 0.45
VWC (%)
Matric potential |m|

(7)

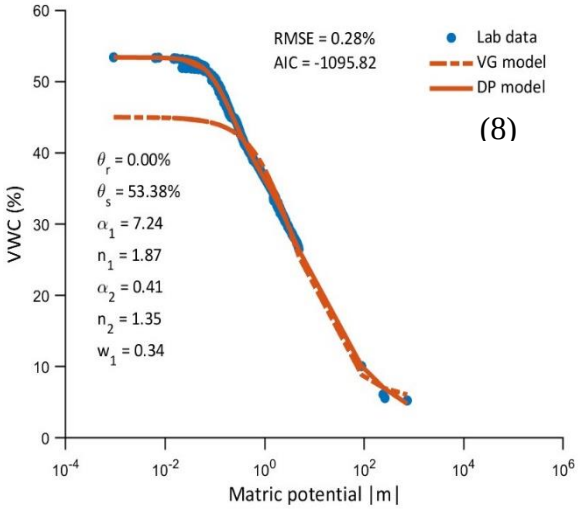
RMSE = 0.28%
AIC = -1095.82
Lab data
VG model
DP model
θ_r = 0.00%
θ_s = 53.38%
α_1 = 7.24
n_1 = 1.87
α_2 = 0.41
n_2 = 1.35
w_1 = 0.34
VWC (%)
Matric potential |m|

(8)

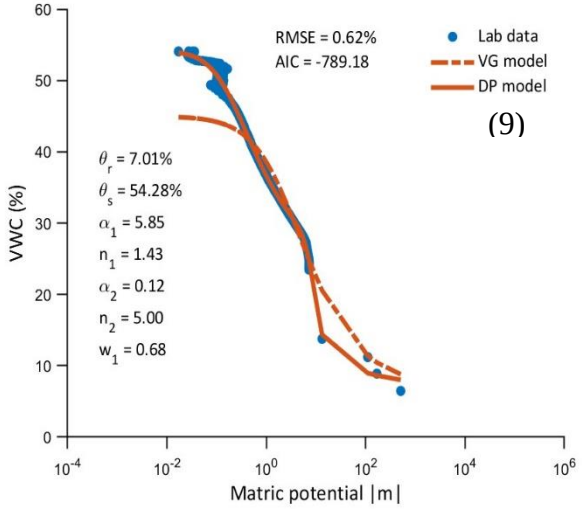
RMSE = 0.62%
AIC = -789.18
Lab data
VG model
DP model
θ_r = 7.01%
θ_s = 54.28%
α_1 = 5.85
n_1 = 1.43
α_2 = 0.12
n_2 = 5.00
w_1 = 0.68
VWC (%)
Matric potential |m|

(9)

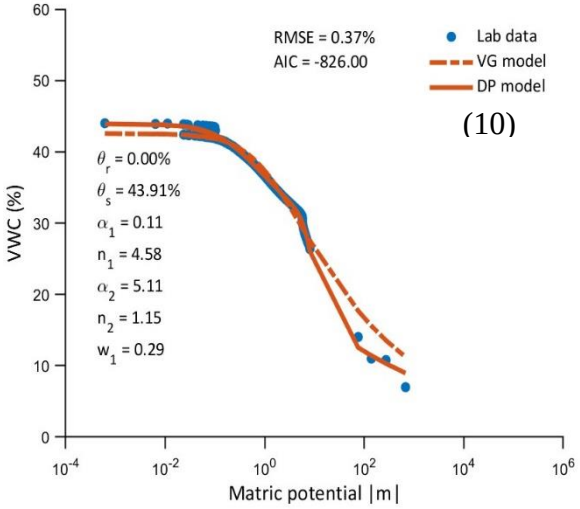
RMSE = 0.37%
AIC = -826.00
Lab data
VG model
DP model
θ_r = 0.00%
θ_s = 43.91%
α_1 = 0.11
n_1 = 4.58
α_2 = 5.11
n_2 = 1.15
w_1 = 0.29
VWC (%)
Matric potential |m|

(10)

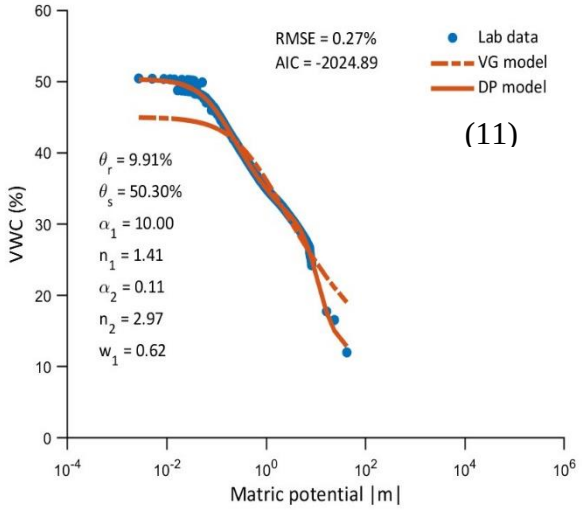
RMSE = 0.27%
AIC = -2024.89
Lab data
VG model
DP model
θ_r = 9.91%
θ_s = 50.30%
α_1 = 10.00
n_1 = 1.41
α_2 = 0.11
n_2 = 2.97
w_1 = 0.62
VWC (%)
Matric potential |m|

(11)

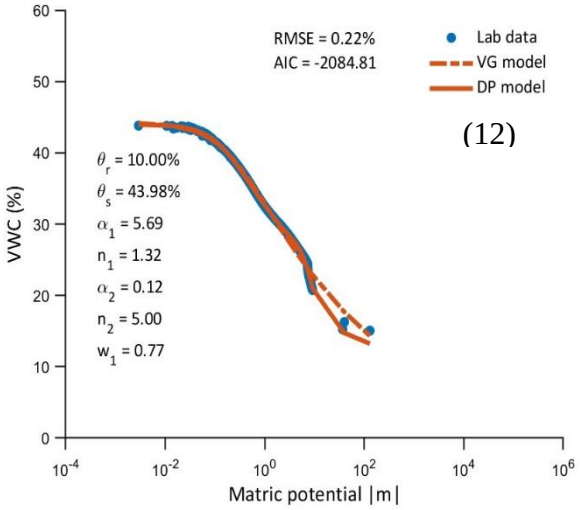
RMSE = 0.22%
AIC = -2084.81
Lab data
VG model
DP model
θ_r = 10.00%
θ_s = 43.98%
α_1 = 5.69
n_1 = 1.32
α_2 = 0.12
n_2 = 5.00
w_1 = 0.77
VWC (%)
Matric potential |m|

(12)

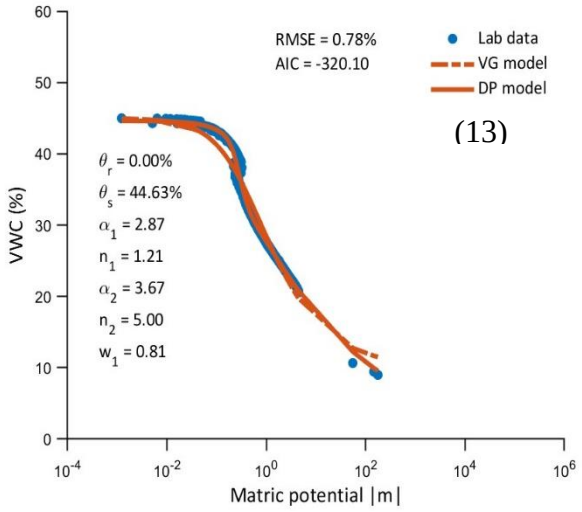

(13)

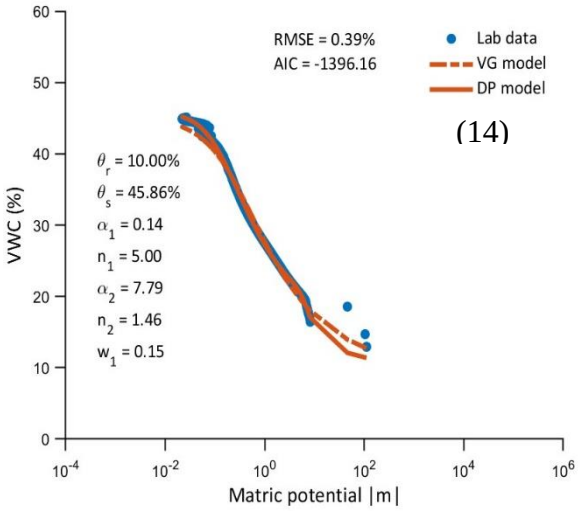

(14)

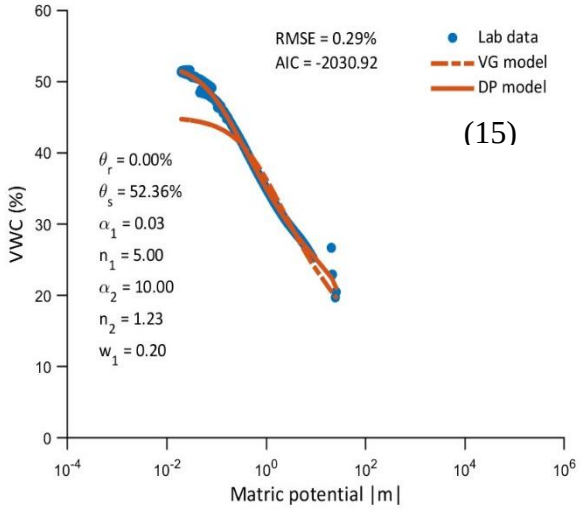

(15)

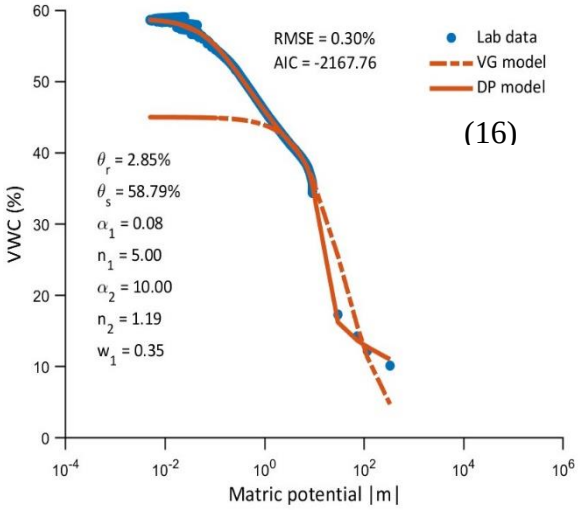

(16)

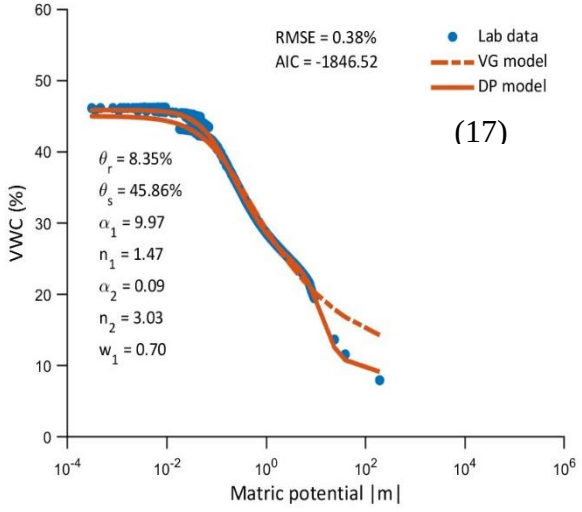

(17)

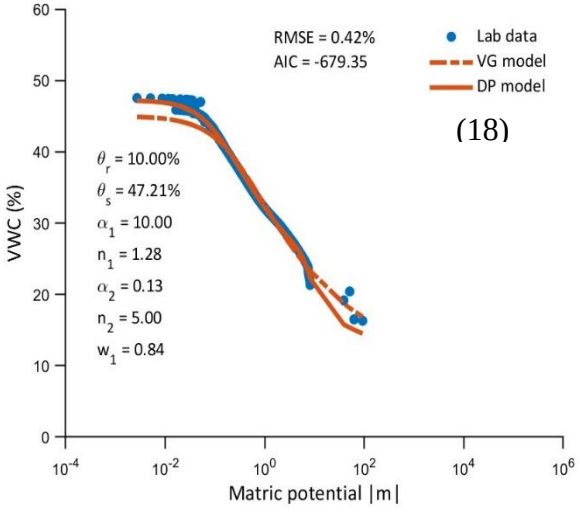

(18)

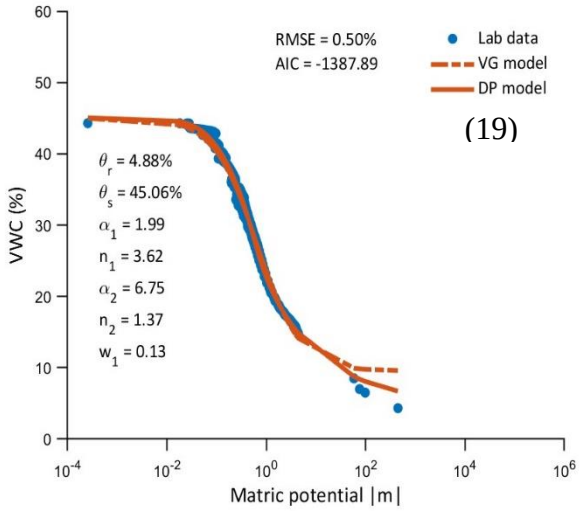

(19)

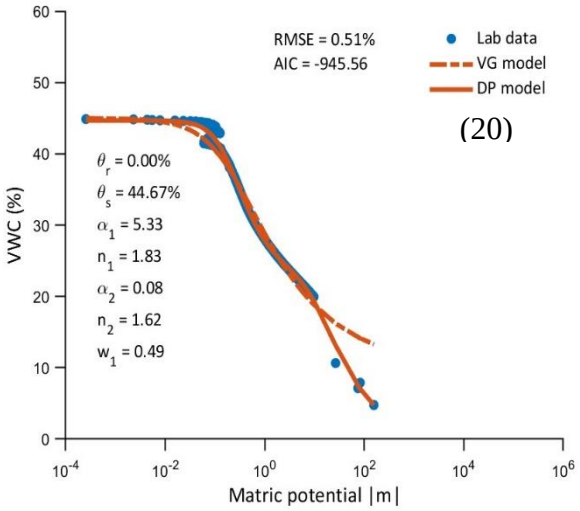

(20)

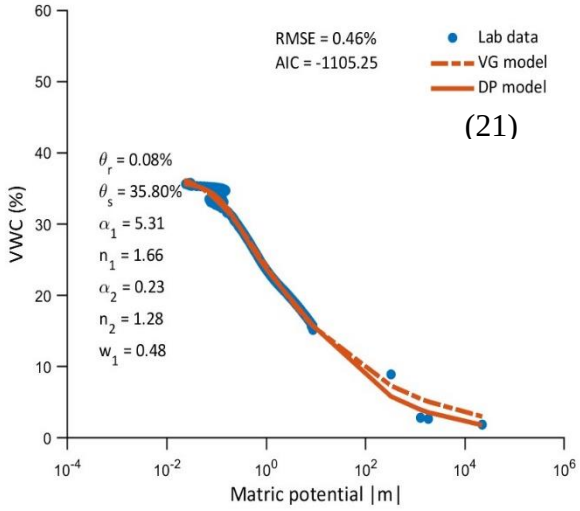

(21)

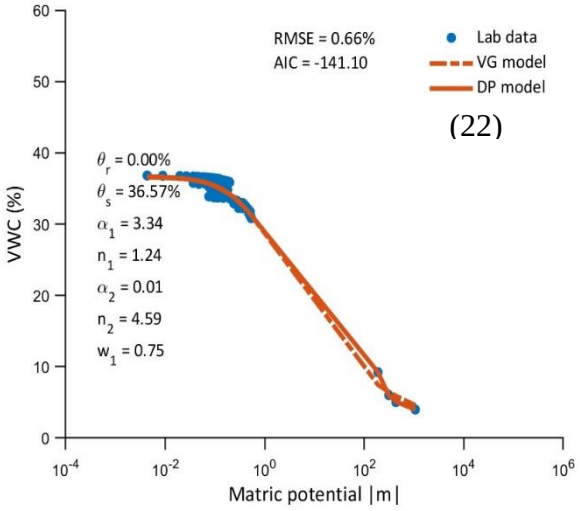

(22)

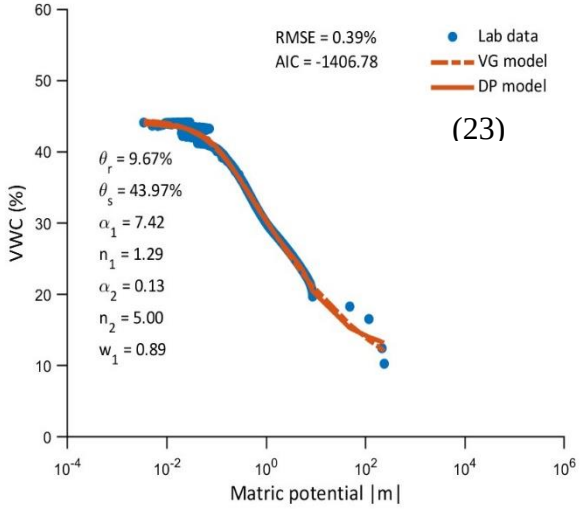

(23)

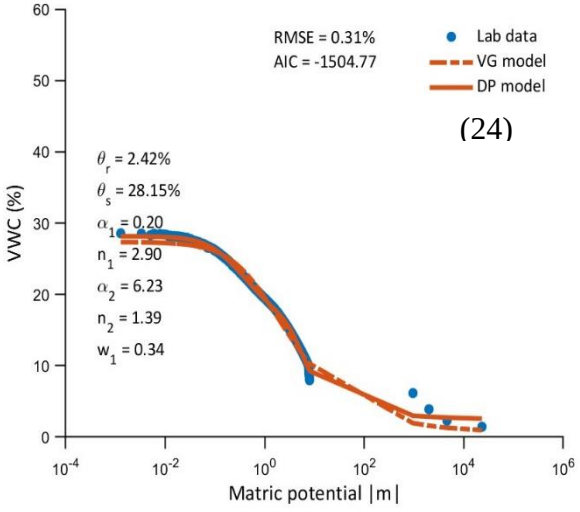

(24)

Appendix A1. van Genuchten and Dual porosity models fitted to lab measured volumetric water content (VWC) and matric potential for 24 soil cores. The blue dots are the measured VWC at different matric potentials. The dotted yellow line indicates van Genuchten model while the solid yellow line indicates dual porosity model. The performance of models was compared based on Root mean square error (RMSE) and Akaike information criterion (AIC). Lower values of these estimates indicate better model. The number in brackets () reflects soil core number.

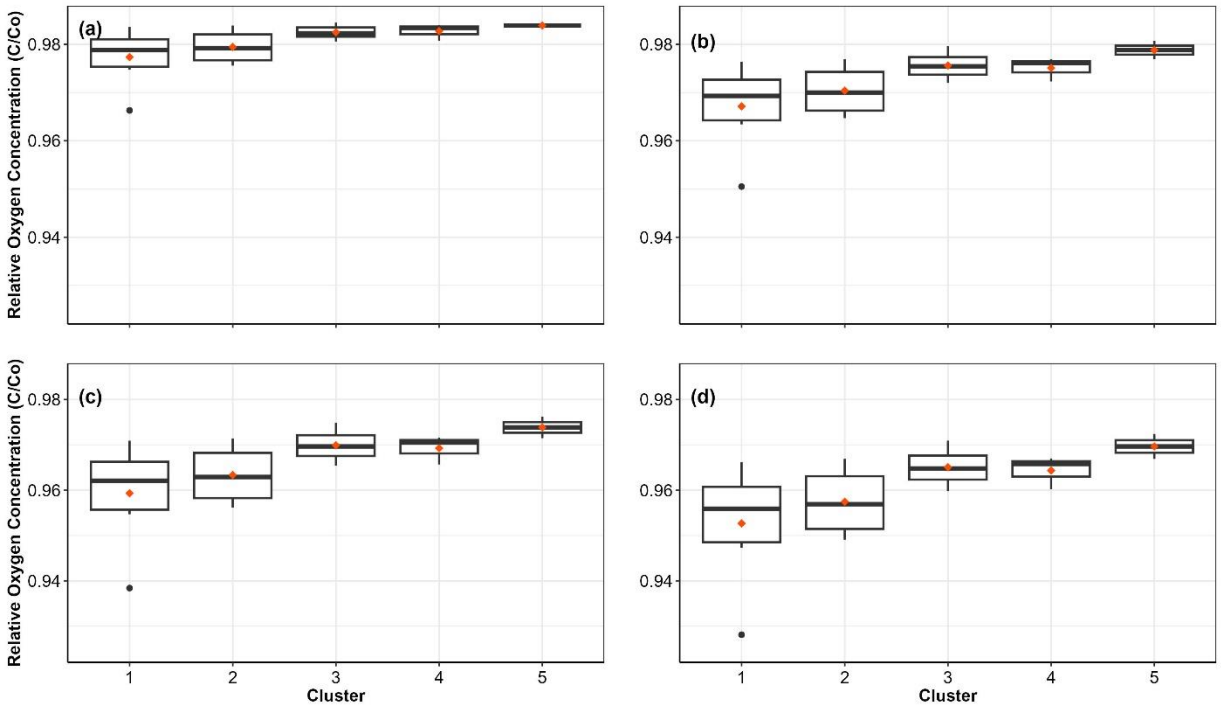

Appendix A2. Distribution of relative O_2 concentration in clusters for diffusivity at threshold moisture at (a) 12 hours, (b) 24 hours, (c) 36 hours, and (d) 48 hours after equilibrium concentration with atmosphere. The centerline of the box plots indicates the median, the upper and lower represent the 25^{th} and 75^{th} quantiles, and the red dot reflects the arithmetic mean of relative O_2 concentration for clusters. The relative oxygen concentrations were statistically insignificant ($p > 0.05$) among clusters at all time points. Dunn test by correcting p value for multiple comparisons using Benjamini and Hochberg (1995).

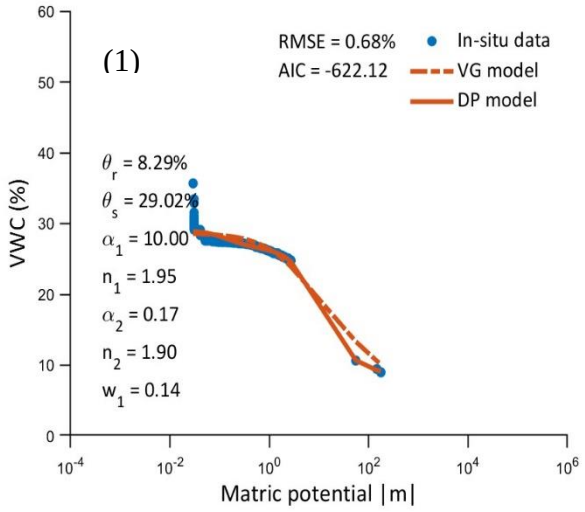
(1)
RMSE = 0.68%
AIC = -622.12
In-situ data
VG model
DP model
θr = 8.29%
θs = 29.02%
α1 = 10.00
n1 = 1.95
α2 = 0.17
n2 = 1.90
w1 = 0.14
VWC (%)
Matric potential |m|

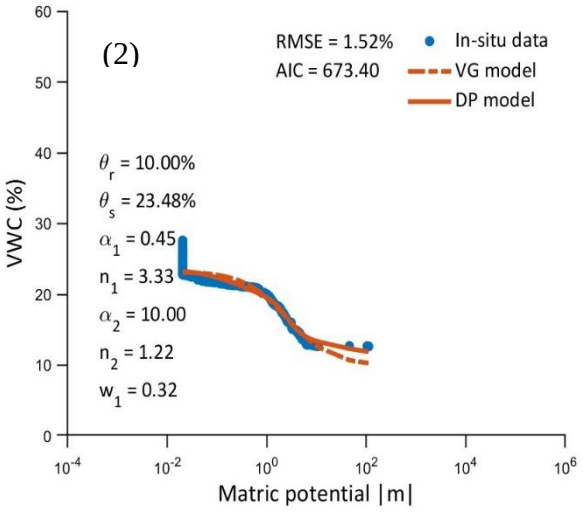
(2)
RMSE = 1.52%
AIC = 673.40
In-situ data
VG model
DP model
θr = 10.00%
θs = 23.48%
α1 = 0.45
n1 = 3.33
α2 = 10.00
n2 = 1.22
w1 = 0.32
VWC (%)
Matric potential |m|

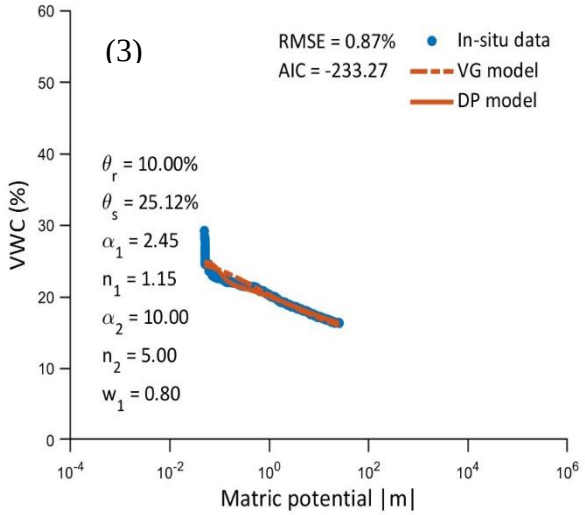
(3)
RMSE = 0.87%
AIC = -233.27
In-situ data
VG model
DP model
θr = 10.00%
θs = 25.12%
α1 = 2.45
n1 = 1.15
α2 = 10.00
n2 = 5.00
w1 = 0.80
VWC (%)
Matric potential |m|

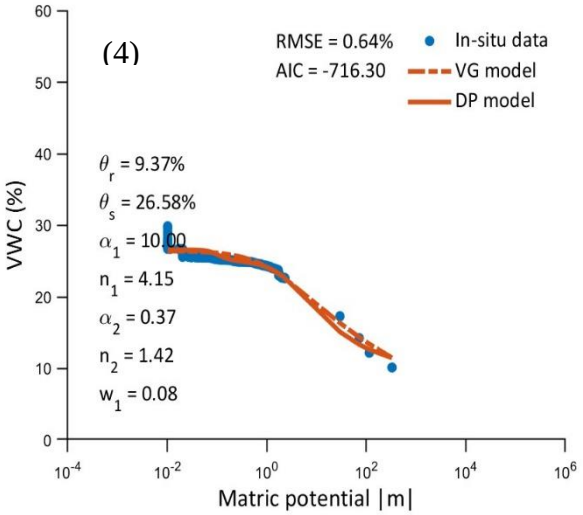
(4)
RMSE = 0.64%
AIC = -716.30
In-situ data
VG model
DP model
θr = 9.37%
θs = 26.58%
α1 = 10.00
n1 = 4.15
α2 = 0.37
n2 = 1.42
w1 = 0.08
VWC (%)
Matric potential |m|

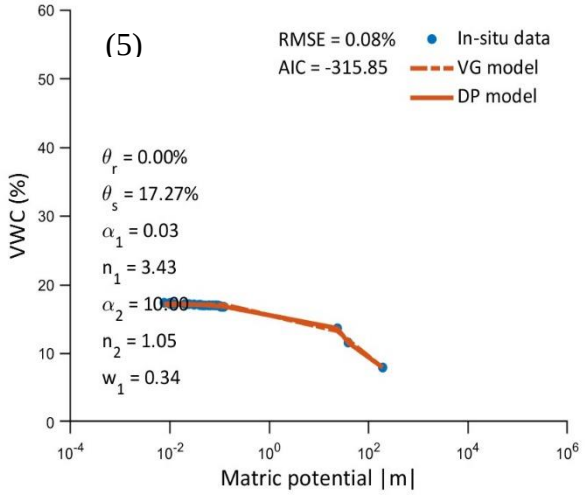
(5)
RMSE = 0.08%
AIC = -315.85
In-situ data
VG model
DP model
θr = 0.00%
θs = 17.27%
α1 = 0.03
n1 = 3.43
α2 = 10.00
n2 = 1.05
w1 = 0.34
VWC (%)
Matric potential |m|

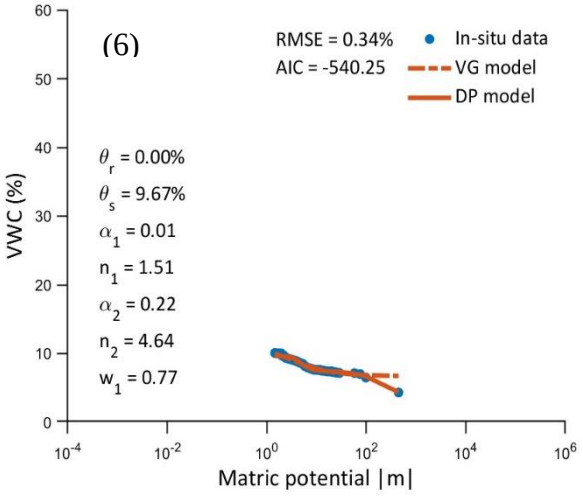
(6)
RMSE = 0.34%
AIC = -540.25
In-situ data
VG model
DP model
θr = 0.00%
θs = 9.67%
α1 = 0.01
n1 = 1.51
α2 = 0.22
n2 = 4.64
w1 = 0.77
VWC (%)
Matric potential |m|

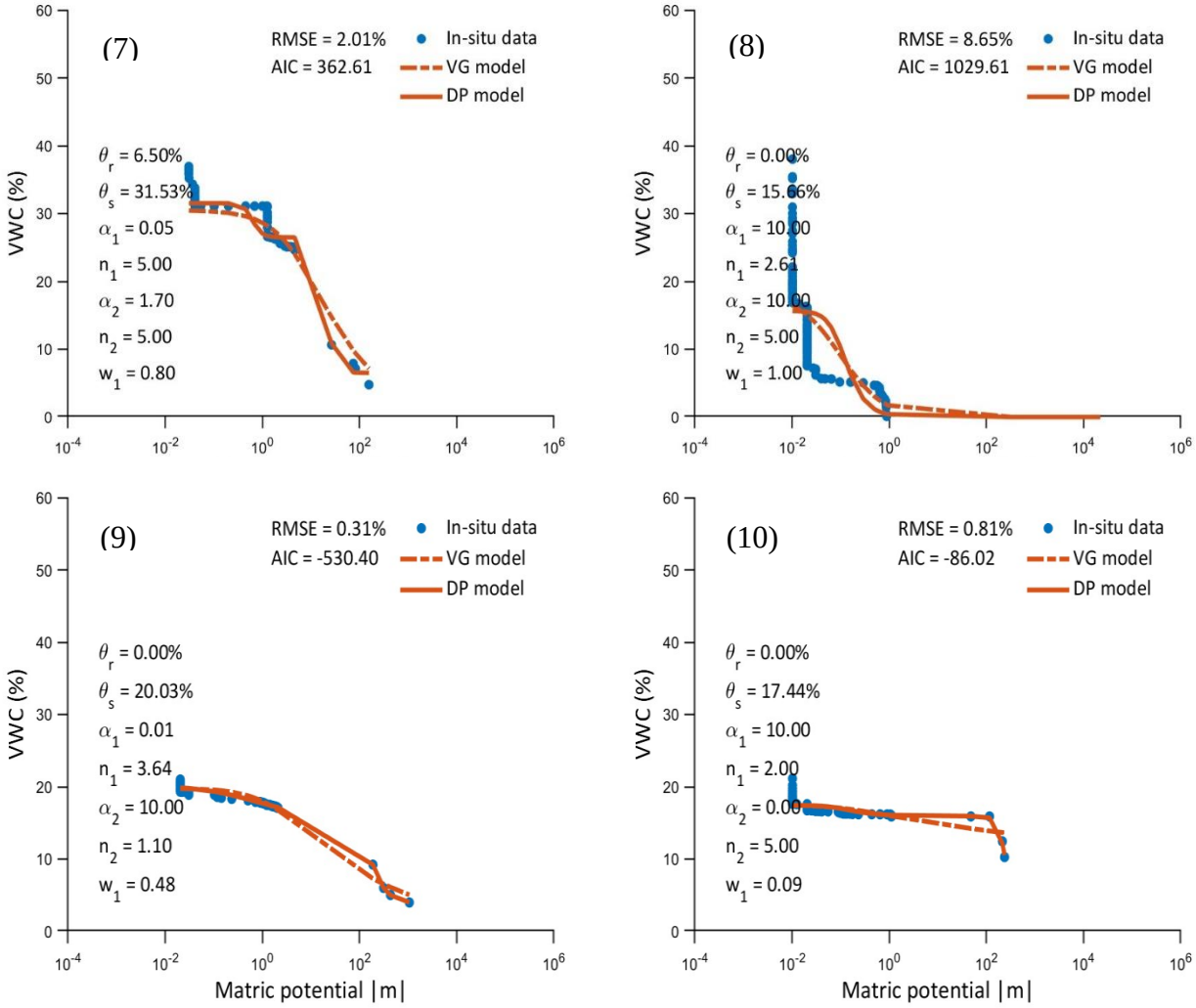

Appendix A3. van Genuchten and Dual porosity models fitted to in situ derived volumetric water content (VWC) and matric potential for 10 points. The blue dots are the measured VWC at different matric potentials. The dotted yellow line indicates van Genuchten model while the solid yellow line indicates dual porosity model. The performance of models was compared based on Root mean square error (RMSE) and Akaike information criterion (AIC). Lower values of these estimates indicate better model. The number in brackets () reflects measurement points.

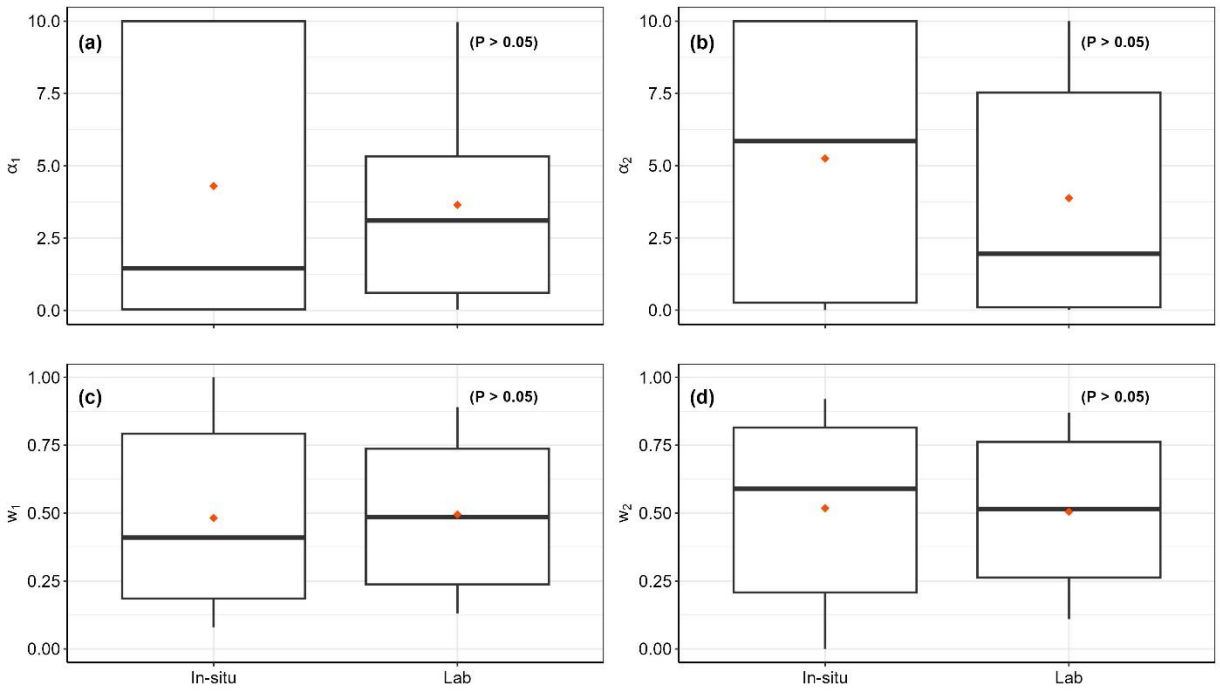

Appendix A4. Distribution of soil hydraulic parameters such as (a) α_1, (b) α_2, (c) w_1, and (d) w_2 between lab and in situ field conditions. The normally distributed data were compared using Student's t-test, while non-normal data were compared using the Mann-Whitley-Wilcoxon test. The centerline of the box plots indicates the median, the upper and lower represent the 25^{th} and 75^{th} quantiles, and the red dot reflects the arithmetic mean of hydraulic parameters for clusters. The mean estimates of these hydraulic parameters were statistically insignificant ($p > 0.05$) between the lab and the field

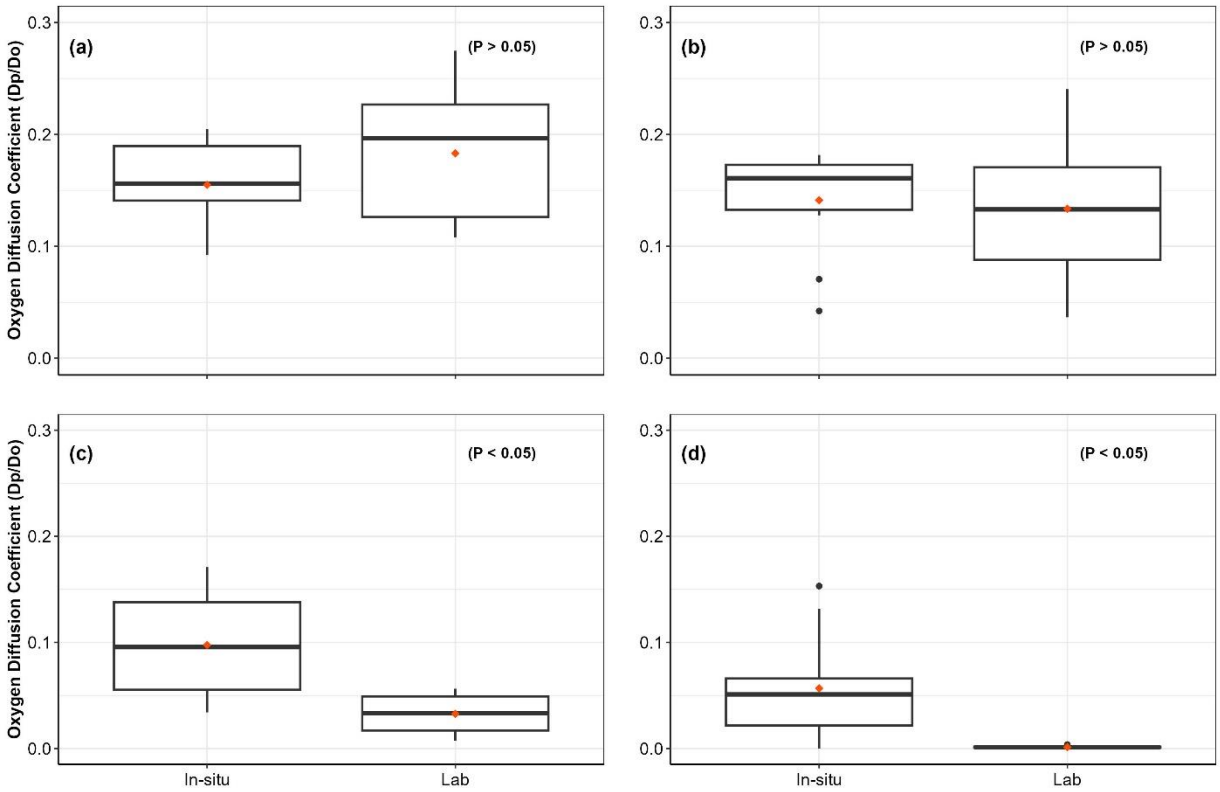

Appendix A5. Distribution of O_2 diffusivity at (a) residual moisture, (b) threshold moisture, (c) field capacity (FC), and (d) saturation between in situ and lab conditions. The centerline of the box plots indicates the median, the upper and lower represent the 25^{th} and 75^{th} quantiles, and the red dot reflects the arithmetic mean O_2 diffusivity/diffusion coefficients. The p value ($p < 0.05$) represents a significant cluster difference.

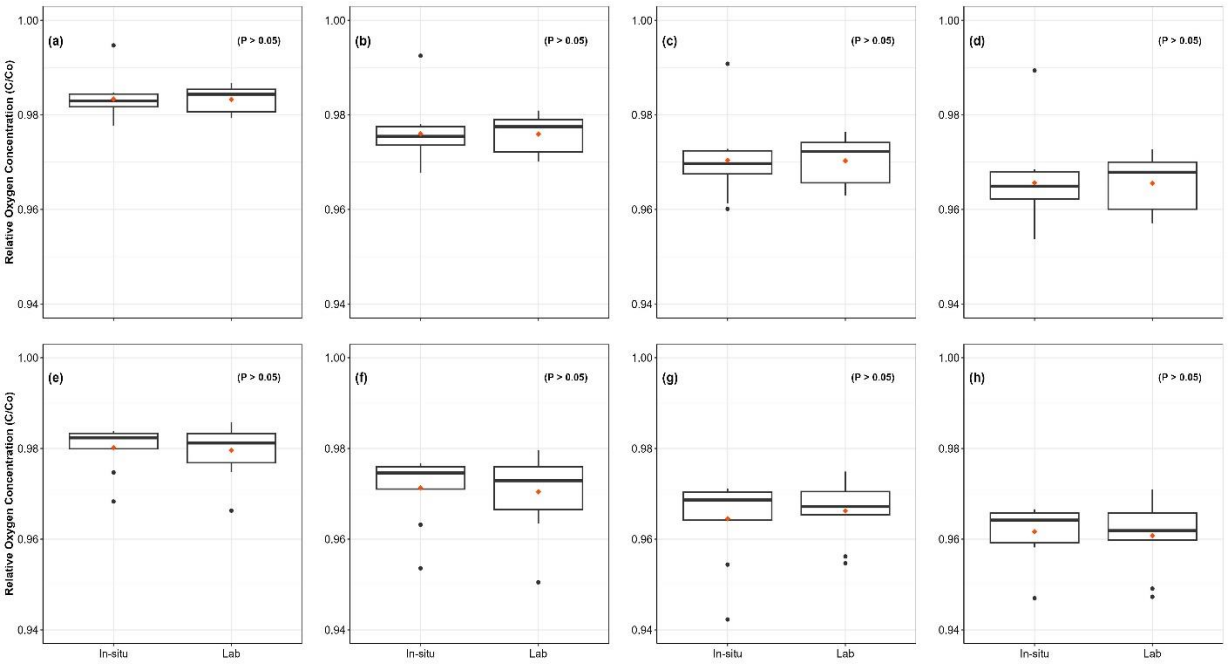

Appendix A6. Distribution of relative O_2 concentration in clusters estimated for O_2 diffusivity at residual moisture at (a) 12 hours, (b) 24 hours, (c) 36 hours, and (d) 48 hours and diffusivity at threshold moisture at (e) 12 hours (f) 24 hours (g) 36 hours, and (h) 48 hours after equilibrium concentration with atmosphere. The centerline of the box plots indicates the median, the upper and lower represent the 25^{th} and 75^{th} quantiles, and the red dot reflects the arithmetic mean of relative O_2 concentration for clusters. The relative oxygen concentrations were statistically insignificant and different ($p > 0.05$) in situ and lab conditions.

CHAPTER 3

PHYSICAL CONTROLS OF SOIL ANOXIA IN AGRICULTURAL FIELDS AND IMPLICATIONS FOR NITROUS OXIDE EMISSION[2]

[2] Yadav, H and Gaur, N. To be Submitted to [Water Resources Research]

ABSTRACT

Anoxic pores in the near-surface influence land-atmosphere interactions by affecting ecosystem fluxes and the persistence of soil carbon stocks. Specifically, in agricultural systems, they can trigger the conversion of applied fertilizers into potent greenhouse gases (GHGs) like nitrous oxide (N_2O) and methane (CH_4). Therefore, quantifying the volume of anoxic microsites at the field scale is essential for predicting soil carbon and nitrogen dynamics. However, the potential for soil pores to become anoxic depends on soil pore distribution and their wetting dynamics. Since soil structure and pore size distribution are highly variable in the space-time domain, especially for agricultural soils exposed to several land-management practices, it has been impractical to estimate soil anoxia at the field scale. This study aimed to estimate the potential anoxic volume at the field scale by characterizing and quantifying pores having a higher potential for becoming anoxic. We collected 24 soil cores from cropland planted with corn and developed high-resolution and complete soil moisture release curves. The relation between cumulative soil moisture as a function of pore diameter was deduced from a release curve and used for estimating lower (1 μm) and upper (3 μm) thresholds. These thresholds were applied to estimate field-scale potential anoxic volume at 24 and 48 hours after rainfall. The peak N_2O emission time along with the temporal variation in soil moisture during 6 months period were used to validate the thresholds. The field-scale estimations were done by interpolating point measurements using inverse distance weighted (IDW) and co-kriging. Random forest regression was performed to predict thresholds based on sand, clay, loss-on-ignition carbon, and porosity. The result showed that almost all tiny pores (< 1 μm) distributed in the field remained saturated and potentially anoxic, while large pores were partially filled and oxic at 24 and 48 hours after rainfall. The thresholds captured the N_2O peaks; most of these peaks were observed when soil moisture was above the upper threshold.

Moreover, the best predictors of the lower and upper thresholds were clay and sand, respectively. This field-scale estimation suggests that the spatial distribution of the potential anoxic volume depends on the density of small pores (≤ 1 μm), which can stay saturated for at least 48 hours. This spatio-temporal estimation approach provides insights into macroscale ecological processes, including soil nutrient dynamics and organic carbon stabilization. This estimation can support optimizing fertilizer application and curtain GHGs production from agricultural fields, eventually enhancing ecosystem sustainability.

1 INTRODUCTION

Agricultural soils play a crucial role in regulating the sustainability of our global ecosystem. They act as a major sink and a source of potent greenhouse gases (GHGs) such as nitrous oxide (N_2O), methane (CH_4), and carbon dioxide (CO_2) (Henault et al., 2012; Keiluweit et al., 2018; Smith, 2017). A substantial amount of carbon (C) stored in cultivated soils is vulnerable to land use and management practices (Keiluweit et al., 2018; Lacroix et al., 2022). Around 60% of the total N_2O emission has been from agricultural soils since the industrial age (Smith, 2017; Xing et al., 2023). However, the release of C and N in the form of GHGs depends on the heterogeneous distribution of saturated soil pores having a higher proclivity to become anoxic (Lacroix et al., 2021; Mathieu et al., 2006; Schlüter et al., 2019). The variation in physical attributes, such as pore architecture and pore continuity, and soil hydraulic properties in combination with soil organic C governs the generation and persistence of anoxic conditions, affecting the biogeochemistry of soils. Saturated pores that are anoxic can enhance the production of N_2O by reducing nitrate (NO^-_3) and support carbon storage since oxygen is needed to remove soil C efficiently in the form of CO_2 into the atmosphere (Keiluweit et al., 2017; Rohe et al., 2021; Schlüter et al., 2019). Quantifying the distribution of O_2-deficit saturated pores in agricultural soils could support developing strategies for decreasing N_2O and CH_4 emissions and increasing the residence time of soil C in agricultural soils (Boye et al., 2017; Lin et al., 2021). Since the emission of GHGs affects soil management practices such as tillage, fertilizer application, and irrigation, proper knowledge of the distribution of anoxia could help in developing climate-smart agricultural practices that can substantially enhance the longevity of agricultural systems (Henault et al., 2012).

The generation of soil anoxia is governed by multiple factors, such as soil hydro-physical attributes that drive oxygen transport in the soil, the spatial distribution of microbial hotspots and

substrate availability that drive oxygen consumption, and temperature and soil pH that determine the rate of oxygen consumption (Ambus & Christensen, 1994; Schlüter et al., 2019; Smith, 2017). Various studies have demonstrated the impact of soil physical properties, such as soil texture and structure, on anoxic volume (Keiluweit et al., 2018; Lacroix et al., 2022; Rohe et al., 2021). Keiluweit et al. (2018) found a negative correlation between clay content and oxygen concentration, indicating the existence of anoxic pores in clay-rich microstructures. Lacroix et al. (2022) illustrated the presence of transient anoxic pores in coarse-textured soils due to enhanced microbial respiration and, thus, oxygen demand. On the other hand, Ball (2013) demonstrated that soil structure influences anoxia by controlling inter-aggregate pore space, which substantially affects soil water content and pore continuity. Pore continuity and water content regulate the diffusion of oxygen and water-extractable organic matter toward and away from the microbial hotspots (Rohe et al., 2021). As a result, many researchers have found a strong correlation between soil moisture and nitrous oxide peaks (Ball, 2013; Schlüter et al., 2019; Smith, 2017; Yanai et al., 2003). Anthony et al. (2023) observed significantly greater N_2O fluxes during irrigation and rainfall events from an alfalfa field, which was periodically flood-irrigated during the growing season. Although ample evidence relates soil moisture to anoxic volume, specific soil moisture conditions and physical descriptors of soil moisture status that create anoxia at a larger scale have not been identified.

Variation in soil physical properties, such as soil texture and structure, often obscures the correlation between soil moisture estimates and related anoxic volume of croplands at a larger scale. Although the soil texture remains constant at a short-temporal scale, soil structure can vary substantially due to above-ground biomass, soil organic C, microbial activity, and management practices, such as tillage and fertilization strategies (Eden et al., 2012; Iqbal et al., 2005; Kheir et

al., 2010; Or et al., 2007). Agricultural practices affect the distribution and mineralization of soil organic C, affecting soil aggregate size and pore-size distribution (Eden et al., 2012; Lipiec et al., 2006; Nath & Rattan, 2017). In addition, the combination of soil particles could greatly vary the size of soil aggregates and intra-aggregate pore sizes (Neira et al., 2015). These changes in soil structural attributes can increase field-scale heterogeneity of soil physical parameters, such as water-filled porosity, total porosity, water retention, and preferential flow paths. Changes in these soil physical parameters substantially influence the spatial and temporal scale variabilities of water content in soil pores, affecting the chemical and biological properties of soils. Peterson et al. (2019) attributed field-scale soil moisture heterogeneity to changes in topography and soil physical factors and demonstrated higher soil moisture variability for wet and dry conditions than intermediate wetness. Or et al. (2007) found the dependency of microbial respiration on microbial habitats and diffusion pathways in unsaturated porous media, which is attributed to soil structure. Therefore, it is essential to quantify the effect of structural variability on soil moisture of agricultural soils for modeling processes, particularly soil anoxia affected by soil moisture.

Various biogeochemical models have been developed to estimate N_2O and CO_2 emissions from agricultural soils, but these models do not adequately incorporate the descriptors of soil anoxic volume. Some of these models, such as traditional Day Cent and Roth C, assumed the soil system to be completely oxic (Gottschalk et al., 2012), while others do not precisely delineate the effect of oxygen availability in aerobic soils (Davidson et al., 2012; Moyano et al., 2013). Recently developed biogeochemical models, however, have considered anoxic volume using an approximation of aggregate model but still do not address the heterogeneity of soil structures by considering a constant microbial response (Keiluweit et al., 2018). More pronounced estimations of anoxic volume considering soil heterogeneity and observed patterns of pore-scale oxygen

concentration are limited to aggregate and core scales (Keiluweit et al., 2018; Lacroix et al., 2021). Although small-scale estimation accurately estimates anoxia, the results are not directly transferable in the field owing to soil's physical, chemical, and biological heterogeneity. Such field scale estimates are required to develop and evaluate mitigation strategies related to GHG emissions and carbon restoration.

This study estimated the spatial and temporal distribution of potential anoxic volume at the field scale by integrating lab and in situ field measurements. Moisture contents corresponding to two soil pore sizes: lower (1 micron) and upper (3 microns), that serve as anoxic volume thresholds in soil were estimated from lab-developed soil moisture release curves for undisturbed soil cores (N = 24) and interpolated using Inverse Distance Weighted (IDW) method to develop field-scale lower and upper threshold moisture maps. These threshold maps represent the spatial distribution of soil moisture in the field required to saturated soil pores smaller than or equal to 1 micron (μm) and 3 microns (μm), respectively. Thresholds were determined based on the Lacroix et al. findings, who reported that saturated pores having diameters less or equal to 1 μm and greater than 3 μm have a higher potential to become anoxic (Lacroix et al., 2021). The threshold maps were deducted from bulk soil moisture maps, developed by co-kriging soil moisture with an auxiliary variable: soil electrical conductivity, to estimate potential anoxic volume distribution of smaller (≤ 1 μm) and larger pores (> 3 μm) at the field scale. Soil moisture maps were developed to represent soil moisture status at 24 and 48 hours after rainfall, and the spatio-temporal variation in field scale anoxia was estimated by comparing these maps with the threshold maps. The computed thresholds were validated for the field based on in situ weekly measurements of nitrous oxide gas using manual gas chambers. The ability of thresholds to capture nitrous oxide peaks simultaneously with soil moisture peaks was evaluated over 6 months. Additionally, in order to enhance the

transferability of this study, a model was developed to predict lower and upper thresholds based on clay, sand, loss-on-ignition carbon, and porosity.

2 MATERIALS AND METHODS

2.1 SITE DESCRIPTION

The field-scale estimation of potential anoxic volume was conducted at the University of Georgia's Iron Horse Farm (IHF), located in the blue ridge and Piedmont region in Oconee County, Georgia (GA), USA. The IHF soil is characterized as very deep, well-drained, moderately permeable, and eroded, formed on the ridges and the sides of the Piedmont uplands (California Soil Resource Lab and USDA Natural Resources Conservation Service). According to USDA taxonomy, the soil is classified as Cecil (Fine, Kaolinitic, thermic Typic Kanhapludults) with sandy loam texture (Soil Survey Staff Natural Resources Conservation Service United States Department of Agriculture (USDA), 2017), having 2 to 10 percent (%) slopes. The average annual temperature and precipitation are 19.6 ^{o}C and 1354.1 mm yr^{-1}, respectively (University of GA Environmental Monitoring Network, 1957–2016).

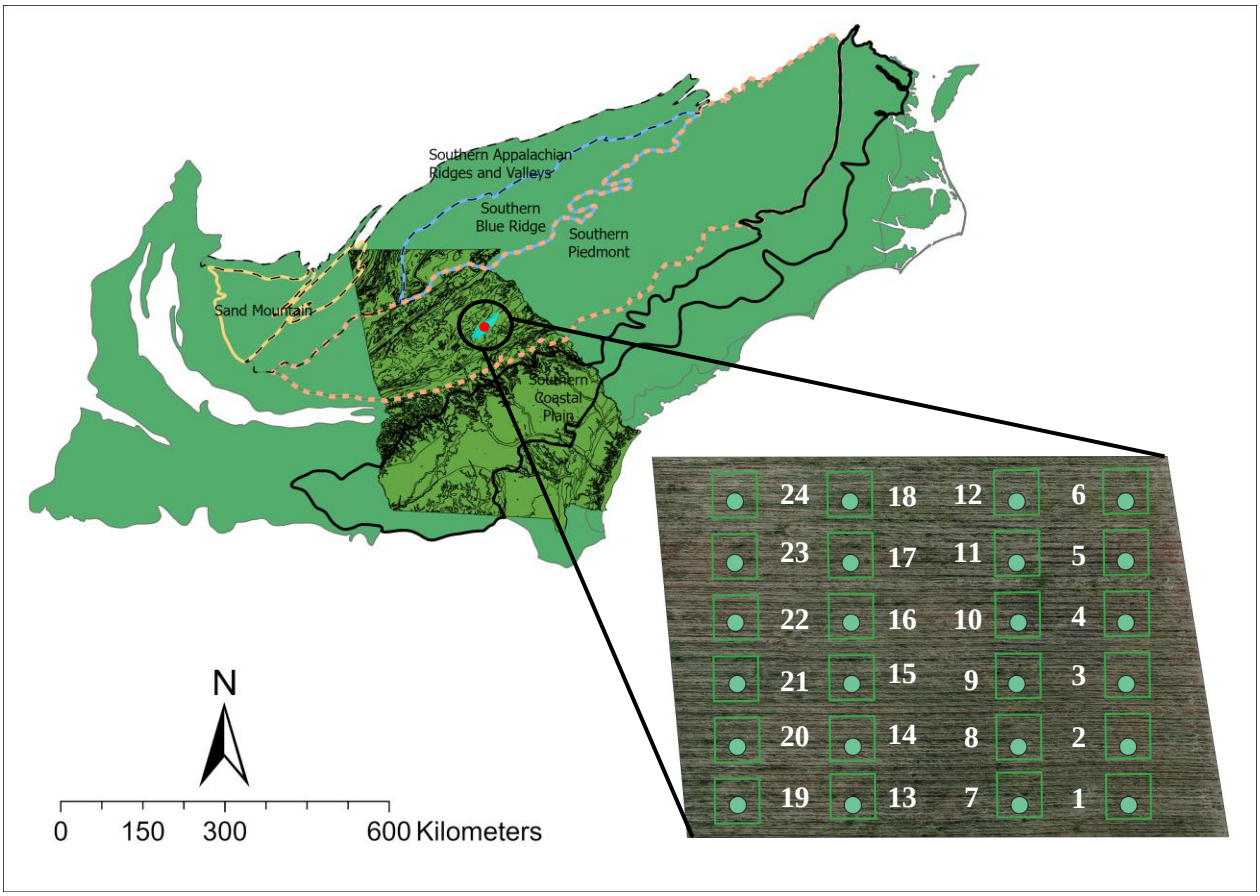

Figure 3.1. Map of the study area. The red dot inside the black circle on the Georgia map reflects the location of the study site. The green rectangular boxes on the study site indicate plots, and the green circles represent points from where soil samples were collected.

Field and lab measurements were conducted simultaneously with another field experiment, which aimed at finding the best combination of herbicides and cover crops for corn production. For the field research, the site (Figure 3.1) was divided into 24 plots (0.06 ha each), and treatment combinations of cover crops (rye or conventional) and different levels of herbicides (High, Low, No) were applied randomly. Manual gas chambers were installed in each plot to measure greenhouse gases, such as N_2O, CH_4, and CO_2, once per week in the morning over 6 months period. Soil management practices, such as fertilizers (NPK) and irrigation, were similar among the plots.

2.2 SOIL CORE COLLECTION

Undisturbed soil cores, having a diameter of 8 cm and a height of 6.3 cm, were collected from the site to develop complete, high-resolution soil moisture release curves in August 2022. In total, 24 soil cores were collected, one from each experimental plot, from the top horizon close to installed manual gas chambers using stainless steel cores and rubber mallets. The soil cores were capped with plastic caps and brought to Environmental Soil Physics Lab at the University of Georgia. The cores were placed in a refrigerator in the lab to avoid moisture loss.

2.3 LAB MEASUREMENTS

The high-resolution, complete soil moisture release curves were developed to analyze the relationship between volumetric water content (VWC) and the matric potential (ψ) for each soil core. Two instruments, HYPROP (Meter Group, Inc., Pullman, WA, USA) and WP4C (Meter Group, Inc., Pullman, WA, USA), were used for developing soil moisture release curves. The detailed descriptions of these instruments are illustrated in Chapter 2.

After developing moisture release curves, soil cores were used to estimate particle size distribution (sand, silt, and clay) and loss-on-ignition carbon. The procedures for the estimation are presented in Chapter 2.

2.4 ESTIMATION OF THRESHOLDS

Soil moisture and matric potential, measured using HYPROP and WP4C, were combined to develop a complete soil moisture release curve, representing moisture fluctuation at wide ranges of matric potential. Two retention models, namely van Genuchten (Van Genuchten, 1980) and Dual porosity (Durner, 1994), were fitted, and the best model, evaluated based on root mean square error (RMSE) and akaike information criterion (AIC), was used to simulate soil moisture behavior at different pressure suction for a specific soil core. A curve representing volumetric water content

(VWC) as a function of a pore diameter was developed from the fitted soil moisture release curve for estimating lower and upper thresholds (Appendix B3). For this, the matric potential was converted to pore diameter using the Laplace equation, which is expressed as follows:

$$h = \frac{2\sigma cos\beta}{\rho r g} \quad [1]$$

where r is the radius of the pore (m), σ is the surface tension (kg s^{-1}), h is the matric potential (cm), ρ is the density of water (kg m^{-3}), g is the acceleration due to gravity (ms^{-2}) and β is the contact angle between soil particle and water. This equation assumes that the density and surface tension of the liquid phase is constant and is only valid for steady-state conditions. Assuming for water at 25 ^{0}C, σ = 7.5 × 10^{-2} kg s^{-2}, ρ = 998.2 kg m^{-3}, and β = 0^o (Chang et al., 2019; Mohammadi & Vanclooster, 2011), pore diameter was estimated corresponding to specific matric potential. The sensitivity of upper and lower thresholds to changes in contact angle was explored by comparing thresholds estimated at 0^o and 40^o contact angles. The lower and upper thresholds represent water required to saturate pores with diameters less or equal to 1 μm and 3 μm, respectively. These thresholds were determined to quantify soil moisture in small (≤ 1 μm) and large (> 3 μm) pores after rainfall. They were determined based on Lacroix et al. (2021), who demonstrated that saturated soil pores less or equal to 1 μm and greater than 3 μm have a higher potential to become anoxic (2021). They found that larger pores inhabit a relatively high microbial population that increases oxygen demand and makes soil pores periodically anoxic; however, smaller pores become oxygen-limited for longer due to constraints in oxygen supply due to poor pore connectivity and high tortuosity. The thresholds were validated based on the ability to capture N_2O peaks. To check the saturation of large pores, we used θ_s parameter fitted to the soil moisture

release curve (Chapter 2), representing soil moisture needed for complete saturation of capillary pores.

2.5 IN SITU FIELD MEASUREMENTS

Soil moisture readings were taken at three points around manual gas chambers (N = 24) using an HH2 Moisture Meter connected to ML3 Theta Probe (Delta-T Devices Ltd, Cambridge, UK) simultaneously after measuring the electrical conductivity (EC) of the field. The EC measurements were taken by dragging Ground Conductivity Meter (EM38-MK2, Geonics Ltd, Ontario, Canada) throughout the field at 24 and 48 hours after rainfall to estimate their temporal variation at the field scale. Two such rainfall dry-downs were measured. One end of the instrument (transmitter coil) injects current into the soil, while the other (receiver coil) measures the induced secondary magnetic field. Using EC measurement as an auxiliary variable, soil moisture was then interpolated by co-kriging to develop bulk soil moisture maps, representing field scale moisture status at 24 and 48 hours after rainfall (Molin & Faulin, 2013). Additionally, soil moisture sensors (ECH20 10 HS and 5 TE, Decagon Devices, Inc., Pullman, WA, USA) were installed at 10 cm depth in ten plots near manual gas chambers to measure in situ variation in VWC (accuracy: ± 2% VWC) every minute during 6 months period (April to September). The moisture sensors were connected to two different data loggers that were ZL6 (Meter Group, Inc., Pullman, WA, USA) and Em50 data logger (Decagon Devices, Inc., Pullman, WA, USA), based on availability. Moreover, the information regarding nitrous oxide peak emissions was obtained from a concurrent study done by Saikawa et al. (2022), who measured nitrous oxides emission weekly during a 6-month period using manual gas chambers and Picarro G2508 analyzer (Picarro, Inc., CA 95054, USA).

2.6 GEOSPATIAL INTERPOLATION AND STATISTICAL ANALYSIS

Geostatistical analysis, including inverse distance weighted (IDW) and ordinary co-kriging, were performed to develop field-scale thresholds and bulk soil moisture maps using ArcGIS Pro (version 3.0.0, Esri, Redlands, CA, USA). A field-scale saturation map using θs was developed to examine the saturation of large pores. The field-scale texture (sand and clay), bulk density, porosity, and loss-on-ignition C maps were also developed using the IDW method. IDW and ordinary co-kriging are commonly used spatial techniques for interpolating variables scattered in space (Belkhiri et al., 2020; Chen & Liu, 2012). The former creates spatial weights matrices for interpolation by assigning greater weights to points closest to the prediction location. This method assumes that each measured point has a local influence that diminishes with the distance of interest. The latter method uses spatially correlated secondary variables to the variable of interest for interpolation. Co-kriging assumes that the primary and secondary variables have a linear relationship and share a common spatial structure.

The R software (R Foundation for Statistical Computing, Vienna, Austria) was used for statistical analysis. Considering high collinearity among explanatory variables: clay, sand, loss-on-ignition carbon, and porosity, a random forest model was run with 1000 iterations, and the mean variable importance plot was made to identify variables contributing more to the dependent variables. The model performance was gauged based on root mean squared error (RMSE). Figures were produced using the ggplot2 package (Wickham et al., 2016).

3 RESULTS AND DISCUSSION

3.1 SPATIO-TEMPORAL DISTRIBUTION OF POTENTIAL ANOXIC VOLUME

Potential anoxic volume distribution was determined by estimating the volume of saturated soil pores less than or equal to 1 μm and greater than 3 μm. The saturated pore sizes were quantified by deducting the threshold maps: upper (3 μm) and lower (1 μm) thresholds from each bulk soil moisture map developed at 24 and 48 hours after rainfall. The saturation map, developed using fitted θ_s parameter to the soil moisture release curve, was used for inspecting the saturation of large pores (> 3 μm).

Figure 3.2 reflects the soil moisture required to saturate soil pores less than or equal to 1 μm (lower threshold) and 3 μm (upper threshold) of the field. The changes in liquid-soil contact angle have an insignificant influence on moisture thresholds as the thresholds were similar when compared between 0^o and 40^o (Appendix B1). The volumetric distribution of soil moisture depends on the pore-size distribution and structural heterogeneity, influenced by soil texture and organic matter content (Eden et al., 2012). Lower and upper threshold maps revealed that relatively higher soil moisture is needed to saturate soil pores distributed in the northwest region (Figure 3.2a, b). This anomaly suggests a high density of connected smaller (≤ 1 μm) and medium-sized pores (1 – 3 μm) in the northwest compared to other regions. The high concentration of small and medium-sized pores is attributed to a greater percentage of small-sized particles (clay and silt) and loss-on-ignition C, facilitating aggregation and uniform pore-size distribution (Chang et al., 2019; Kutílek, 2004) (Appendix B2 a, e). However, the sand content was also higher in the northwest region, contributing to the formation of large pores (> 3 μm) (Appendix B2 b). The presence of large structural pores embedded in the soil matrix containing small and medium-sized pores in this region is evident from the study conducted in Chapter 2. They found a higher α_1/α_2 ratio of soil

cores collected from the northwest field region, indicating large pores enmeshed in the soil matrix (Zhang et al., 2022). Moreover, the higher density of small and medium-sized pores was also reflected in field-scale porosity and bulk density maps (Appendix B2 d); porosity was higher while bulk density was lower in the northwest region.

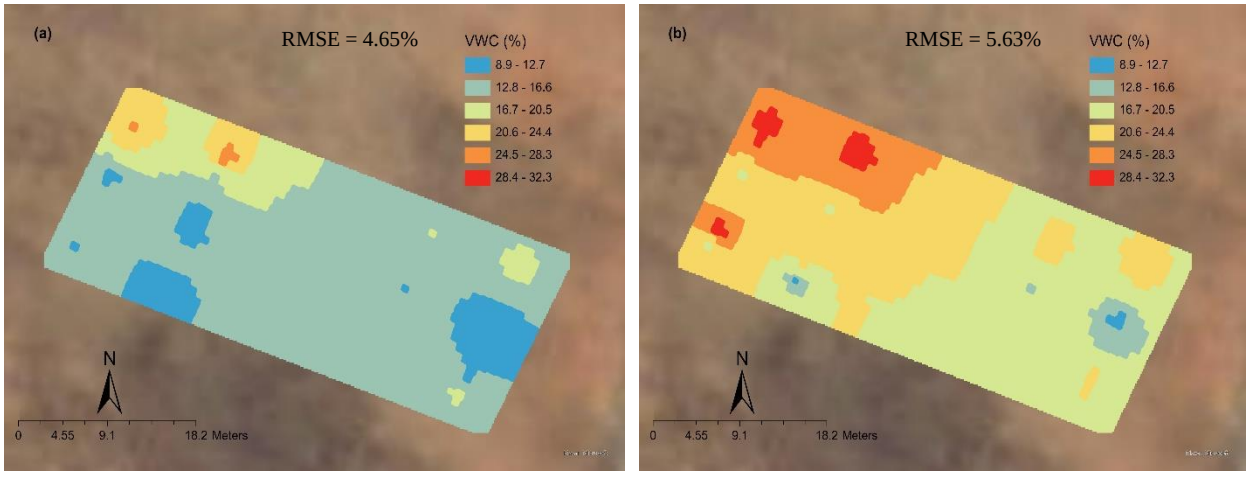

Figure 3.2. Spatial distribution of volumetric water content (VWC) (%) in pores (a) ≤ 1 µm (b) ≤ 3 µm. The root mean square value (RMSE) indicates the difference between predicted and measured water contents.

The volumetric distribution of soil moisture at 24 and 48 hours after rainfall is illustrated in Figure 3.3. Gaur and Mohanty (2013) demonstrated that spatial soil moisture distribution is mainly dominated by soil properties as opposed to topography and vegetation variability at the field scale. In our study, soil moisture was comparatively higher in the east and west regions of the field at 24 hours, although porosity was lower on the east side of the field (Figure 3.3a). After 48 hours, moisture substantially declined on the east side of the field while moisture on the west side remained primarily unchanged (Figure 3.3b). This anomaly in the drainage pattern could be attributed to the dominance of soil structural features and pore-size distribution. The east side of the field had comparatively higher clay than sand but lower loss-on-ignition C (Appendix B2 a, e). The lower soil C is related to poor structural features and thus narrow pore-size distribution, as

soil C enhances soil structural attributes (Eden et al., 2012). Moreover, the fitted weighting parameter, w, of soil moisture release curves, developed for soil samples collected from the east region of the field, showed a significant contribution of macropores to the total soil moisture in this region (Chapter 2). As macropores have a higher tendency to get drained, soil moisture could have declined relatively faster in this region. However, despite higher sand content in the west region of the field, the relatively constant soil moisture may have been due to comparatively higher silt and loss-on-ignition C, contributing to the soil moisture retention capacity. Previous studies have accounted for the role of pore architecture and their physico-chemical composition in moisture retention in soil (Crawford et al., 1995; Young et al., 2008). The influence of texture and organic carbon on pore-size distribution has been documented by several studies (Beckett & Augarde, 2013; de Lima et al., 2022; Mtambanengwe et al., 2004; Nimmo, 2004). These studies revealed that organic carbon could substantially contribute to the formation of structured pores in soils with higher clay or silt fraction.

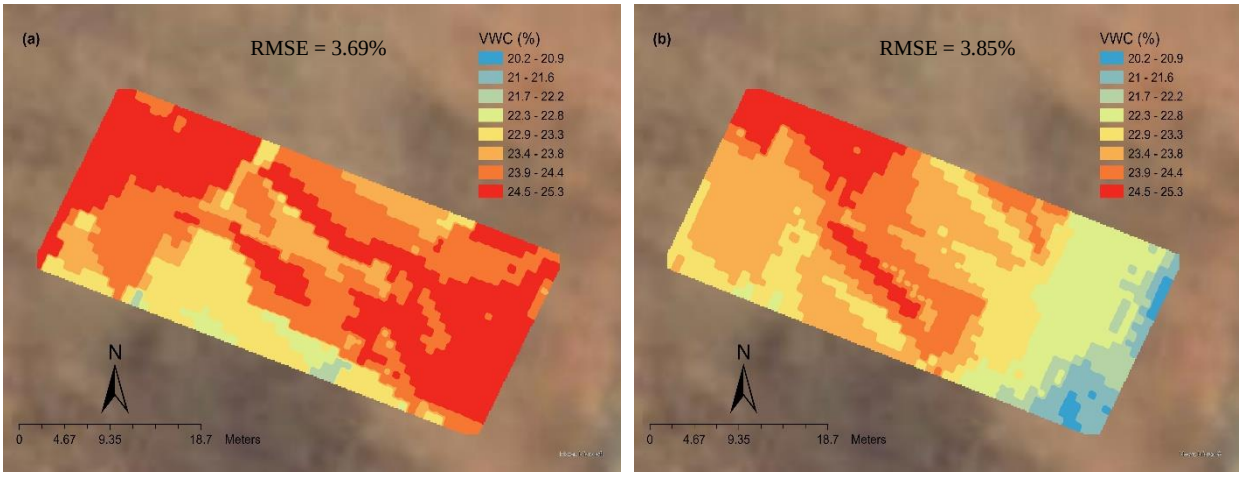

Figure 3.3. Spatial distribution of volumetric water content (VWC) (%) at (a) 24 hours and (b) 48 hours after rainfall. The root mean square value (RMSE) indicates the difference between predicted and measured water contents.

Figure 3.4 illustrates the spatial distribution of potential oxic and anoxic volume in the field at 24 and 48 hours after rainfall. Most of the small pores (≤ 1 μm) were potentially anoxic at 24 hours after rainfall except for a small portion (indicated by dark blue) in the northwest region (Figure 3.4a). The dark blue region in the northwest needed a greater amount of threshold moisture (average: 26.4% VWC) for saturation than was supplied by the rainfall that raised the VWC to only 24.9%. But the large pores (> 3 μm) were unsaturated throughout the field because the moisture contributed by the rainfall was inadequate to saturate them completely. In addition to the soil moisture contributed by the rainfall, the large pores of the field needed 10.9 to 30.4% VWC on average for saturation at 24 and 48 hours after rainfall (Figure 3.5a, b).

The distribution of potentially anoxic pores contributed by saturated small pores remained almost constant within 24 hours (Figure 3.4c). The persistence of anoxic conditions in small pores can be explained by the strong capillary forces (adhesion and cohesion) in small pores that enable them to hold water against the forces of gravity (Gardner, 1979; Tuller et al., 2004). Moreover, this effect could be due to the redistribution of water from large to small pores (Figure 3.4d) as a result of Haines instability, which forces the non-wetting phase (air) into larger pores, thus

displacing the water from the large pores. This phenomenon is a dominant pore-scale water displacement event during drainage conditions (Bakhshian et al., 2021).

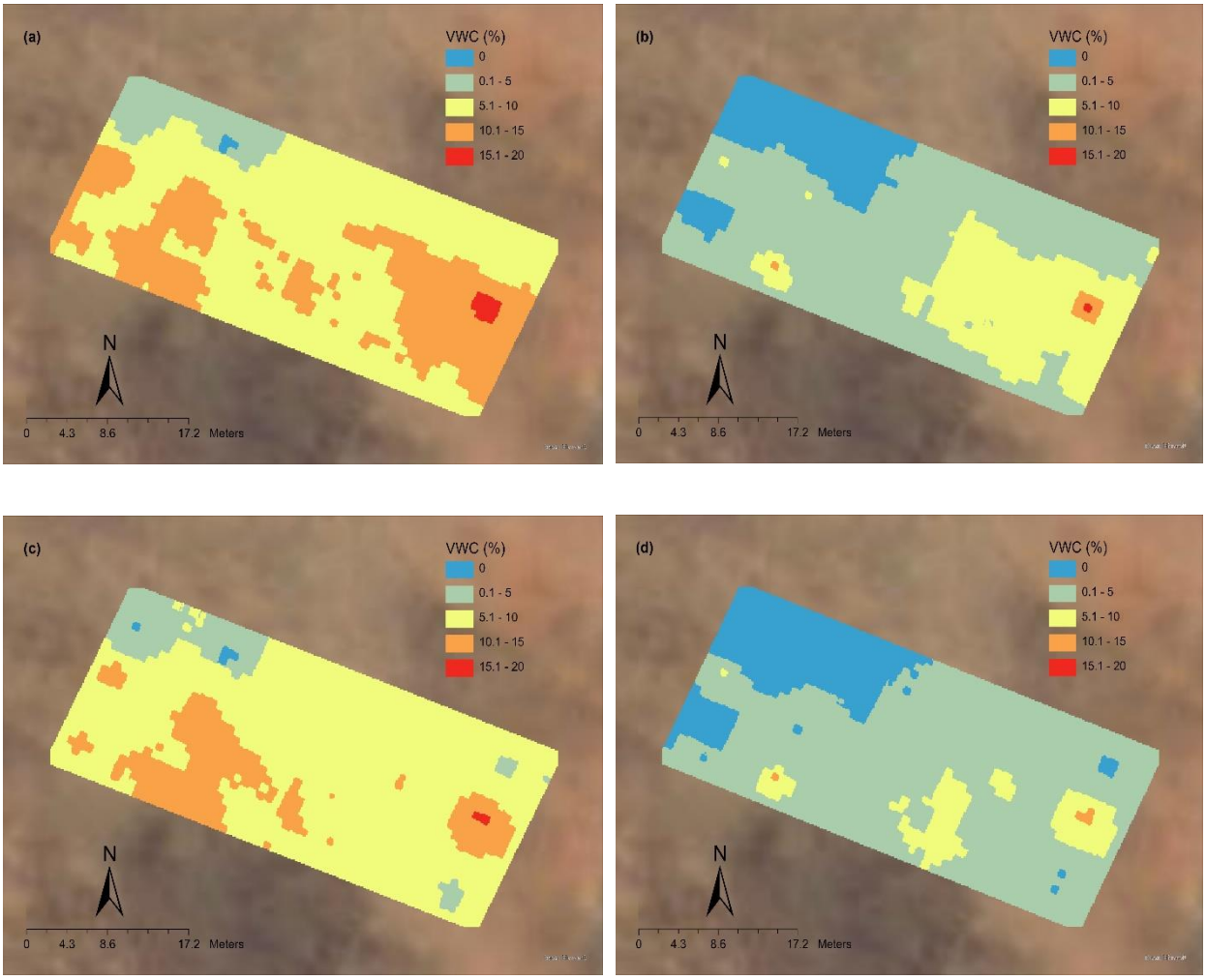

Figure 3.4. Spatio-temporal variation of potential anoxic volume at 24 hours in pores (a) less or equal to 1 μm and (b) greater than 3 μm; at 48 hours in pores (c) less than or equal to 1 μm and (d) greater than 3 μm after rainfall.

The result indicated that although large pores have a higher potential to become anoxic (Lacroix et al., 2021) due to the high oxygen demand created by microbial activity, these large pores barely get saturated in the field. And even if large pores get saturated due to intensive rainfall, they drain quickly compared to small pores, rendering soil oxic. But the tiny pores become

saturated after rainfall and can stay potentially anoxic by limiting oxygen diffusion through them for at least 48 hours in the field, contributing more to potential anoxic volume. Therefore, small pores play a crucial role in making soil conducive for the emission of nitrous oxides and soil organic carbon preservation in the field condition for at least 48 hours after rainfall under field conditions.

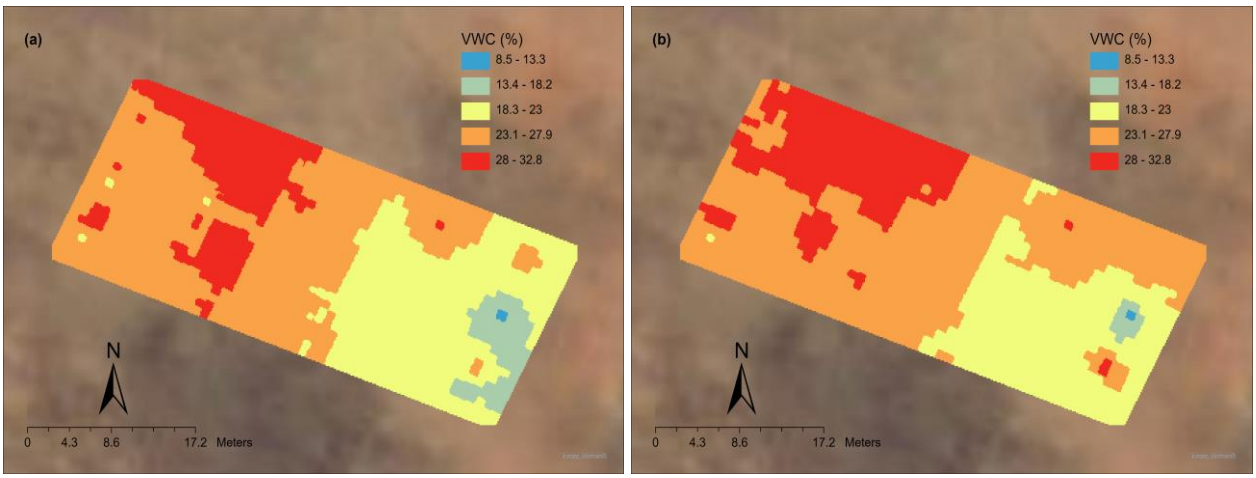

Figure 3.5. Spatial distribution of soil moisture deficit at (a) 24 hours (b) 48 hours after rainfall for complete saturation of large pores (> 3 microns).

3.2 VALIDATION OF THRESHOLDS

The lower and upper thresholds, estimated using θ(r) curve, represent the volumetric distribution of small (1μm) and large (3 μm) pores in the field. The θ(r) curve depicts the variation in soil moisture as a function of pore sizes. These lower and upper thresholds were computed in terms of volumetric water contents corresponding to volumetric pore size distribution. All the pores less or equal to 1 μm and 3 μm were assumed to be saturated at moisture equal to lower and upper thresholds, respectively. In the field, the lower and upper thresholds were mainly in the range of 10 - 20% of the total soil moisture (Figure 3.6a-j). The upper thresholds were higher than

20% soil moisture at two measurement points, indicating a higher percentage of small and medium-sized pores (Figure 3.6c, d).

Soil moisture greater than lower and upper thresholds mostly coincided with nitrous oxide (N_2O) peaks (Figure 3.6a-j) except for two points where N_2O peaks were observed when bigger pores were empty (Figures 3.6c, d). However, the lower thresholds captured the N_2O peaks at these two points. The observed anomaly was possibly due to the higher contribution of small and medium-sized pores to soil moisture, which is evident from the fact that soil moisture barely touched the upper threshold. The significant contribution of micropores to the total soil moisture at these two locations, as indicated by the lower weighting parameter, w_1, is also evident in Chapter 2. The weighting parameter, w_1, of the soil moisture release curve was lower at these points, reflecting the substantial role of micropores in soil moisture retention at different matric potentials. Additionally, the single N_2O peak per site might have been due to the lower sampling frequency of manual chambers (Smith, 2017). Consequently, it can be inferred that soil moisture greater than the upper threshold makes soil pores highly conducive for nitrous oxide emission. However, some peaks can be observed even at moisture slightly greater than or equal to the lower threshold.

Several studies have documented nitrous oxide pulses after rainfall and applying fertilizers (Anthony et al., 2023; Butterbach-Bahl et al., 2013; Smith, 2017); however, they do not relate N_2O pulses to the actual soil moisture corresponding to specific pore sizes. This study provides insights into the soil moisture distribution in soil pores that contribute to nitrous oxide emission.


(a)
(b)
(c)
(d)
(e)
(f)
(g)
(h)
(i)
(j)
Upper Threshold (3 µm)
Lower Threshold (1 µm)
Soil moisture (%)
Rainfall (mm/day)
Time (days)
Apr-21
May-05
May-19
Jun-02
Jun-16
Jun-30
Jul-14
Jul-28
Aug-11
Aug-25
Sep-08
Sep-22

Figure 3.6. In situ soil moisture variation and nitrous oxide (N_2O) peak emission at 10 points (a-j) in the field. The yellow and black lines represent lower and upper thresholds, indicating the volumetric distribution of pores equal to 1 μm and 3 μm in terms of soil moisture. The dotted red line reflects peak N_2O emission in the field at respective points. The light blue line represents precipitation that occurred in the field. The gaps between soil moisture and precipitation were subsidized by irrigation.

3.3 EXPLANATORY VARIABLES FOR THRESHOLDS

The upper and lower thresholds were determined based on the θ(r) curve derived from a soil moisture release curve. This threshold estimation method generally takes longer (more than a week). However, identifying explanatory variables that are highly correlated with thresholds could offer opportunities to estimate them directly for a field. A random forest model was implemented using explanatory variables such as sand (%), clay (%), porosity (%), and loss-on-ignition C to predict lower and upper thresholds. Around 1000 iterations were done to find the mean performance of the model using explanatory variables. The model explained 79% variation in the dependent variables: upper (R^2 = 0.79) and lower (R^2 = 0.79) thresholds. The RMSE of the model for upper and lower thresholds was found to be 1.46% and 1.16%, respectively. For the lower threshold, clay and porosity were the best predictors, while sand and porosity were the best predictors in the case of the upper threshold (Figure 3.7a, b). Clay content increased small-sized pores, contributing to lower thresholds, while sand content enhanced bigger pores in soils, increasing upper thresholds. Studies have presented similar findings where small pores were related to higher clay-sized particles (de Lima et al., 2022; Nimmo, 2004; Zaffar & Lu, 2015).

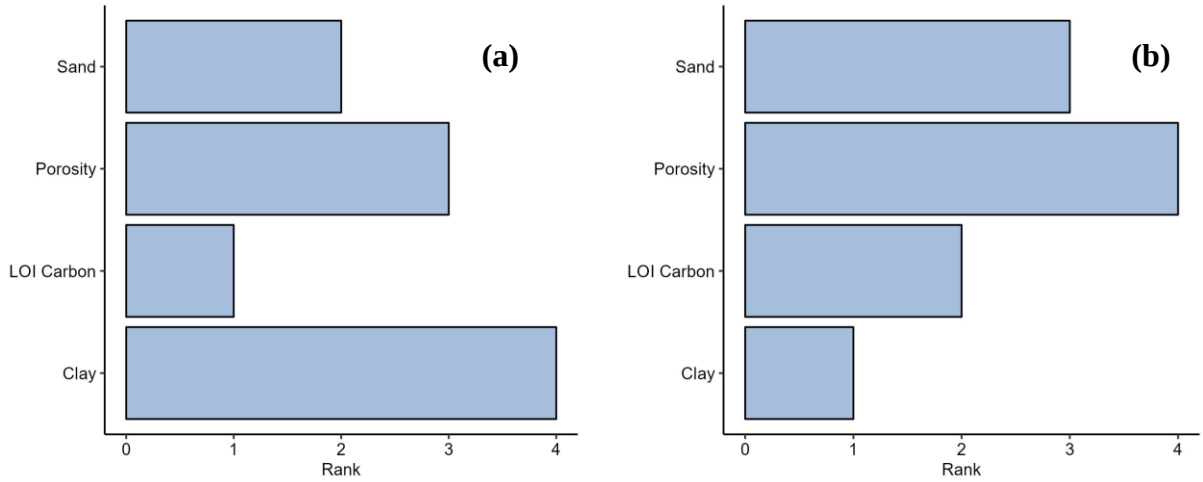

Figure 3.7. Variable importance plot developed using random forest model. The Y-axis represents explanatory variables and X-axis reflects their respective ranks/importance for the prediction of (a) lower threshold (b) upper threshold.

4 CONCLUSIONS

Soil anoxia is a crucial soil phenomenon influencing soil C and nitrogen dynamics. However, quantifying soil anoxia is difficult due to the highly variable soil ecosystem in terms of physical, chemical, and biological properties. Soil physical conditions, specifically soil structure and moisture, can prime the system to become anoxic. This study endeavored to estimate the spatial distribution and temporal change in potential anoxic volume by characterizing and estimating pores based on their potential to become anoxic. The spatial distribution of potential anoxia was compared between 24 and 48 hours after rainfall to quantify the temporal variation in anoxia. At the field scale, smaller pores ($\leq$ 1 μm) have a higher contribution to potential anoxic volume than larger pores (> 3 μm) because of their higher density and strong water retention capacity. While larger pores barely remain saturated in the field, lowering their contribution to the spatial distribution of potential anoxic volume, peaks of N_2O emission in the field were primarily observed when these larger pores became saturated. Consequently, the volumetric distribution of

pore sizes determines the contribution of respective pore sizes to the potential anoxic volume. In addition, the upper and lower thresholds, used for estimating the potential anoxic volume, can be predicted based on the soil's physical attributes, including sand, clay, porosity, and chemical properties such as organic carbon.

This spatio-temporal estimation of soil anoxia provides insights into the contribution of specific soil moisture and their descriptors to potential anoxic volume in an agricultural field. This information can be used to regulate and monitors soil and crop management practices such as fertilization, irrigation, and tillage, enhancing the sustainability of agricultural production. The distribution of potential anoxic zones could explain the dynamics of various soil nutrients such as Fe and Al. Incorporating potential anoxic volume estimation in N and C turnover models would support in accurate prediction of N_2O, CO_2, and CH_4 fluxes from agricultural soils. Consequently, this will offer opportunities to curtain GHGs and increase the residence time of carbon in the soil, eventually enhancing environmental sustainability.

REFERENCES

Agathokleous, E., Feng, Z., Oksanen, E., Sicard, P., Wang, Q., Saitanis, C. J., Araminiene, V., Blande, J. D., Hayes, F., Calatayud, V., Domingos, M., Veresoglou, S. D., Peñuelas, J., Wardle, D. A., De Marco, A., Li, Z., Harmens, H., Yuan, X., Vitale, M., & Paoletti, E. (2020). Ozone affects plant, insect, and soil microbial communities: A threat to terrestrial ecosystems and biodiversity. *Science Advances*, *6*(33), eabc1176. https://doi.org/doi:10.1126/sciadv.abc1176

Ambus, P., & Christensen, S. (1994). Measurement of N_2O emission from a fertilized grassland: An analysis of spatial variability. *Journal of Geophysical Research: Atmospheres*, *99*(D8), 16549-16555.

Anthony, T. L., Szutu, D. J., Verfaillie, J. G., Baldocchi, D. D., & Silver, W. L. (2023). Carbon-sink potential of continuous alfalfa agriculture lowered by short-term nitrous oxide emission events. *Nature Communications*, *14*(1), 1926. https://doi.org/10.1038/s41467-023-37391-2

Arriaga, F. J., Lowery, B., & Mays, M. D. (2006). A fast method for determining soil particle size distribution using a laser instrument. *Soil Science*, *171*(9), 663-674.

Bakhshian, S., Rabbani, H. S., & Shokri, N. (2021). Physics-driven investigation of wettability effects on two-phase flow in natural porous media: Recent advances, new insights, and future perspectives. *Transport in Porous Media*, *140*, 85-106.

Ball, B. (2013). Soil structure and greenhouse gas emissions: a synthesis of 20 years of experimentation. *European Journal of Soil Science*, *64*(3), 357-373.

Beckett, C. T. S., & Augarde, C. E. (2013). Prediction of soil water retention properties using pore-size distribution and porosity. *Canadian Geotechnical Journal*, *50*(4), 435-450. https://doi.org/10.1139/cgj-2012-0320

Belkhiri, L., Tiri, A., & Mouni, L. (2020). Spatial distribution of the groundwater quality using kriging and Co-kriging interpolations. *Groundwater for Sustainable Development*, *11*, 100473.

Berg, S., Ott, H., Klapp, S. A., Schwing, A., Neiteler, R., Brussee, N., Makurat, A., Leu, L., Enzmann, F., Schwarz, J.-O., Kersten, M., Irvine, S., & Stampanoni, M. (2013). Real-time 3D imaging of Haines jumps in porous media flow. *Proceedings of the National Academy of Sciences*, *110*(10), 3755-3759. https://doi.org/doi:10.1073/pnas.1221373110

Bodner, G., Leitner, D., & Kaul, H.-P. (2014). Coarse and fine root plants affect pore size distributions differently. *Plant and Soil*, *380*, 133 - 151.

Boye, K., Noël, V., Tfaily, M. M., Bone, S. E., Williams, K. H., Bargar, J. R., & Fendorf, S. (2017). Thermodynamically controlled preservation of organic carbon in floodplains. *Nature Geoscience*, *10*(6), 415-419.

Brussaard, L., Behan-Pelletier, V. M., Bignell, D. E., Brown, V. K., Didden, W. A. M., Folgarait, P. J., Fragoso, C. E., Freckman, D. W., Gupta, V. V. S. R., & Hattori, T. (1997). Biodiversity and ecosystem functioning in soil. *AMBIO: A Journal of the Human Environment*, *26*, 563-570.

Butterbach-Bahl, K., Baggs, E. M., Dannenmann, M., Kiese, R., & Zechmeister-Boltenstern, S. (2013). Nitrous oxide emissions from soils: how well do we understand the processes and their controls? *Philosophical transactions of the royal Society B: Biological Sciences*, *368*(1621), 20130122.

Campbell, G. S. (1974). A simple method for determining unsaturated conductivity from moisture retention data. *Soil Science*, *117*(6), 311-314.

Campbell, G. S. (1985). *Soil physics with BASIC: transport models for soil-plant systems*. Elsevier.

Castellano, M. J., Schmidt, J. P., Kaye, J. P., Walker, C., Graham, C. B., Lin, H., & Dell, C. J. (2010). Hydrological and biogeochemical controls on the timing and magnitude of nitrous oxide flux across an agricultural landscape. *Global change biology*, *16*(10), 2711-2720.

Chang, C.-c., Cheng, D.-h., & Qiao, X.-y. (2019). Improving estimation of pore size distribution to predict the soil water retention curve from its particle size distribution. *Geoderma*, *340*, 206-212. https://doi.org/https://doi.org/10.1016/j.geoderma.2019.01.011

Chen, F.-W., & Liu, C.-W. (2012). Estimation of the spatial rainfall distribution using inverse distance weighting (IDW) in the middle of Taiwan. *Paddy and Water Environment*, *10*(3), 209-222. https://doi.org/10.1007/s10333-012-0319-1

Cook, G. D., So, H. B., & Dalal, R. C. (1992). Structural degradation of two Vertisols under continuous cultivation. *Soil and Tillage Research*, *24*(1), 47-64. https://doi.org/https://doi.org/10.1016/0167-1987(92)90071-I

Crawford, J., Matsui, N., & Young, I. (1995). The relation between the moisture-release curve and the structure of soil. *European Journal of Soil Science*, *46*(3), 369-375.

CURRIE, J. A. (1984). Gas diffusion through soil crumbs: the effects of compaction and wetting. *Journal of Soil Science*, *35*(1), 1-10. https://doi.org/https://doi.org/10.1111/j.1365-2389.1984.tb00253.x

Davidson, E. A., Samanta, S., Caramori, S. S., & Savage, K. (2012). The Dual Arrhenius and Michaelis–Menten kinetics model for decomposition of soil organic matter at hourly to seasonal time scales. *Global change biology*, *18*(1), 371-384.

de Lima, R. P., Rolim, M. M., Toledo, M. P. S., Tormena, C. A., da Silva, A. R., e Silva, I. A. C., & Pedrosa, E. M. R. (2022). Texture and degree of compactness effect on the pore size distribution in weathered tropical soils. *Soil and Tillage Research*, *215*, 105215. https://doi.org/https://doi.org/10.1016/j.still.2021.105215

Durner, W. (1994). Hydraulic conductivity estimation for soils with heterogeneous pore structure. *Water Resources Research*, *30*(2), 211-223.

Eden, M., Moldrup, P., Schjønning, P., Scow, K. M., & de Jonge, L. W. (2012). Soil-gas phase transport and structure parameters for a soil under different management regimes and at two moisture levels. *Soil Science*, *177*(9), 527-534.

Fatichi, S., Or, D., Walko, R., Vereecken, H., Young, M. H., Ghezzehei, T. A., Hengl, T., Kollet, S., Agam, N., & Avissar, R. (2020). Soil structure is an important omission in Earth System Models. *Nature Communications*, *11*(1), 522. https://doi.org/10.1038/s41467-020-14411-z

Frederick, R. T., Jalal, D. J., & Don, K. (1982). Gaseous diffusion equations for porous materials. *Geoderma*. https://doi.org/10.1016/0016-7061(82)90033-7

Gardner, W. H. (1965). Water Content. In *Methods of Soil Analysis* (pp. 82-127). https://doi.org/https://doi.org/10.2134/agronmonogr9.1.c7

Gardner, W. H. (1979). How water moves in the soil. *Crops Soils*, *32*(2), 13-18.

Gaur, N., & Mohanty, B. P. (2013). Evolution of physical controls for soil moisture in humid and subhumid watersheds. *Water Resources Research*, *49*(3), 1244-1258.

Gottschalk, P., Smith, J. U., Wattenbach, M., Bellarby, J., Stehfest, E., Arnell, N., Osborn, T., Jones, C., & Smith, P. (2012). How will organic carbon stocks in mineral soils evolve under future climate? Global projections using RothC for a range of climate change scenarios. *Biogeosciences*, *9*(8), 3151-3171.

Gregory, P. J., Ingram, J. S. I., Andersson, R., Betts, R. A., Brovkin, V., Chase, T. N., Grace, P. R., Gray, A. J., Hamilton, N., Hardy, T. B., Howden, S. M., Jenkins, A., Meybeck, M., Olsson, M., Ortiz-Monasterio, I., Palm, C. A., Payn, T. W., Rummukainen, M., Schulze, R. E., . . . Wilkinson, M. J. (2002). Environmental consequences of alternative practices for intensifying crop production. *Agriculture, Ecosystems & Environment*, *88*(3), 279-290. https://doi.org/https://doi.org/10.1016/S0167-8809(01)00263-8

Haghighi, F., Gorji, M., & Shorafa, M. (2010). A study of the effects of land use changes on soil physical properties and organic matter. *Land Degradation & Development*, *21*(5), 496-502.

Haws, N. W., Rao, P. S. C., Simunek, J., & Poyer, I. C. (2005). Single-porosity and dual-porosity modeling of water flow and solute transport in subsurface-drained fields using effective field-scale parameters. *Journal of Hydrology*, *313*(3-4), 257-273.

Hayes, A. (2017). Soil Physical Properties. *Properties and Management of Soils in the Tropics*.

Henault, C., Grossel, A., Mary, B., Roussel, M., & LÉOnard, J. (2012). Nitrous Oxide Emission by Agricultural Soils: A Review of Spatial and Temporal Variability for Mitigation. *Pedosphere*, *22*(4), 426-433. https://doi.org/https://doi.org/10.1016/S1002-0160(12)60029-0

Hendricks, T., Franklin, D., Dahal, S., Hancock, D., Stewart, L., Cabrera, M., & Hawkins, G. (2019). Soil carbon and bulk density distribution within 10 Southern Piedmont grazing systems. *Journal of Soil and Water Conservation*, *74*(4), 323-333.

Horel, Á., Tóth, E., Gelybó, G., Kása, I., Bakacsi, Z., & Farkas, C. (2015). Effects of Land Use and Management on SoilHydraulic Properties. *Open Geosciences*, *7*(1). https://doi.org/doi:10.1515/geo-2015-0053

Iqbal, J., Thomasson, J. A., Jenkins, J. N., Owens, P. R., & Whisler, F. D. (2005). Spatial variability analysis of soil physical properties of alluvial soils. *Soil Science Society of America Journal*, *69*(4), 1338-1350.

Jiao, W., Zhou, D., & Wang, Y. (2021). Effects of Clay Content on Pore Structure Characteristics of Marine Soft Soil. *Water*, *13*(9), 1160. https://www.mdpi.com/2073-4441/13/9/1160

Jirků, V., Kodešová, R., Nikodem, A., Mühlhanselová, M., & Žigová, A. (2013). Temporal variability of structure and hydraulic properties of topsoil of three soil types. *Geoderma*, *204-205*, 43-58. https://doi.org/https://doi.org/10.1016/j.geoderma.2013.03.024

Jones, T. H., & Bradford, M. A. (2001). Assessing the functional implications of soil biodiversity in ecosystems. *Ecological Research, 16*, 845-858.

Kanwar, R. (1986). Analytical solutions of the transient state oxygen diffusion equation in soils with a production term. *Journal of Agronomy and Crop Science*, *156*(2), 101-109.

Kanwar, R. S., Mukhtar, S., & Singh, P. K. (1989). Transient-State Oxygen Diffusion Through Undisturbed Soil Columns. *Transactions of the ASABE*, *32*, 1645-1650.

Keiluweit, M., Gee, K., Denney, A., & Fendorf, S. (2018). Anoxic microsites in upland soils dominantly controlled by clay content. *Soil Biology and Biochemistry, 118*, 42-50.

Keiluweit, M., Wanzek, T., Kleber, M., Nico, P., & Fendorf, S. (2017). Anaerobic microsites have an unaccounted role in soil carbon stabilization. *Nature Communications*, *8*(1), 1771.

Kheir, R. B., Greve, M. H., Bøcher, P. K., Greve, M. B., Larsen, R., & McCloy, K. (2010). Predictive mapping of soil organic carbon in wet cultivated lands using classification-tree based models: The case study of Denmark. *Journal of Environmental Management*, *91*(5), 1150-1160.

Kibret, K., Beyene, S., & Erkossa, T. (2023). Soil Fertility and Soil Health. In S. Beyene, A. Regassa, B. B. Mishra, & M. Haile (Eds.), *The Soils of Ethiopia* (pp. 157-192). Springer International Publishing. https://doi.org/10.1007/978-3-031-17012-6_8

Kutílek, M. (2004). Soil hydraulic properties as related to soil structure. *Soil and Tillage Research*, *79*(2), 175-184. https://doi.org/https://doi.org/10.1016/j.still.2004.07.006

Lacroix, E. M., Mendillo, J., Gomes, A., Dekas, A., & Fendorf, S. (2022). Contributions of anoxic microsites to soil carbon protection across soil textures. *Geoderma*, *425*, 116050.

Lacroix, E. M., Rossi, R. J., Bossio, D., & Fendorf, S. (2021). Effects of moisture and physical disturbance on pore-scale oxygen content and anaerobic metabolisms in upland soils. *Science of The Total Environment*, *780*, 146572. https://doi.org/https://doi.org/10.1016/j.scitotenv.2021.146572

Lai, S.-H., Tiedje, J. M., & Erickson, A. E. (1976). In situ Measurement of Gas Diffusion Coefficient in Soils. *Soil Science Society of America Journal*, *40*(1), 3-6. https://doi.org/https://doi.org/10.2136/sssaj1976.03615995004000010006x

Li, H., Yao, Y., Zhang, X., Zhu, H., & Wei, X. (2021). Changes in soil physical and hydraulic properties following the conversion of forest to cropland in the black soil region of

Northeast China. *CATENA, 198*, 104986. https://doi.org/https://doi.org/10.1016/j.catena.2020.104986

Lin, Y., Campbell, A. N., Bhattacharyya, A., DiDonato, N., Thompson, A. M., Tfaily, M. M., Nico, P. S., Silver, W. L., & Pett-Ridge, J. (2021). Differential effects of redox conditions on the decomposition of litter and soil organic matter. *Biogeochemistry*, *154*(1), 1-15.

Lipiec, J., Kuś, J., Słowińska-Jurkiewicz, A., & Nosalewicz, A. (2006). Soil porosity and water infiltration as influenced by tillage methods. *Soil and Tillage Research*, *89*(2), 210-220.

Lipovetsky, T., Zhuang, L., Teixeira, W. G., Boyd, A., Pontedeiro, E. M., Moriconi, L., Alves, J. L., Couto, P., & van Genuchten, M. T. (2020). HYPROP measurements of the unsaturated hydraulic properties of a carbonate rock sample. *Journal of Hydrology*, *591*, 125706.

Mathieu, O., Lévêque, J., Hénault, C., Milloux, M.-J., Bizouard, F., & Andreux, F. (2006). Emissions and spatial variability of N_2O, N_2 and nitrous oxide mole fraction at the field scale, revealed with 15N isotopic techniques. *Soil Biology and Biochemistry*, *38*(5), 941-951.

Matson, P. A., Parton, W. J., Power, A. G., & Swift, M. J. (1997). Agricultural Intensification and Ecosystem Properties. *Science*, *277*(5325), 504-509. https://doi.org/doi:10.1126/science.277.5325.504

Millington, R. (1959). Gas diffusion in porous media. *Science*, *130*(3367), 100-102.

Millington, R., & Quirk, J. (1960). Transport in porous media. p. 97–106. FA Van Beren et al.(ed.) Trans. Int. Congr. of Soil Sci., 7th, Madison, WI. 14–24 Aug. 1960. Vol. 1. Elsevier, Amsterdam. *Transport in porous media. p. 97–106. In FA Van Beren et al.(ed.)*

Trans. Int. Congr. of Soil Sci., 7th, Madison, WI. 14–24 Aug. 1960. Vol. 1. Elsevier, Amsterdam.

Millington, R., & Quirk, J. (1961). Permeability of porous solids. *Transactions of the Faraday Society*, *57*, 1200-1207.

Minasny, B., & McBratney, A. B. (2007). Estimating the Water Retention Shape Parameter from Sand and Clay Content. *Soil Science Society of America Journal*, *71*(4), 1105-1110. https://doi.org/https://doi.org/10.2136/sssaj2006.0298N

Mohammadi, M. H., & Vanclooster, M. (2011). Predicting the soil moisture characteristic curve from particle size distribution with a simple conceptual model. *Vadose Zone Journal*, *10*(2), 594-602.

Moldrup, P., Kruse, C., Rolston, D., & Yamaguchi, T. (1996). Modeling diffusion and reaction in soils: III. Predicting gas diffusivity from the Campbell soil-water retention model. *Soil Science*, *161*(6), 366-375.

Moldrup, P., Olesen, T., Schjonning, P., Yamaguchi, T., & Rolston, D. E. (2000). Predicting the gas diffusion coefficient in undisturbed soil from soil water characteristics. *Soil Science Society of America Journal*, *64*(1), 94-100. https://doi.org/DOI10.2136/sssaj2000.64194x

Moldrup, P., Olesen, T., Yoshikawa, S., Komatsu, T., & Rolston, D. E. (2004). Three-porosity model for predicting the gas diffusion coefficient in undisturbed soil. *Soil Science Society of America Journal*, *68*(3), 750-759.

Molin, J. P., & Faulin, G. D. C. (2013). Spatial and temporal variability of soil electrical conductivity related to soil moisture. *Scientia Agricola*, *70*, 01-05.

Moyano, F. E., Manzoni, S., & Chenu, C. (2013). Responses of soil heterotrophic respiration to moisture availability: An exploration of processes and models. *Soil Biology and Biochemistry*, *59*, 72-85.

Mtambanengwe, F., Mapfumo, P., & Kirchmann, H. (2004). Decomposition of organic matter in soil as influenced by texture and pore size distribution. *Managing nutrient cycles to sustain soil fertility in sub-Saharan Africa*, *261*.

Mullins, C. E., Smith, K., & Mullins, C. (2000). Matric potential. *Soil and environmental analysis: Physical methods. eds ka smith and ce mullins*, 65-93.

Nath, A. J., & Rattan, L. (2017). Effects of tillage practices and land use management on soil aggregates and soil organic carbon in the north Appalachian region, USA. *Pedosphere*, *27*(1), 172-176.

Neira, J., Ortiz, M., Morales, L., & Acevedo, E. (2015). Oxygen diffusion in soils: Understanding the factors and processes needed for modeling. *Chilean journal of agricultural research*, *75*, 35-44. http://www.scielo.cl/scielo.php?script=sci_arttext&pid=S0718-58392015000300005&nrm=iso

Nimmo, J. R. (2004). Porosity and pore size distribution. *Encyclopedia of Soils in the Environment*, *3*(1), 295-303.

Nimmo, J. R., & Likens, G. (2009). Vadose water.

Noelia, R.-R., & Eguren, G. (2022). Evaluation of Sustainability of Cropping Sequences on Production Systems: Agricultural Intensification Indices.

Or, D., Smets, B. F., Wraith, J., Dechesne, A., & Friedman, S. (2007). Physical constraints affecting bacterial habitats and activity in unsaturated porous media–a review. *Advances in Water Resources*, *30*(6-7), 1505-1527.

Ortega-Ramírez, P., Pot, V., Laville, P., Schlüter, S., Amor-Quiroz, D. A., Hadjar, D., Mazurier, A., Lacoste, M., Caurel, C., Pouteau, V., Chenu, C., Basile-Doelsch, I., Henault, C., & Garnier, P. (2023). Pore distances of particulate organic matter predict N_2O emissions from intact soil at moist conditions. *Geoderma*, *429*, 116224. https://doi.org/https://doi.org/10.1016/j.geoderma.2022.116224

Paul, E. A., Paustian, K. H., Elliott, E., & Cole, C. V. (1996). *Soil Organic Matter in Temperate AgroecosystemsLong Term Experiments in North America*. CRC Press.

Peng, H., Dan, L., Hua, X., Chaoli, L., Hayat, U., Yang, X., Changhong, S., Chunsheng, D., Yuanlai, C., & Yufeng, L. (2022). Assessment of paddy expansion impact on regional climate using WRF model: a case study in Sanjiang Plain, Northeast China. https://doi.org/10.1007/S00704-022-04145-X

Peterson, A., Helgason, W., & Ireson, A. (2019). How spatial patterns of soil moisture dynamics can explain field-scale soil moisture variability: Observations from a sodic landscape. *Water Resources Research*, *55*(5), 4410-4426.

Pires, L. F., Auler, A. C., Roque, W. L., & Mooney, S. J. (2020). X-ray microtomography analysis of soil pore structure dynamics under wetting and drying cycles. *Geoderma*, *362*, 114103. https://doi.org/10.1016/j.geoderma.2019.114103

Pulido Moncada, M., Helwig Penning, L., Timm, L. C., Gabriels, D., & Cornelis, W. M. (2017). Visual examination of changes in soil structural quality due to land use. *Soil and Tillage Research*, *173*, 83-91. https://doi.org/https://doi.org/10.1016/j.still.2016.08.011

Rohe, L., Apelt, B., Vogel, H.-J., Well, R., Wu, G.-M., & Schlüter, S. (2021). Denitrification in soil as a function of oxygen availability at the microscale. *Biogeosciences*, *18*(3), 1185-1201.

Schlüter, S., Zawallich, J., Vogel, H.-J., & Dörsch, P. (2019). Physical constraints for respiration in microbial hotspots in soil and their importance for denitrification. *Biogeosciences*, *16*(18), 3665-3678.

Schwen, A., Bodner, G., Scholl, P., Buchan, G. D., & Loiskandl, W. (2011). Temporal dynamics of soil hydraulic properties and the water-conducting porosity under different tillage. *Soil and Tillage Research*, *113*(2), 89-98. https://doi.org/https://doi.org/10.1016/j.still.2011.02.005

Selassie, Y. G., Anemut, F., & Addisu, S. (2015). The effects of land use types, management practices and slope classes on selected soil physico-chemical properties in Zikre watershed, North-Western Ethiopia. *Environmental Systems Research*, *4*(1), 1-7.

Sergey, B., & Pete, S. (2012). Soil physics meets soil biology: Towards better mechanistic prediction of greenhouse gas emissions from soil. *Soil Biology & Biochemistry*. https://doi.org/10.1016/J.SOILBIO.2011.12.015

Smith, K. (2017). Changing views of nitrous oxide emissions from agricultural soil: key controlling processes and assessment at different spatial scales. *European Journal of Soil Science*, *68*(2), 137-155.

Stevenson, A., Hartemink, A. E., & Zhang, Y. (2023). Measuring sand content using sedimentation, spectroscopy, and laser diffraction. *Geoderma*, *429*, 116268. https://doi.org/https://doi.org/10.1016/j.geoderma.2022.116268

Stolze, K., Barnes, A. D., Eisenhauer, N., & Totsche, K. U. (2022). Depth-differentiated, multivariate control of biopore number under different land-use practices. *Geoderma*, *418*, 115852. https://doi.org/https://doi.org/10.1016/j.geoderma.2022.115852

Subedi, A., Franklin, D., Cabrera, M., Dahal, S., Hancock, D., McPherson, A., & Stewart, L. (2022). Extreme Weather and Grazing Management Influence Soil Carbon and Compaction. *Agronomy*, *12*(9), 2073.

Suzanne, E. A., Jonathan, A. L., Alexandre, R. C., & Sébastien, F. L. (2008). Measurement of gas diffusion through soils: comparison of laboratory methods. *Journal of Environmental Monitoring*. https://doi.org/10.1039/B809461F

Troeh, F. R., Jabro, J. D., & Kirkham, D. (1982). Gaseous diffusion equations for porous materials. *Geoderma*, *27*(3), 239-253.

Tuller, M., Or, D., & Hillel, D. (2004). Retention of water in soil and the soil water characteristic curve. *Encyclopedia of Soils in the Environment*, *4*, 278-289.

Turkeltaub, T., Mannheim, R., Furman, A., & Weisbrod, N. (2023). Elucidating the relationship between gaseous O2 and redox potential in a soil aquifer treatment system using data driven approaches and an oxygen diffusion model. *Journal of Hydrology*, *618*, 129168. https://doi.org/https://doi.org/10.1016/j.jhydrol.2023.129168

van Dam, J. C., Wösten, J. H. M., & Nemes, A. (1996). Unsaturated soil water movement in hysteretic and water repellent field soils. *Journal of Hydrology*, *184*(3), 153-173. https://doi.org/https://doi.org/10.1016/0022-1694(95)02996-6

Van Genuchten, M. T. (1980). A closed-form equation for predicting the hydraulic conductivity of unsaturated soils. *Soil Science Society of America Journal*, *44*(5), 892-898.

Wang, R., Wen, S., & Sun, Z. (2022). Analytical Solution of Rainfall Infiltration in Unsaturated Soil Slopes Considering Initial Water Content Distribution. *KSCE Journal of Civil Engineering*, *26*(11), 4419-4431. https://doi.org/10.1007/s12205-022-1750-5

Wei, C., Gao, M., Shao, J., Xie, D., & Pan, G. (2006). Soil aggregate and its response to land management practices. *China Particuology*, *4*(05), 211-219.

Wendel, A. S., Bauke, S. L., Amelung, W., & Knief, C. (2022). Root-rhizosphere-soil interactions in biopores. *Plant and Soil*, *475*(1-2), 253-277.

West, J. R., Lauer, J. G., & Whitman, T. (2023). Tillage homogenizes soil bacterial communities in microaggregate fractions by facilitating dispersal. *bioRxiv*, 2023.2003. 2008.531801.

Wickham, H., Chang, W., & Wickham, M. H. (2016). Package 'ggplot2'. *Create elegant data visualisations using the grammar of graphics. Version*, *2*(1), 1-189.

Wittwer, R. A., Bender, S. F., Hartman, K., Hydbom, S., Lima, R. A. A., Loaiza, V., Nemecek, T., Oehl, F., Olsson, P. A., Petchey, O., Prechsl, U. E., Schlaeppi, K., Scholten, T., Seitz, S., Six, J., & van der Heijden, M. G. A. (2021). Organic and conservation agriculture promote ecosystem multifunctionality. *Science Advances*, *7*(34), eabg6995. https://doi.org/doi:10.1126/sciadv.abg6995

Xing, H., Smith, C. J., Wang, E., Macdonald, B., & Wårlind, D. (2023). Modelling nitrous oxide emissions: comparing algorithms in six widely used agro-ecological models. *Soil Research*.

Xue, J., & Gavin, K. (2008). Effect of Rainfall Intensity on Infiltration into Partly Saturated Slopes. *Geotechnical and Geological Engineering*, *26*(2), 199-209. https://doi.org/10.1007/s10706-007-9157-0

Yanai, J., Sawamoto, T., Oe, T., Kusa, K., Yamakawa, K., Sakamoto, K., Naganawa, T., Inubushi, K., Hatano, R., & Kosaki, T. (2003). Spatial variability of nitrous oxide emissions and their soil-related determining factors in an agricultural field. *Journal of environmental quality*, *32*(6), 1965-1977.

Ye, L., Zengming, C., Ji, C., Michael, J. C., Chenglong, Y., Nan, Z., Yuncai, M., Huijie, Z., Junjie, L., Weixin, D., Ye, L., Zengming, C., Ji, C., Michael, J. C., Chenglong, Y., Nan, Z., Yuncai, M., Huijie, Z., Junjie, L., & Weixin, D. (2022). Oxygen availability regulates the quality of soil dissolved organic matter by mediating microbial metabolism and iron oxidation. https://doi.org/10.1111/GCB.16445

Young, I. M., Crawford, J. W., Nunan, N., Otten, W., & Spiers, A. (2008). Chapter 4 Microbial Distribution in Soils: Physics and Scaling. In *Advances in Agronomy* (Vol. 100, pp. 81-121). Academic Press. https://doi.org/https://doi.org/10.1016/S0065-2113(08)00604-4

Zaffar, M., & Lu, S.-G. (2015). Pore Size Distribution of Clayey Soils and Its Correlation with Soil Organic Matter. *Pedosphere*, *25*(2), 240-249. https://doi.org/https://doi.org/10.1016/S1002-0160(15)60009-1

Zeleke, T. B., & Si, B. C. (2005). Scaling relationships between saturated hydraulic conductivity and soil physical properties. *Soil Science Society of America Journal*, *69*(6), 1691-1702.

Zhang, Y., Weihermüller, L., Toth, B., Noman, M., & Vereecken, H. (2022). Analyzing dual porosity in soil hydraulic properties using soil databases for pedotransfer function development. *Vadose Zone Journal*, *21*(5), e20227.

APPENDIX 3.1

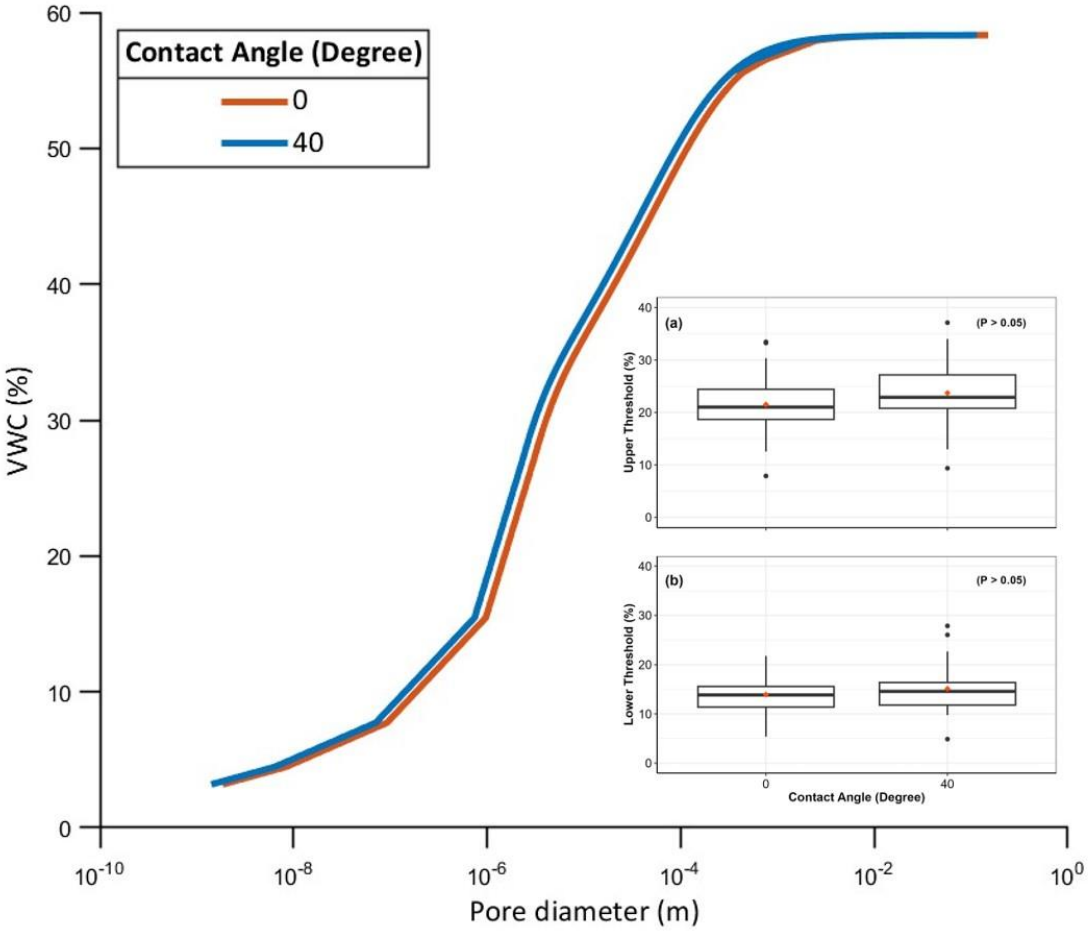

Appendix B1. Effect of changes in liquid-solid contact angle from 0 to 40 degree (°) on the relationship of volumetric water content (VWC) (%) and pore diameter (m). The boxplots depict the distribution of (a) upper threshold (b) lower threshold at contact angle 0° and 40°. The centerline of the box plots indicates the median, the upper and lower represent the 25th and 75th quantiles, and the red dot reflects the arithmetic mean of thresholds. The p value ($p < 0.05$) represents a significant cluster difference.

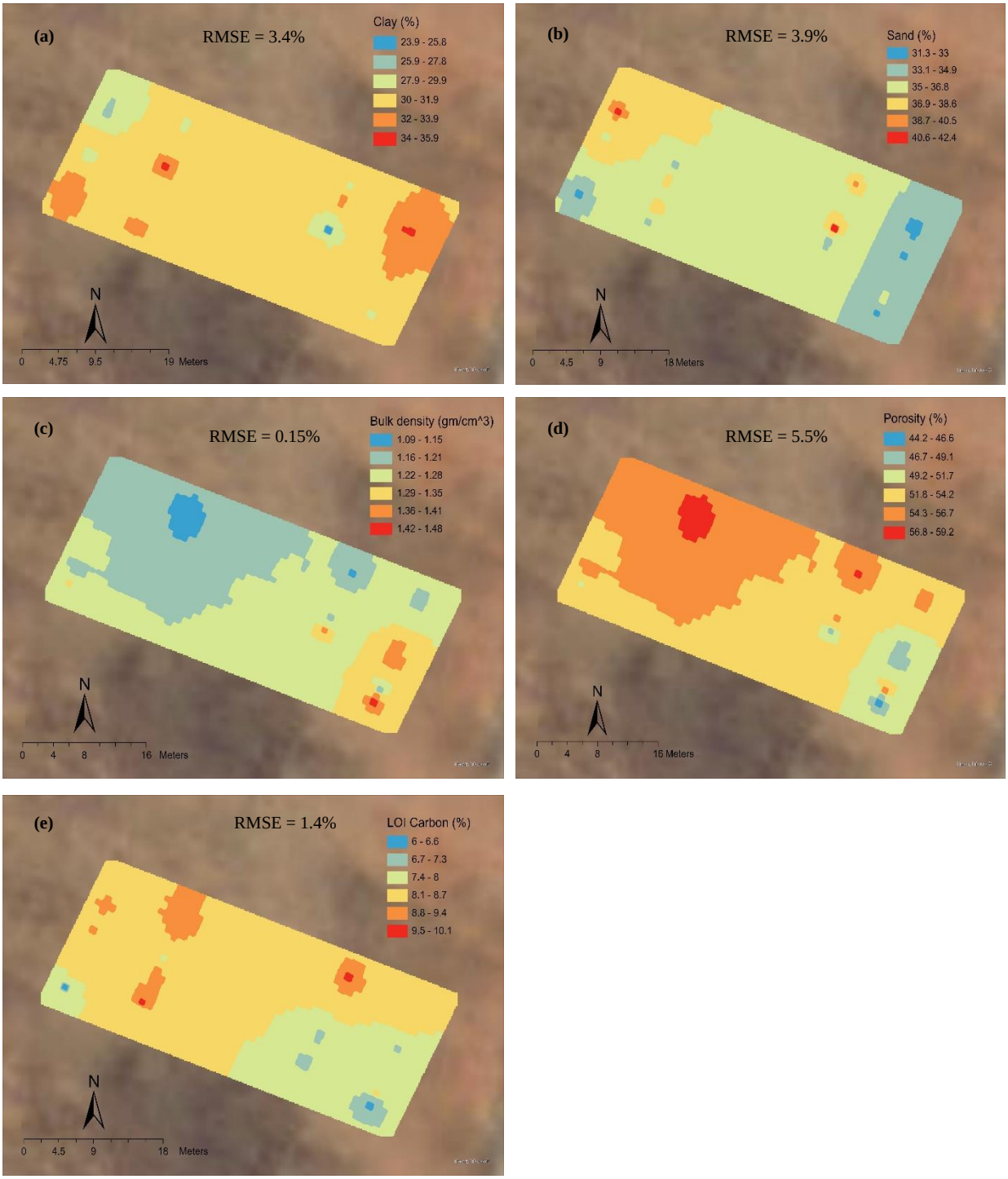

Appendix B2. Spatial distribution of (a) clay (%) (b) sand (%) (c) bulk density (gm cm^^{3}) (d) porosity (%) (e) loss-on-ignition carbon (%) in the field. The root mean square value (RMSE) indicates the difference between predicted and measured water contents.

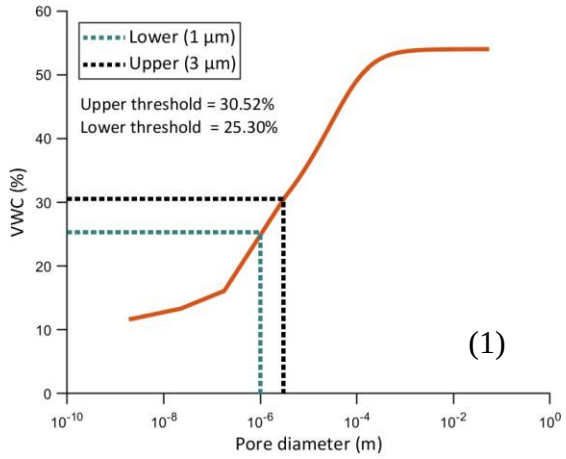
Lower (1 µm)
Upper (3 µm)
Upper threshold = 30.52%
Lower threshold = 25.30%
VWC (%)
Pore diameter (m)
(1)

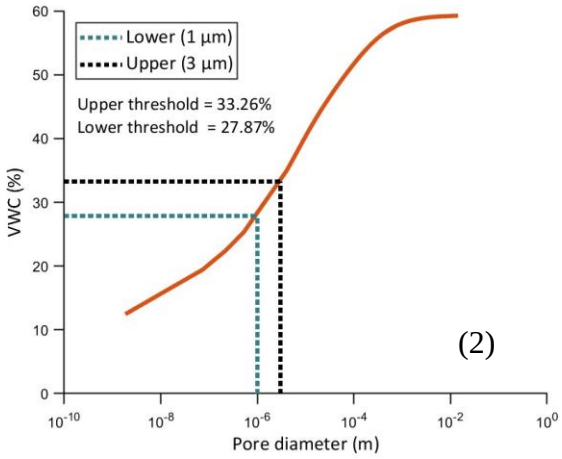
Lower (1 µm)
Upper (3 µm)
Upper threshold = 33.26%
Lower threshold = 27.87%
VWC (%)
Pore diameter (m)
(2)

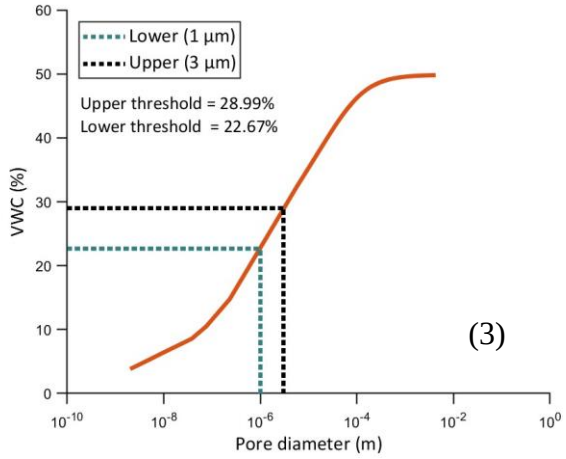
Lower (1 µm)
Upper (3 µm)
Upper threshold = 28.99%
Lower threshold = 22.67%
VWC (%)
Pore diameter (m)
(3)

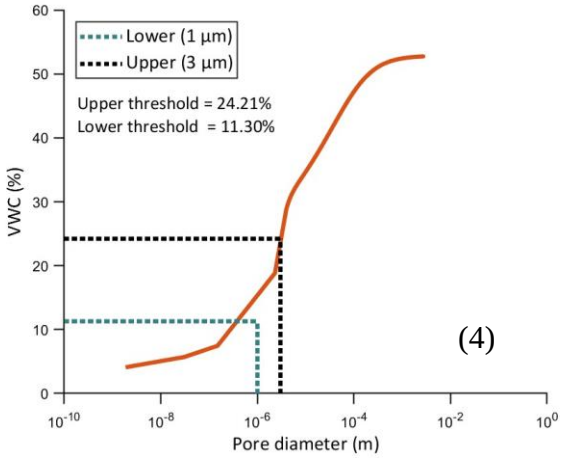
Lower (1 µm)
Upper (3 µm)
Upper threshold = 24.21%
Lower threshold = 11.30%
VWC (%)
Pore diameter (m)
(4)

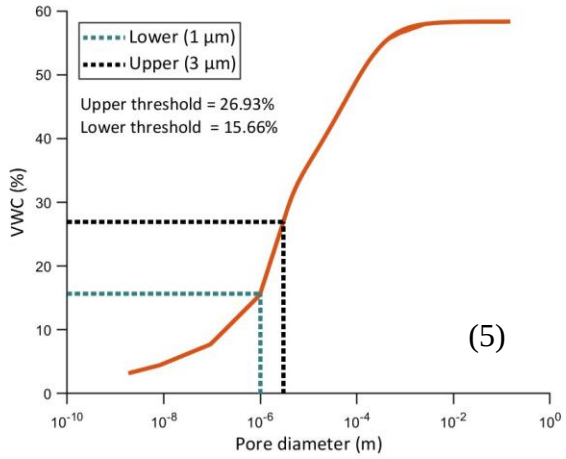
Lower (1 µm)
Upper (3 µm)
Upper threshold = 26.93%
Lower threshold = 15.66%
VWC (%)
Pore diameter (m)
(5)

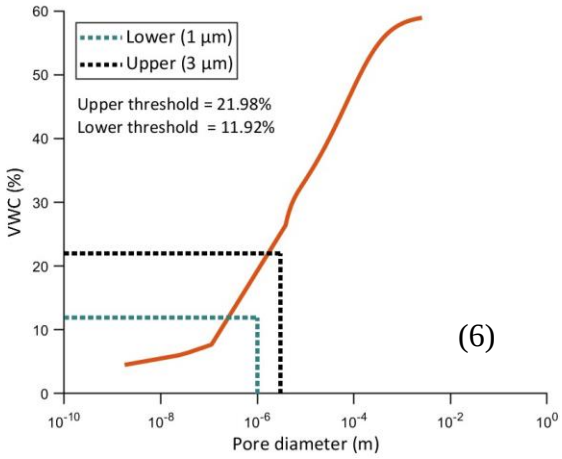
Lower (1 µm)
Upper (3 µm)
Upper threshold = 21.98%
Lower threshold = 11.92%
VWC (%)
Pore diameter (m)
(6)

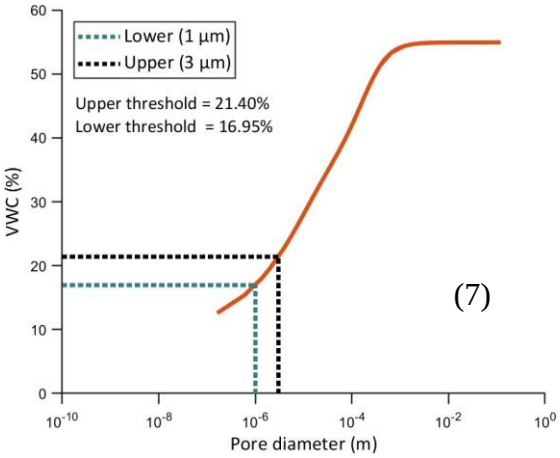
Lower (1 µm)
Upper (3 µm)
Upper threshold = 21.40%
Lower threshold = 16.95%
VWC (%)
Pore diameter (m)

(7)

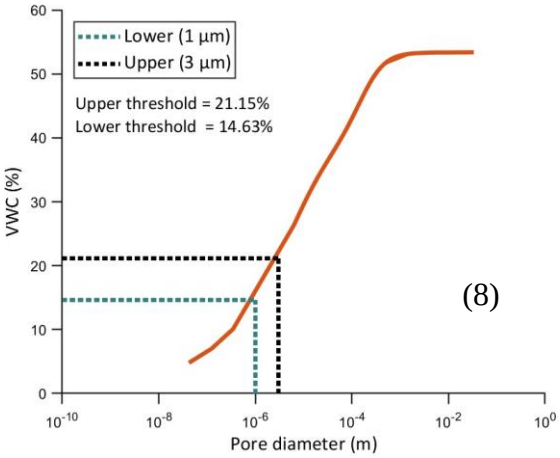
Lower (1 µm)
Upper (3 µm)
Upper threshold = 21.15%
Lower threshold = 14.63%
VWC (%)
Pore diameter (m)

(8)

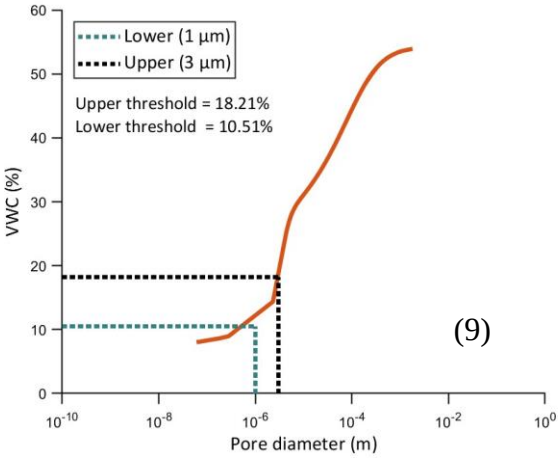
Lower (1 µm)
Upper (3 µm)
Upper threshold = 18.21%
Lower threshold = 10.51%
VWC (%)
Pore diameter (m)

(9)

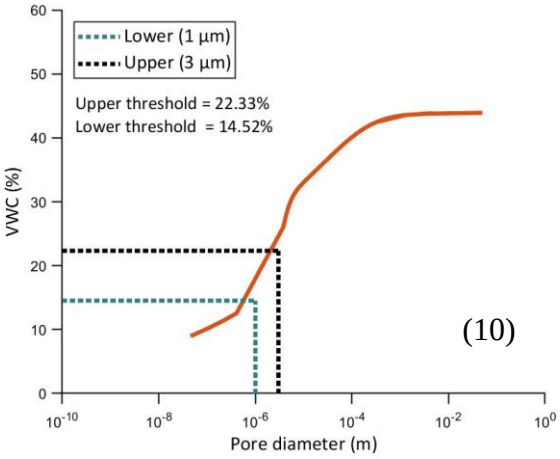
Lower (1 µm)
Upper (3 µm)
Upper threshold = 22.33%
Lower threshold = 14.52%
VWC (%)
Pore diameter (m)

(10)

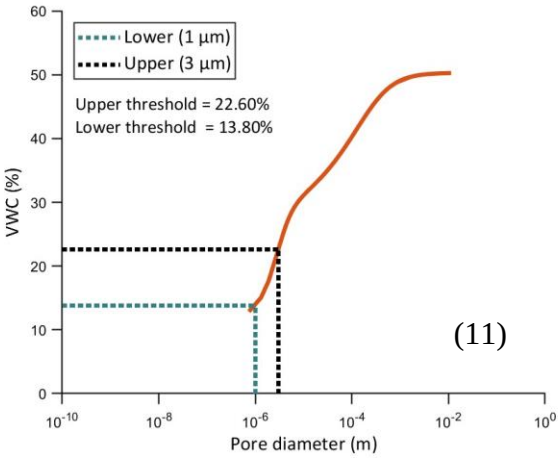
Lower (1 µm)
Upper (3 µm)
Upper threshold = 22.60%
Lower threshold = 13.80%
VWC (%)
Pore diameter (m)

(11)

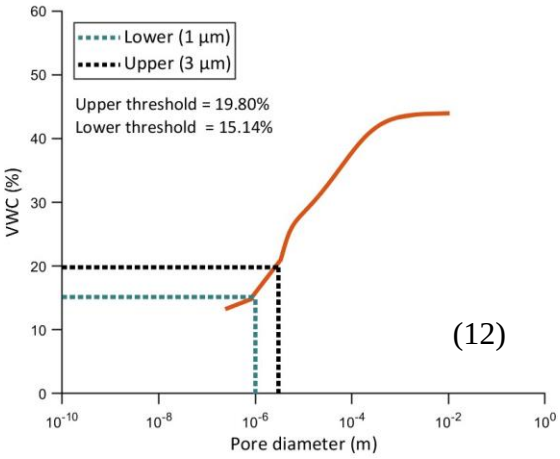
Lower (1 µm)
Upper (3 µm)
Upper threshold = 19.80%
Lower threshold = 15.14%
VWC (%)
Pore diameter (m)

(12)

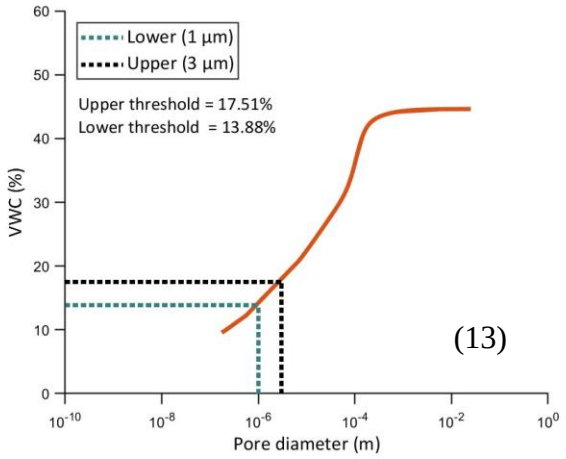

(13)

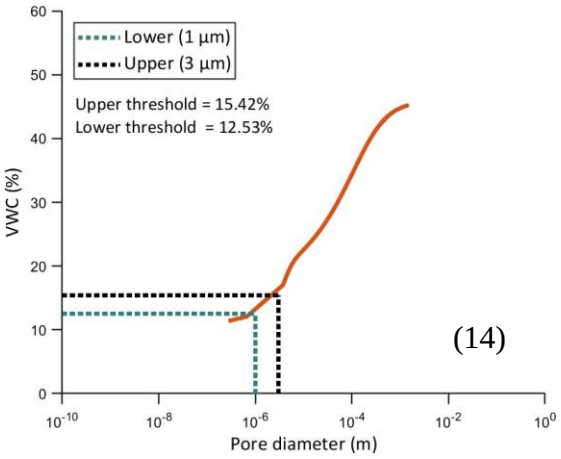

(14)

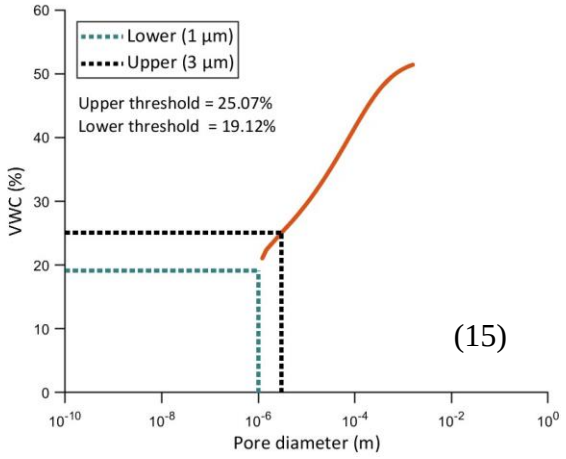

(15)

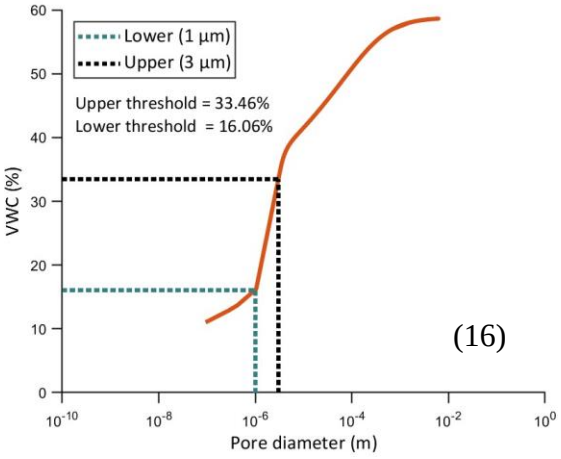

(16)

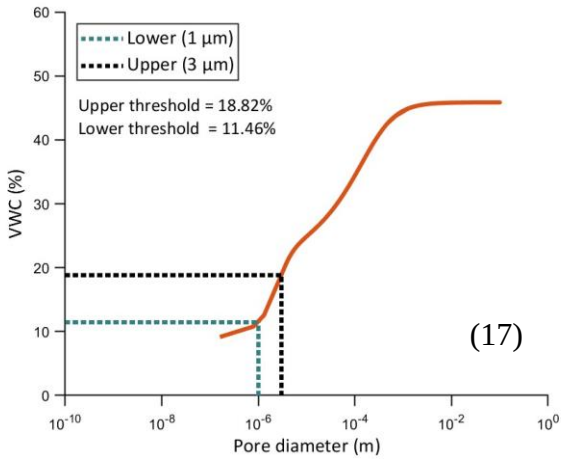

(17)

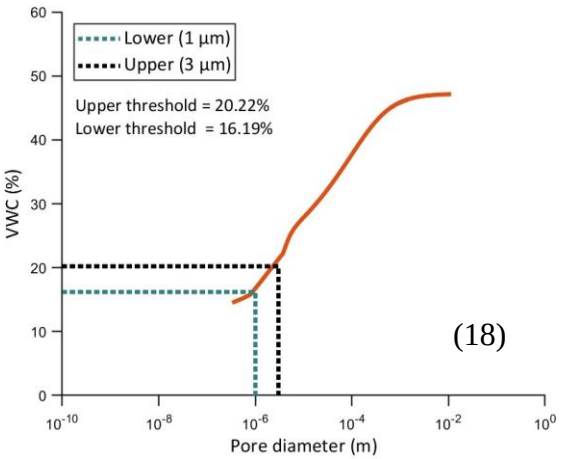

(18)

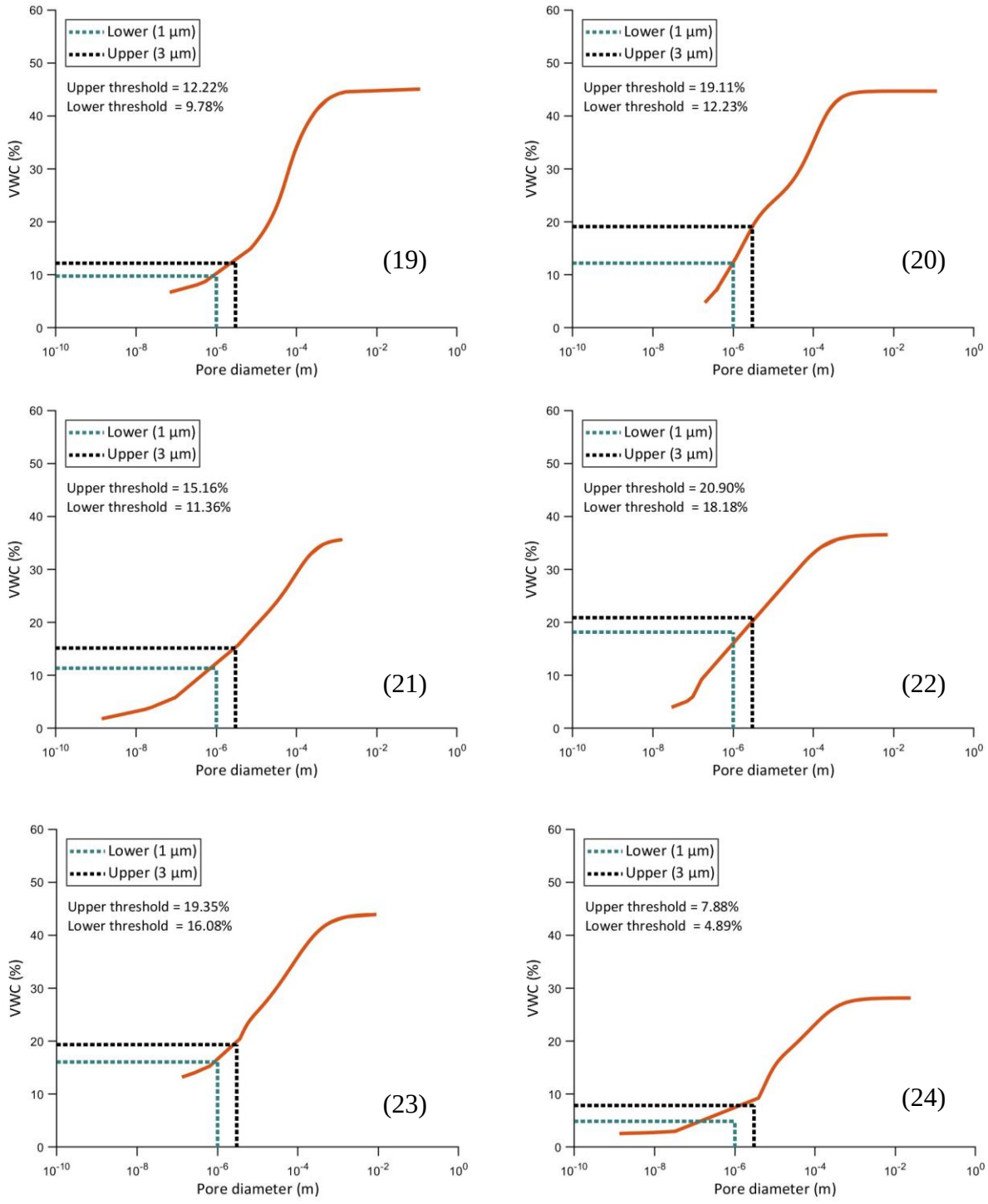

Appendix B3. Volumetric water content in surface soil as a function of pore diameter for 24 soil cores. The dotted black line represents upper thresholds (3 microns) while the dotted green line indicates lower threshold (1 micron).

CHAPTER 4

CONCLUSION

Soil physical properties, interconnected with chemical and biological attributes, are heavily impacted by land management practices. Variations in physical properties, especially soil structure, significantly affect nutrient redox processes, microbial community diversity, distribution, and activity within the soil ecosystem. These alterations are reflected in soil hydraulic properties, which dictate the division of rainfall into surface runoff and infiltration and impact the wetting behavior of soil profiles. The arrangement of air and water phases within the soil system plays a crucial role in determining oxygen diffusivity and the formation and longevity of anoxic soil pores.

The impact of soil structure on oxygen diffusivity was assessed at different moisture conditions—residual, threshold, field capacity, and saturation. The residual moisture represents dry soil condition, while threshold moisture reflects soil condition when pores less than or equal to 1 micron are only saturated. Soil structure impacted oxygen diffusion at residual and threshold moisture in the soil ecosystem. When soil moisture increased beyond the threshold, the water phase became extensively connected by trapping air, which decreased air phase connectivity and obliterated the effect of soil structure on O_2 diffusivity. We found that oxygen diffusivity at residual and threshold moisture was relatively higher in soil structures with uniform pore size distribution (PSD) and highly connected pores than with non-uniform PSD and disconnected pores. The transferability of oxygen diffusivity estimates based on lab-derived soil hydraulic parameters was also assessed for field conditions. It was found that O_2 diffusivity estimated at field capacity and

saturation from lab measurements for simulating in situ O_2 transport was not directly transferable but was transferable for the residual and threshold soil moisture. It was also found that the oxygen diffusivity/ diffusion coefficient determines the oxygen concentration in the soil profile at different depths at residual moisture. However, oxygen diffusivity does not influence oxygen concentration when soil pores representing a greater fraction of pore volume are filled with water (i.e., threshold moisture).

Soil moisture distribution governs the potential of distinct soil pores to become anoxic, influencing the release of nitrous oxide and methane gases from the soil ecosystem. The intensity of rainfall and irrigation controls moisture in soil pores, while the duration of the saturation state depends on soil structural attributes, such as pore connectivity, pore-size distribution, and the architecture of the pore. The macropores (> 3 μm) distributed throughout the field quickly drain water compared to micropores in the soil matrix. Soil matrix retains water for an extended period due to strong adhesive and cohesive forces between water and soil pore, rendering highly potent anoxic pores (≤ 1 μm) to remain O_2 deficit for at least 48 hours. Although macropores have a relatively higher proclivity to become anoxic after saturation, they barely get saturated in the field due to insufficient rainfall and the inability to retain water.

The results from this study are based upon several assumptions, and consequently, any inferences based on these results have limitations that must be considered during applications. The hydraulic parameters fitted to the dual porosity model represent water flow through capillary pores under equilibrium conditions; they do not account for macropore water flow prevalent in non-capillary pores under non-equilibrium conditions. Moreover, the influence of changes in contact angle on pore throat diameter is not accounted while estimating pore diameter based on matric potential. The water meniscus is assumed to be flat, with a contact angle equal to zero. Lastly,

oxygen concentration decline is assumed to be primarily influenced by soil physical properties and oxygen diffusivity, which is not the case in actual conditions where oxygen concentration is also impacted by microbial activity, organic C concentration, soil redox potential, and temperature.

Considering the limitations above, the findings of this study offer valuable insights into oxygen diffusion as well as the temporal and spatial distribution of anoxic soil volume in agricultural soils. These insights can be used to develop a parsimonious oxygen diffusion model by utilizing shape-fitting parameters n_1 and n_2, which in turn have significant implications for greenhouse gas (GHG) modeling. Additionally, understanding the spatio-temporal distribution of soil anoxia can significantly contribute to modeling carbon (C) and nitrogen (N) dynamics in croplands. Moreover, the identification of temporal and spatial hotspots within cultivated fields has the potential to optimize land management practices. By pinpointing these hotspots, it becomes possible to implement targeted interventions that can enhance crop productivity, improve soil quality, and promote environmental sustainability. Therefore, this knowledge can be instrumental in achieving the dual goals of maximizing agricultural yields while minimizing the ecological impact of farming activities. In summary, these findings not only shed light on oxygen diffusion and the distribution of anoxic soil volume but also offer practical applications in GHG modeling, C and N dynamics modeling, and optimizing land management practices. By harnessing this information, stakeholders in the agricultural sector can work towards sustainable and efficient agricultural systems that balance productivity and environmental quality.